

FHWA/IN/JTRP-2008/7

Final Report

**ANALYSIS AND DETERMINATION OF AXLE
LOAD SPECTRA AND TRAFFIC INPUT FOR
THE MECHANISTIC-EMPIRICAL
PAVEMENT DESIGN GUIDE**

**Yi Jiang
Shuo Li
Tommy Nantung
Huaxin Chen**

October 2008



INDOT Research

TECHNICAL *Summary*

Technology Transfer and Project Implementation Information

TRB Subject Code: 55-5 Traffic Measurement
Publication No.: FHWA/IN/JTRP-2008/7, SPR-40291

October 2008
Final Report

Analysis and Determination of Axle Load Spectra and Traffic Input for the Mechanistic-Empirical Pavement Design Guide

Introduction

The values of equivalent single axle loads (ESAL) have been used to represent the vehicle loads in pavement design. To improve the pavement design procedures, a new method, called the Mechanistic-Empirical Pavement Design Guide (MEPDG), has been developed to use the axle load spectra to represent the vehicle loads in pavement design. These spectra represent the percentage of the total axle applications within each load interval for single, tandem, tridem, and quad axles. Using axle load spectra as the traffic input, the MEPDG method is able to analyze the impacts of varying traffic loads on pavement and provide an optimal pavement structure design. In addition, the new method can be used to analyze the effects of materials and the impacts of seasons, to compare rehabilitation strategies, and to perform forensic analyses of pavement conditions. The MEPDG utilizes mechanistic-empirical approaches to realistically characterize in-service pavements and

allows the full integration of vehicular traffic loadings, climatic features, soil characteristics, and paving materials properties into the detailed analysis of pavement structural behaviors and the resulting pavement performance.

In order to provide the traffic data input required by the MEPDG, the Indiana Department of Transportation (INDOT) made an effort to obtain truck traffic information from the traffic data collected through weigh-in-motion (WIM) stations. This study was conducted to create the truck traffic spectra and other traffic inputs for INDOT to implement the new pavement design method. Furthermore, the INDOT AADT data were used in this study to analyze the spatial distributions of the traffic volumes in Indiana and to obtain the spatial distributions of traffic volumes.

Findings

A Visual Basic computer program was developed and was successfully utilized to obtain the necessary traffic information for the new pavement design method from the WIM data. The truck traffic data include average annual daily truck traffic, average monthly and hourly truck traffic, adjustment factors, axle load spectra, and axle weight and spacing values. The truck traffic can be expressed in individual vehicle types as well as in combined truck traffic values. It was found that the WIM data contained a noticeable amount of unclassified vehicles, which would affect pavement designs

if their patterns and components could not be reasonably identified.

Furthermore, the INDOT AADT data were used in this study to analyze the spatial distributions of the traffic volumes in Indiana. The spatial distributions of traffic volumes were obtained to provide INDOT with (1) a 3-dimensional perspective of traffic volumes over entire Indiana; and (2) a basis for determining appropriate WIM locations. ArcGIS 9.2 was used in the analysis of the spatial distributions of traffic volumes. ArcGIS 9.2 applies the interpolation techniques in its Geostatistical

Analyst. Geostatistical Analyst uses sample points taken at different locations in a landscape and creates a continuous surface. The sample points in this study are the traffic volumes from the INDOT traffic monitoring stations. It was found that the AADT data were not normally distributed. The data were transformed by log or Box-Cox techniques to make the data more normally distributed in order to satisfy the normal distribution requirement of the geostatistics. Through various types of mathematical modeling techniques, it was concluded that the Inverse Distance Weighing (IDW) method generated the best AADT predictions among the ten modeling methods. The IDW method can be used to predict the AADT at given locations within Indiana.

This study has produced the traffic input for INDOT to implement the new pavement design method. The traffic input is an essential component for using the MEPDG to design pavement structures. In addition to the axle load spectra and truck traffic input, this study also analyzed the AADT distributions in Indiana through geostatistical analysis utilizing ArcGIS tools. The geostatistical analysis resulted in a series of results for spatial AADT predictions and future WIM station location determinations. It is believed that the results of this study will certainly facilitate INDOT's transition process from the current pavement design method to the MEPDG.

Implementation

The axle load spectra and traffic inputs generated from this study will be used for INDOT to implement the new AASHTO Pavement Design Method. The suggested future

WIM station locations can be used for INDOT to consider when additional WIM stations are to be established.

Contacts

For more information:

Prof. Yi Jiang

Department of Building Construction
Management
School of Technology
Purdue University
West Lafayette IN 47907
Phone: (765) 494-5602
Fax: (765) 496-2246

Indiana Department of Transportation

Division of Research
1205 Montgomery Street
P.O. Box 2279
West Lafayette, IN 47906
Phone: (765) 463-1521
Fax: (765) 497-1665

Purdue University

Joint Transportation Research Program
School of Civil Engineering
West Lafayette, IN 47907-1284
Phone: (765) 494-9310
Fax: (765) 496-1105

Final Report

FHWA/IN/JTRP-2008/7

Analysis and Determination of Axle Load Spectra and Traffic Input for the Mechanistic-Empirical Pavement Design Guide

By

Yi Jiang, Ph.D., PE
Department of Building Construction Management
School of Technology
Purdue University

Shuo Li, Ph.D., PE
Office of Research and Development
Indiana Department of Transportation

Tommy Nantung, Ph.D., PE
Office of Research and Development
Indiana Department of Transportation

Huaxin Chen, Ph.D.
Department of Building Construction Management
School of Technology
Purdue University

Joint Transportation Research Program
Project No. C-36-59VVV
File No. 8-4-74
SPR-40291

Conducted in Cooperation with the
Indiana Department of Transportation
and the U.S. Department of Transportation
Federal Highway Administration

The contents of this report reflect the views of the authors who are responsible for the facts and accuracy of the data presented herein. The contents do not necessarily reflect the official views or policies of the Indiana Department of Transportation and Federal Highway Administration. This report does not constitute a standard, specification, or regulation.

Purdue University
West Lafayette, Indiana
October 2008

1. Report No. FHWA/IN/JTRP-2008/7		2. Government Accession No.		3. Recipient's Catalog No.	
4. Title and Subtitle Analysis and Determination of Axle Load Spectra and Traffic Input for the Mechanistic-Empirical Pavement Design Guide				5. Report Date October 2008	
				6. Performing Organization Code	
7. Author(s) Yi Jiang, Shuo Li, Tommy Nantung, and Huaxin Chen				8. Performing Organization Report No. FHWA/IN/JTRP-2008/7	
9. Performing Organization Name and Address Joint Transportation Research Program 1284 Civil Engineering Building Purdue University West Lafayette, IN 47907-1284				10. Work Unit No.	
				11. Contract or Grant No. SPR-40291	
12. Sponsoring Agency Name and Address Indiana Department of Transportation State Office Building 100 North Senate Avenue Indianapolis, IN 46204				13. Type of Report and Period Covered Final Report	
				14. Sponsoring Agency Code	
15. Supplementary Notes Prepared in cooperation with the Indiana Department of Transportation and Federal Highway Administration.					
16. Abstract The values of equivalent single axle loads (ESAL) have been used to represent the vehicle loads in pavement design. To improve the pavement design procedures, a new method, called the Mechanistic-Empirical Pavement Design Guide (MEPDG), has been developed to use the axle load spectra to represent the vehicle loads in pavement design. These spectra represent the percentage of the total axle applications within each load interval for single, tandem, tridem, and quad axles. Using axle load spectra as the traffic input, the MEPDG method is able to analyze the impacts of varying traffic loads on pavement and provide an optimal pavement structure design. In addition, the new method can be used to analyze the effects of materials and the impacts of seasons, to compare rehabilitation strategies, and to perform forensic analyses of pavement conditions. The MEPDG utilizes mechanistic-empirical approaches to realistically characterize in-service pavements and allows the full integration of vehicular traffic loadings, climatic features, soil characteristics, and paving materials properties into the detailed analysis of pavement structural behaviors and the resulting pavement performance. In order to provide the traffic data input required by the MEPDG, the Indiana Department of Transportation (INDOT) made an effort to obtain truck traffic information from the traffic data collected through weigh-in-motion (WIM) stations. This study was conducted to create the truck traffic spectra and other traffic inputs for INDOT to implement the new pavement design method. Furthermore, the INDOT AADT data were used in this study to analyze the spatial distributions of the traffic volumes in Indiana and to obtain the spatial distributions of traffic volumes.					
17. Key Words Pavement design, axle load spectra, geostatistical analysis, weigh-in-motion, traffic input, traffic volume distribution.			18. Distribution Statement No restrictions. This document is available to the public through the National Technical Information Service, Springfield, VA 22161		
19. Security Classif. (of this report) Unclassified		20. Security Classif. (of this page) Unclassified		21. No. of Pages 101	22. Price

ACKNOWLEDGMENTS

This research project was sponsored by the Indiana Department of Transportation (INDOT) in cooperation with the Federal Highway Administration through the Joint Transportation Research Program. The authors would like to thank the study advisory committee members, Kirk Mangold and Scott A. MacArthur of INDOT Traffic Monitoring Section, for their valuable assistance and technical guidance. The authors would also like to express their appreciations to Dr. Karen Q. Zhu for her great help in data processing and in use of the ArcGIS functions.

TABLE OF CONTENTS

CHAPTER 1: INTRODUCTION	1
CHAPTER 2: WIM DATA PROCESSING	6
CHAPTER 3: TRUCK TRAFFIC AND AXLE LOAD SPECTRA	8
CHAPTER 4: EFFECTS OF UNCLASSIFIED VEHICLES	23
CHAPTER 5: GEOSTATISTICAL ANALYSIS OF INDIANA TRAFFIC DISTRIBUTIONS	27
5.1: Exploring AADT Data	28
5.1.1: Histogram	28
5.1.2: Normal QQ Plot	31
5.1.3: Data Transformation	32
5.2: Variograms	44
5.3: Geostatistical Modeling	49
5.3.1: Kriging Methods:	49
5.3.2: Other Modeling Methods:	65
5.3.3: Comparison of the Modeling Methods:	72
CHAPTER 6: TRAFFIC VOLUME LEVELS AND WIM STATION DISTRIBUTIONS	75
6.1: Traffic Volume Levels and AADT Prediction	75
6.2: Possible Locations of Future WIM Stations	78
CHAPTER 7: CONCLUSIONS	89
REFERENCES	91
APPENDIX: TRAFFIC INPUT AT A WIM STATION	92

CHAPTER 1: INTRODUCTION

The values of equivalent single axle loads (ESAL) have been used to represent the vehicle loads in pavement design (AASHTO 1993). To improve the pavement design procedures, a new method, called the Mechanistic-Empirical Pavement Design Guide (MEPDG) (NCHRP 2004), has been developed to use the axle load spectra to represent the vehicle loads in pavement design. These spectra represent the percentage of the total axle applications within each load interval for single, tandem, tridem, and quad axles. This new pavement design method is a mechanistic-empirical approach to designing pavement structures. It is a radical change from the ESAL based method. The axle load spectra approach quantifies the characteristics of traffic loads by directly using all individual axle loads, instead of converting them into ESAL values. Using axle load spectra as the traffic input, the MEPDG method is able to analyze the impacts of varying traffic loads on pavement and provide an optimal pavement structure design. In addition, the new method can be used to analyze the effects of materials and the impacts of seasons, to compare rehabilitation strategies, and to perform forensic analyses of pavement conditions. The MEPDG utilizes mechanistic-empirical approaches to realistically characterize in-service pavements and allows the full integration of vehicular traffic loadings, climatic features, soil characteristics, and paving materials properties into the detailed analysis of pavement structural behaviors and the resulting pavement performance. Although both approaches are based on the same data sources, the axle load spectra approach is more consistent with the state-of-the-practice method for traffic monitoring outlined in the Traffic Monitoring Guide (FHWA 2001). A crucial

distinction between the MEPDG and the previous 1972, 1986, or 1993 AASHTO Pavement Design Guides is the requirement of data.

Vehicular traffic loading is one of the key factors that may cause pavement fatigue cracking, rutting, and other pavement structural failures and functional distresses. In the previous AASHTO Pavement Design Guides, all vehicular loading are required to be converted into ESAL. However, the MEPDG departs completely from the concept of ESAL because of the strict requirement of detailed loadings for evaluating pavement structural behavior and its effect on pavement performance in different time. The MEPDG uses the full axle load spectra. An advantage of using the axle load spectra over the use of ESAL is that the traffic data requirement is consistent with the state-of-the-practice outlined in the FHWA Traffic Monitoring Guide (TMG). This implies that the historical traffic data collected by state highway agencies, such as weigh-in-motion (WIM) data and automatic vehicle classification (AVC) data, can be utilized to create axle load spectra. Therefore, it becomes possible for a state highway agency to develop a harmonious and integrated traffic databank that may be used not only for the MEPDG, but also for congestion management, planning, regulation, pavement management, and asset management.

The MEPDG provides a hierarchical approach for data inputs. This feature allows state highway agencies to maximize the reliability of pavement design based on the accuracy and variability of data available and the needs and capabilities of highway agencies. The MEPDG defines three levels of traffic data input with respect to the number of days of WIM, AVC, and traffic counts as follows:

1. Level 1: Project/Segment Specific AVC and WIM Measurements. Level 1 uses volume, classification and axle load spectra directly related to the project, and is the most accurate level. In order to import traffic data at the level, highway agencies need to collect and traffic volume, classification, and axle weight data along or near the project to be designed through their AVC and WIM stations. Detailed analysis is required so as to provide the distribution of axle loadings by direction and lane with time for the first year after construction.
2. Level 2: Regional AVC and WIM Measurements. Level 2 uses regional AVC and WIM axle load spectra data and traffic volume and classification data related to the project and provides intermediate accuracy of traffic loading data. In order to provide level 2 input, highway agencies need to gather enough truck traffic information on a related site, such as weekly and seasonal truck traffic and truck load variations. However, the truck weights are determined from regional truck weight summaries by highway agencies.
3. Level 3: Site Specific Vehicle Count Data/Default Regional or Statewide Value. Level 3 uses regional or statewide default vehicle classification and axle load spectra data and provides poor accuracy. At this level, the agencies have only average annual daily traffic (AADT) through site vehicle counters. However, the information pertaining to truck traffic, such as truck percentage, truck distribution, and axle load distribution, is in question.

To prepare the transition from equivalent single-axle loads to load spectra, many studies have been conducted by different states to analyze the effects of the new design method. Buchanan (2004) utilized the long term pavement performance (LTPP) data

from Mississippi sites to determine vehicle class distribution, monthly and hourly distribution factors, and axle load spectra. The truck traffic data in Mississippi showed that the single trailer trucks comprised 70% of the truck traffic on interstates and four-lane highways. However, single-unit trucks were the primary type of trucks on the low volume routes in Mississippi.

Al-Yagout et al. (2005) developed truck axle load spectra using the axle load data collected at WIM stations throughout Washington State. The project concluded that the developed load spectra are reasonable for pavement design. For single axles they are comparable to the MEPDG defaults. For tandem and tridem axles they are slightly more conservative than the defaults.

An Alabama study (Timm, Bower and Turochy 2006) evaluated different load spectra in terms of practical effects on resulting flexible pavement thickness design. The study concluded that statewide load spectra are warranted for use and will not adversely affect most pavement designs.

Haider and Harichandran (2007) presented a methodology for using truck weights and proportions on a highway to estimate individual axle load spectra for various axle configurations. Their study results showed that truck weights and proportions on a highway can be used to estimate individual axle load spectra for various axle configurations. They claimed that it was possible to develop reasonable relationships between truck weights and axle loads.

In a Canadian study (Swan et al. 2008), the truck traffic data, collected as part of periodic commercial traffic surveys, were used to obtain best possible default values for traffic input parameters required for the MEPDG. The researchers compared the default

traffic data inputs included in the MEPDG software and the regional traffic data inputs developed in the study in terms of axle load spectra. They found that the axle load spectra from their study have smaller number of heavily overloaded axles and the peaks between loaded and unloaded axles are more pronounced. They also found that the number and type of trucks, followed by the axle load spectra, have the predominant influence on the predicted pavement performance. The MEPDG contains several input parameters which do not have any significant influence on the predicted pavement performance, such as hourly traffic volume adjustment factors, and axle spacing.

In order to provide the traffic data input required by the MEPDG, the Indiana Department of Transportation (INDOT) made an effort to obtain truck traffic information from the traffic data collected through WIM stations. This study was conducted to create the truck traffic spectra and other traffic inputs for INDOT to implement the new pavement design method. This report presents the results of generated truck traffic information with respect to the requirements of the MEPDG. The characteristics of the truck traffic on Indiana highways include the traffic volumes of various types of trucks, the axle load spectra, axle spacing, and adjustment factors of truck traffic. The adjustment factors include hourly and monthly truck traffic adjustment factors, which are used to reflect the changes of truck traffic at different time periods. Furthermore, the INDOT AADT data were used in this study to analyze the spatial distributions of the traffic volumes in Indiana. The spatial distributions of traffic volumes were obtained to provide INDOT with a 3-dimensional perspective of traffic volumes over entire Indiana; and a basis for determining appropriate locations for future WIM stations.

CHAPTER 2: WIM DATA PROCESSING

The INDOT WIM system consists of 47 WIM sites installed on interstate and other state owned primary highways. The following three types of WIM devices are used in Indiana.

- **Bending Plate:** WIM systems utilize plates with strain gauges bonded to the underside. As a vehicle passes over the bending plate, the system records the strain measured by the strain gauge and calculates the dynamic load. The static load is estimated using the measured dynamic load and calibration parameters.
- **Piezoelectric Sensor:** WIM systems utilize piezo sensors to detect a change in voltage caused by pressure exerted on the sensor by an axle and measure the axle's weight. As a vehicle passes over the piezo sensor, the system records the electrical charge created by the sensor and calculates the dynamic load. The static load is estimated using the measured dynamic load and calibration parameters.
- **Load Cell:** WIM systems utilize a single load cell with two scales to detect an axle and weigh both the right and left side of the axle simultaneously. As a vehicle passes over the two load cell, the system records the weights measured by each scale and sums them to obtain the axle weight.

Among the 47 WIM sites, 23 of them are Piezoelectric Sensor WIM systems, 13 are Bending Plate WIM systems, and the rest are Load Cell WIM systems. All WIM raw data have to be screened for errors before they are put in a database in the form of a monthly traffic data file. A monthly WIM data file generally consists of all traffic

information that is necessary to generate traffic summary reports. The traffic database from the WIM measurements is used for many purposes, including the Long-Term Pavement Performance (LTPP) monitoring, pavement design, truck weight enforcement by Indiana State Police (ISP), and WIM system improvements by the contractors. As part of this study, the database is utilized to develop traffic design inputs for the MEPDG.

The WIM raw data files are binary data files containing all traffic information. In general, the binary data files must be converted into American Standard Code for Information Interchange (ASCII) data files that are usually very large in size. In reality, the potential damages to pavement structures caused by passenger vehicles are negligible. Both the AASHTO method and the MEPDG do not consider the effects of passenger vehicles on pavement structure and only take into account the trucks of Class 4 to Class 13 as defined by FHWA (2001). Therefore, in order to process traffic data for pavement design, pavement engineers only focus on truck traffic information, rather than all of the traffic information in the binary WIM data files.

In order to extract the truck traffic information from the binary WIM data files, the authors utilized the vendor's software to generate the ASCII raw vehicle report (IRD 1999). An ASCII raw vehicle report consists solely of the truck traffic information, including time, lane number, vehicle class, speed, axle weight, and axle spacing. Since an ASCII raw vehicle report file is also large in size, a Visual Basic® computer program was developed to generate traffic inputs required by the MEPDG from the ASCII file.

CHAPTER 3: TRUCK TRAFFIC AND AXLE LOAD SPECTRA

The FHWA vehicle classification defines 13 types of vehicles as shown in Figure 1. Since the first three types of vehicles are not considered in pavement design, only vehicles in Classes 4 through 13 are included in the axle load spectra. The five-year WIM data between 2000 and 2004 were used for the data processing and analysis. All of the required traffic inputs for the MEPDG were obtained from the 47 WIM stations. To illustrate of the axle load spectra, the WIM station on I-74 (at reference marker 169.77) is selected in this report to present the processed traffic data. There are four lanes (two lanes in each direction) at the I-74 site. In the eastbound direction, Lane 1 and Lane 2 represent the driving lane and the passing lane, respectively. In the westbound direction, Lane 3 and 4 represent the driving lane and the passing lane, respectively. The traffic inputs for the MEPDG include the following:

- Average annual daily truck traffic;
- Truck volume monthly adjustment factors;
- Truck volume lane distribution factors;
- Truck volume directional distribution factors;
- Truck volume class distributions;
- Traffic volume hourly distribution factors;
- Single-axle load distributions;
- Tandem-axle load distributions;

- Tridem-axle load distributions;
- Quad-axle load distributions;
- All-axle load distributions;
- Average axle weight (kips) and average axle spacing (inches); (Note: 1.0 kip = 1,000 pounds)
- Average number of axle types.

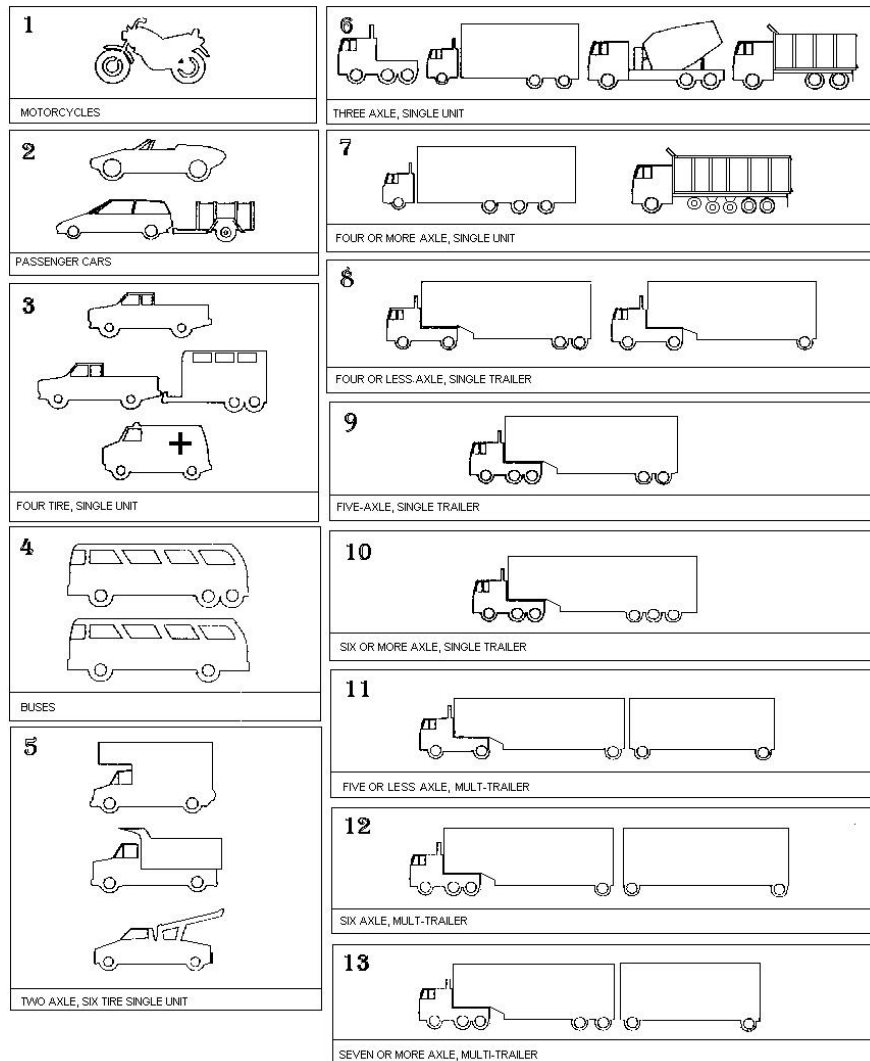


Figure 1: FHWA Vehicle Classifications

An important traffic input for the MEPDG is the average annual daily truck traffic (AADTT). The obtained values of the truck traffic are in the forms of average monthly daily truck traffic (AMDTT) and average hourly truck traffic (AHTT) of a year. Table 1 presents the monthly AMDTT values at the I-74 WIM station. It should be noted that the average values shown in the last row of Table 1 are the values of AADTT of the

corresponding lanes. With the AMDTT values, the monthly adjustment factors (MAF) can be calculated by the following equation (NCHRP 2004):

$$MAF_i = \frac{AMDDT_i}{\sum_{j=1}^{12} AMDDT_j} \times 12 \quad (1)$$

where:

MAF_i: monthly adjustment factor for month i.

AMDDT_i: average monthly daily truck traffic for month i.

Table 1: Monthly Truck Traffic at I-74 WIM Site

Monthly ADTT				
	Lane 1	Lane 2	Lane 3	Lane 4
January	2557	344	2462	489
February	2840	385	2616	492
March	3136	418	2915	555
April	3398	452	3317	1616
May	3715	458	3919	1494
June	4353	515	4660	1599
July	3920	529	4518	1614
August	3739	524	4153	1627
September	3562	488	3886	1551
October	3073	440	3116	1500
November	2802	428	2814	1454
December	2632	464	2689	1538
Average	3311	454	3422	1294

Figure 2 shows the monthly adjustment factors calculated with the data in Table 1. The MEPDG uses MAF values as an input to reflect the monthly and seasonal effects of truck traffic on pavement performance. Therefore, MAF values will certainly affect the results of pavement designs.

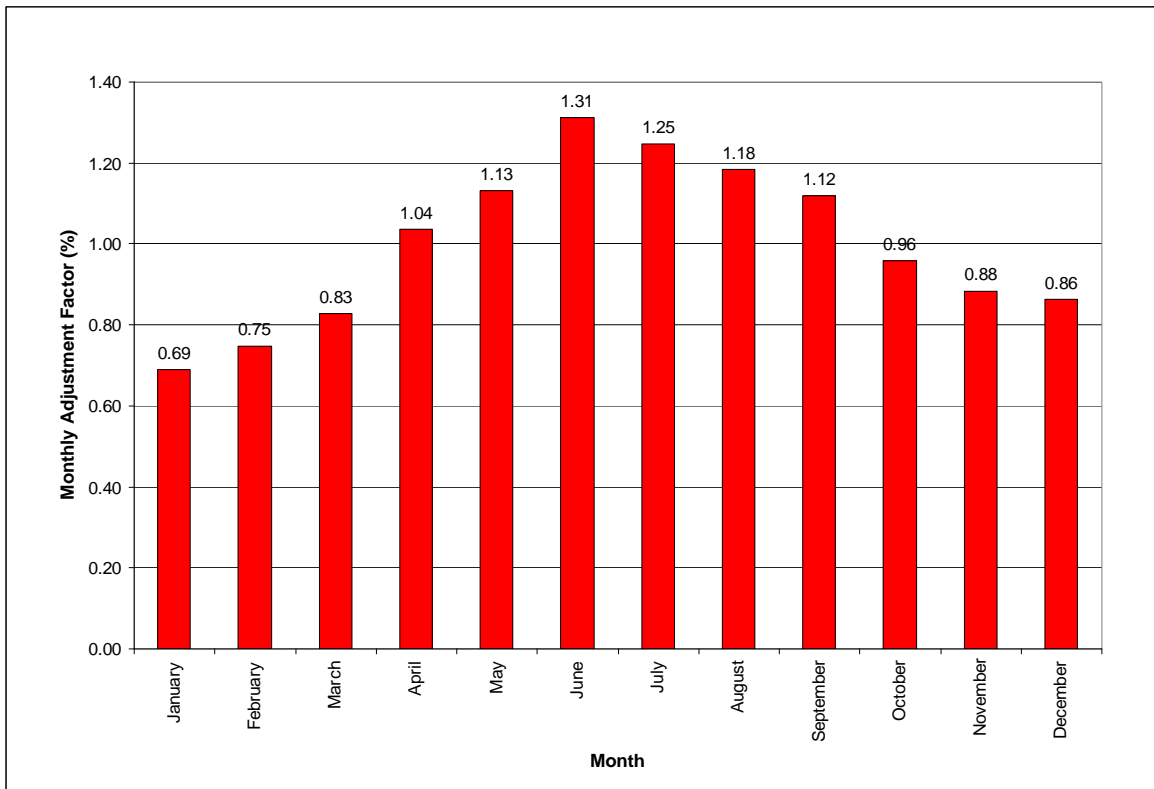


Figure 2: Monthly Adjustment Factors

Similarly, the values of AHTT were also obtained. The values of hourly truck volumes at the I-74 WIM station are graphically shown in Figure 3. The variations of the hourly truck volumes at the site can be clearly seen in the graph. Based on the average hourly truck traffic, the hourly distributions factors were calculated as shown in Figure 4. The hourly distribution factors are the percentages of truck traffic at each hour out of the total truck volume during a 24-hour period.

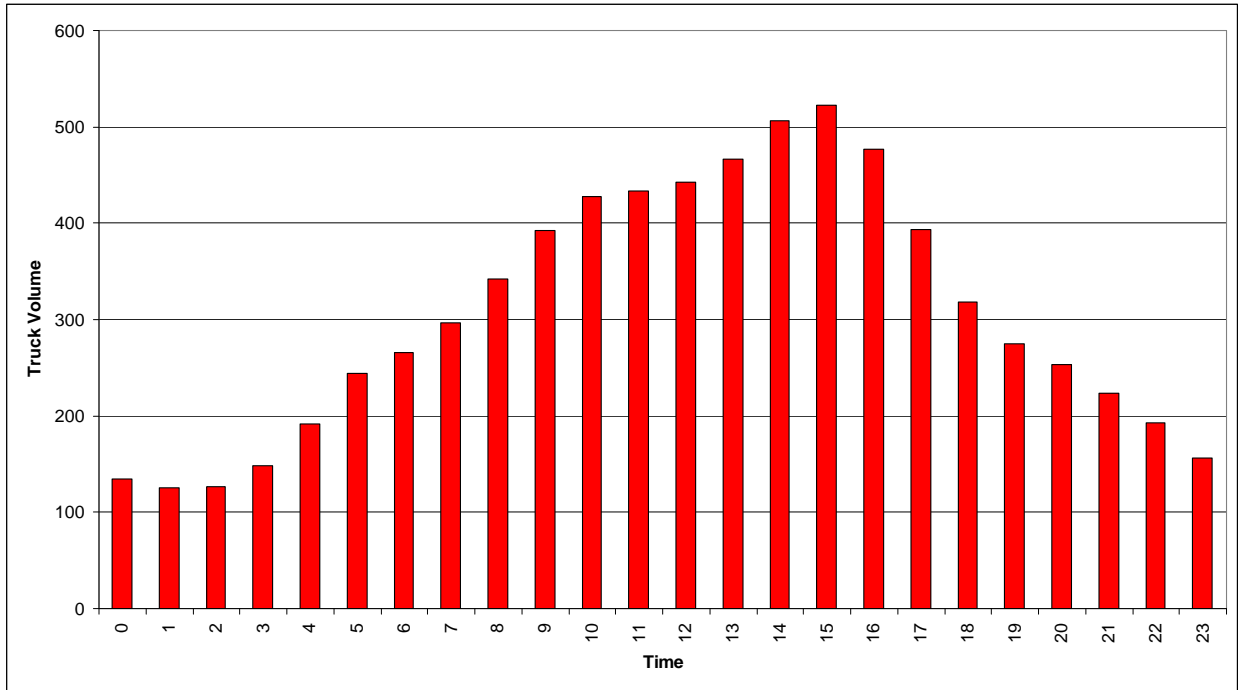


Figure 3: Hourly Truck Volumes

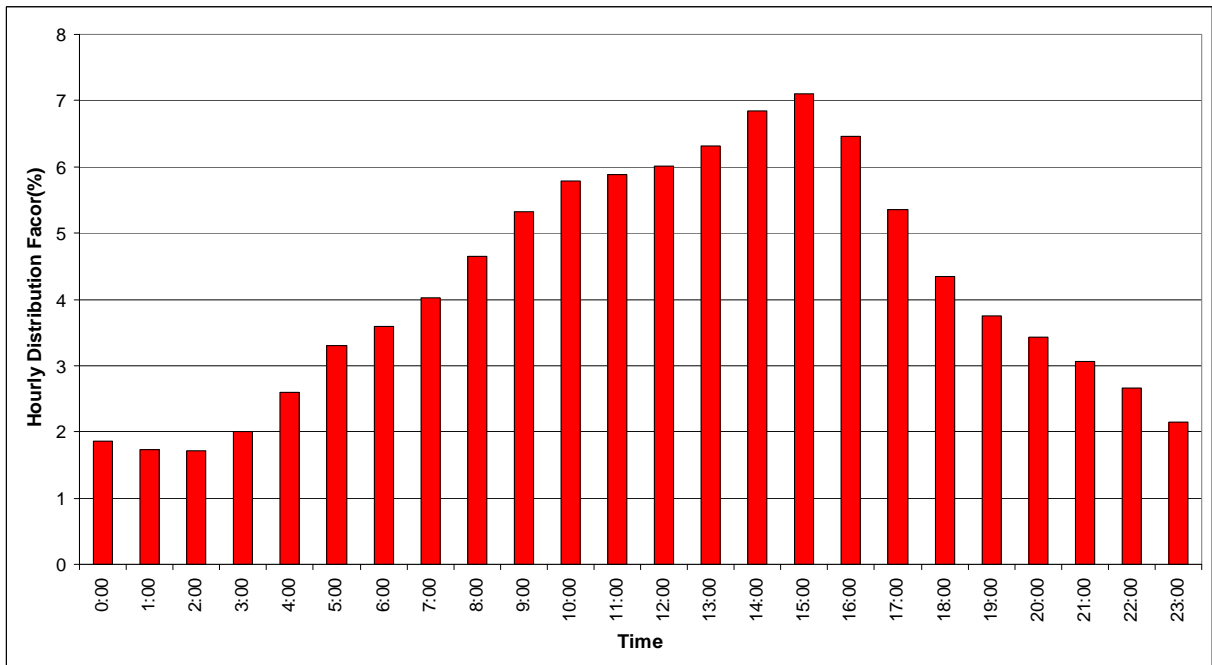


Figure 4: Hourly Distribution Factors of Truck Traffic

In addition to the AADTT, the MEPDG requires information on the components of truck traffic based on the FHWA vehicle classifications. The truck components are represented by the percent of each truck type. The truck classifications at the I-74 WIM station are illustrated in Figure 5, where C_i means the i th vehicle class of the FHWA vehicle classifications and C_0 represents unclassified vehicles. The unclassified vehicles are those that the WIM device failed to identify their vehicle types based on the integrated criteria. They include only the number of unclassified vehicles without any other measurements such as axle loads and axle spaces. The quantities of unclassified vehicles have great effect on pavement design. There are many possible reasons for a vehicle not to be classified, such as vehicle tailgating, lane changing, and irregular vehicle size. An unreasonably large value of unclassified vehicles (C_0) usually indicates that the WIM device is not working properly. Currently, there are no specified threshold values for normal range of unclassified vehicles. The truck classifications in Figure 5 indicate that most of the trucks belong to Class 9, followed by Class 5 vehicles. In fact, this is also true for all of the 47 WIM sites in Indiana. Li et al. (2005) found that the volume of Class 9 vehicles and the total ESAL value on Indiana highways have a highly correlated linear relationship. The truck volumes of the vehicle types in each month are presented in Table 2.

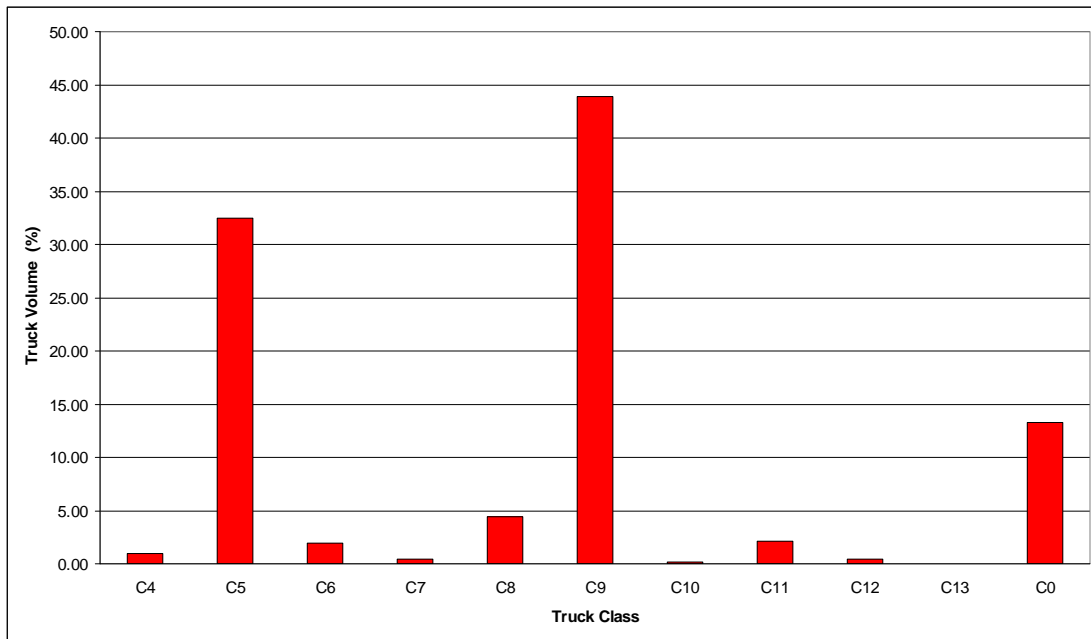


Figure 5: Truck Classification Distribution

Table 2: Average Monthly Daily Truck Volumes

Month	Vehicle Class										
	C4	C5	C6	C7	C8	C9	C10	C11	C12	C13	C0
Jan	32	1006	233	21	240	2420	10	124	19	5	1743
Feb	39	1159	208	18	227	2418	9	119	18	2	2118
Mar	51	1581	340	13	372	2782	10	149	22	0	1704
Apr	103	2886	128	21	389	4195	17	201	41	0	803
May	113	3793	131	48	434	3971	12	191	40	0	853
Jun	108	4820	142	53	490	4282	17	207	44	0	963
Jul	97	4656	130	57	480	3957	13	193	39	0	959
Aug	102	3841	141	50	469	4228	17	202	40	0	953
Sep	107	3353	122	54	445	4261	16	197	41	0	891
Oct	102	2297	119	43	361	4150	14	199	41	0	803
Nov	94	1851	123	31	287	4141	15	185	39	0	732
Dec	76	1772	123	27	267	3836	12	174	33	0	1004
Total	1023	33016	1941	435	4461	44640	162	2141	416	8	13524

Distributions of truck traffic on roadway lanes and in travel directions are also required by the MEPDG. The total truck volume and truck volumes on the four lanes at the I-74 WIM station are depicted in Figure 6. Based on the data in Figure 6, the lane distribution factors of truck traffic can be computed as shown in Figure 7. A lane

distribution factor in Figure 7 is the proportion of the vehicles on the travel lane. For example, the lane distribution factor of 0.94 for Class 9 vehicles in the east bound direction means that 94% of the Class 9 vehicles were on the driving lane and 6% of the vehicles were on the passing lane. Similarly, the directional distribution factors can be obtained as shown in Figure 8. A directional distribution factor represents the higher percent of a given vehicle type among the two travel directions of the roadway. For example, in Figure 8 the directional distribution factor of 0.92 for C7 means that 92% of the Class 7 vehicles traveled in one direction of the roadway and 8% of the Class 7 vehicles traveled in the opposite direction of the roadway.

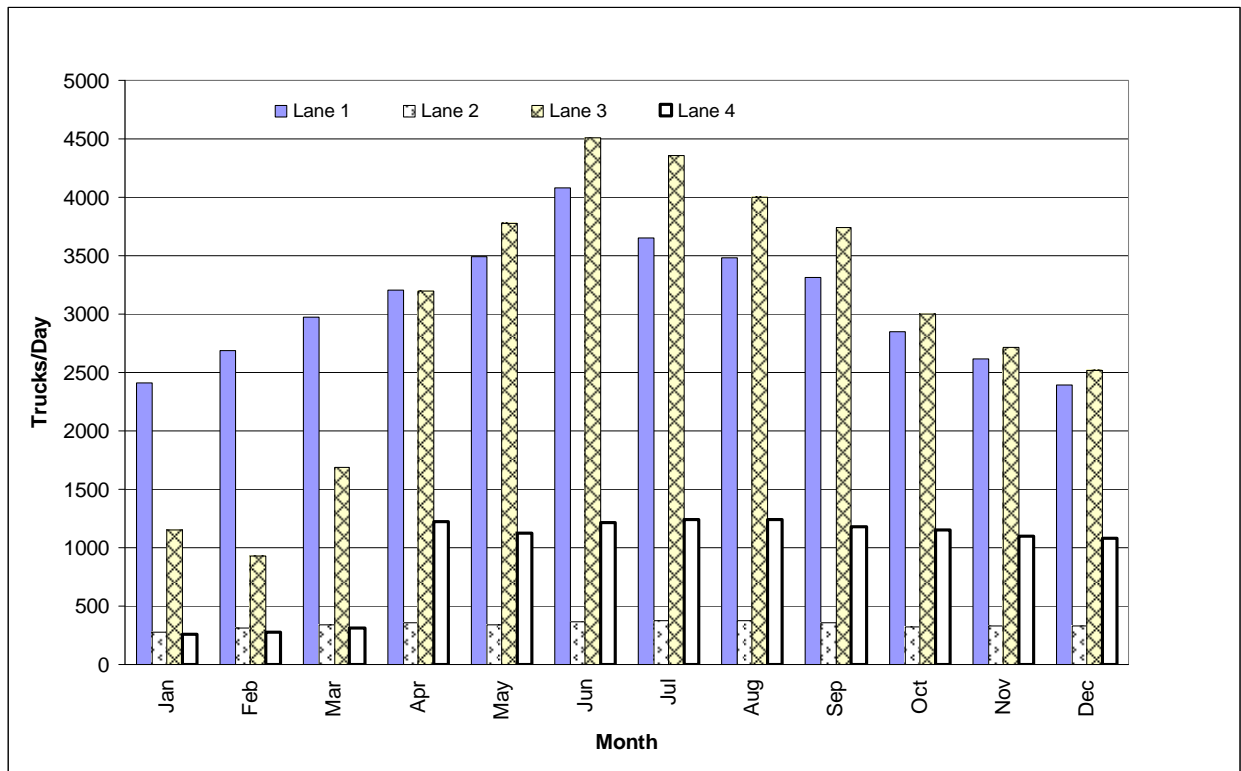


Figure 6: Truck Traffic Distributions on Highway Lanes

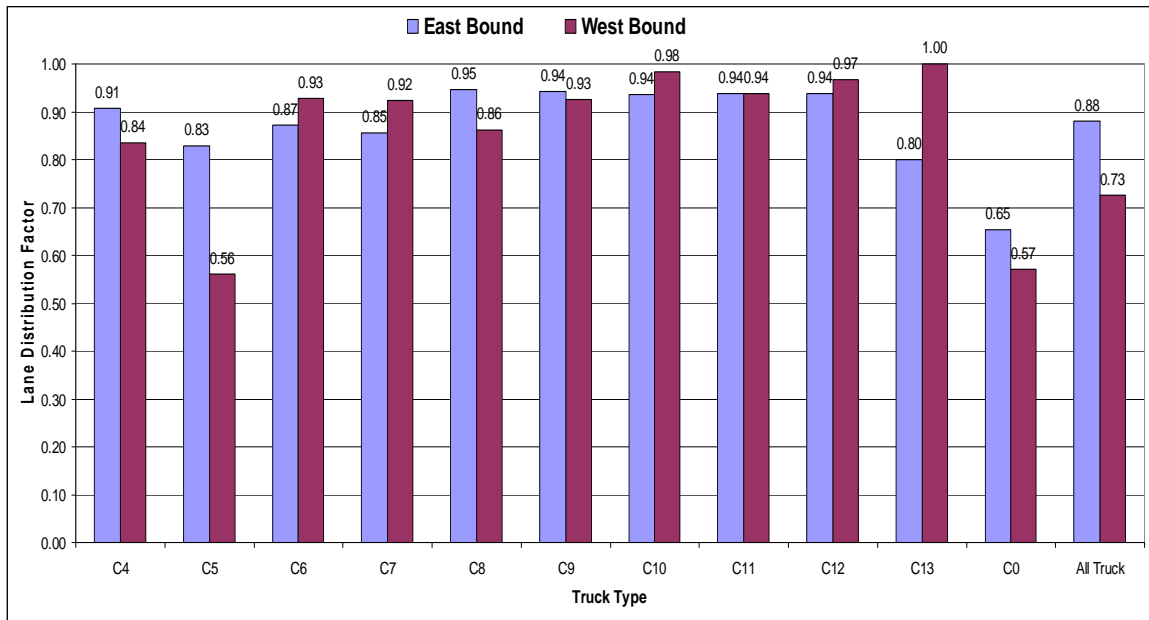


Figure 7: Lane Distribution Factors

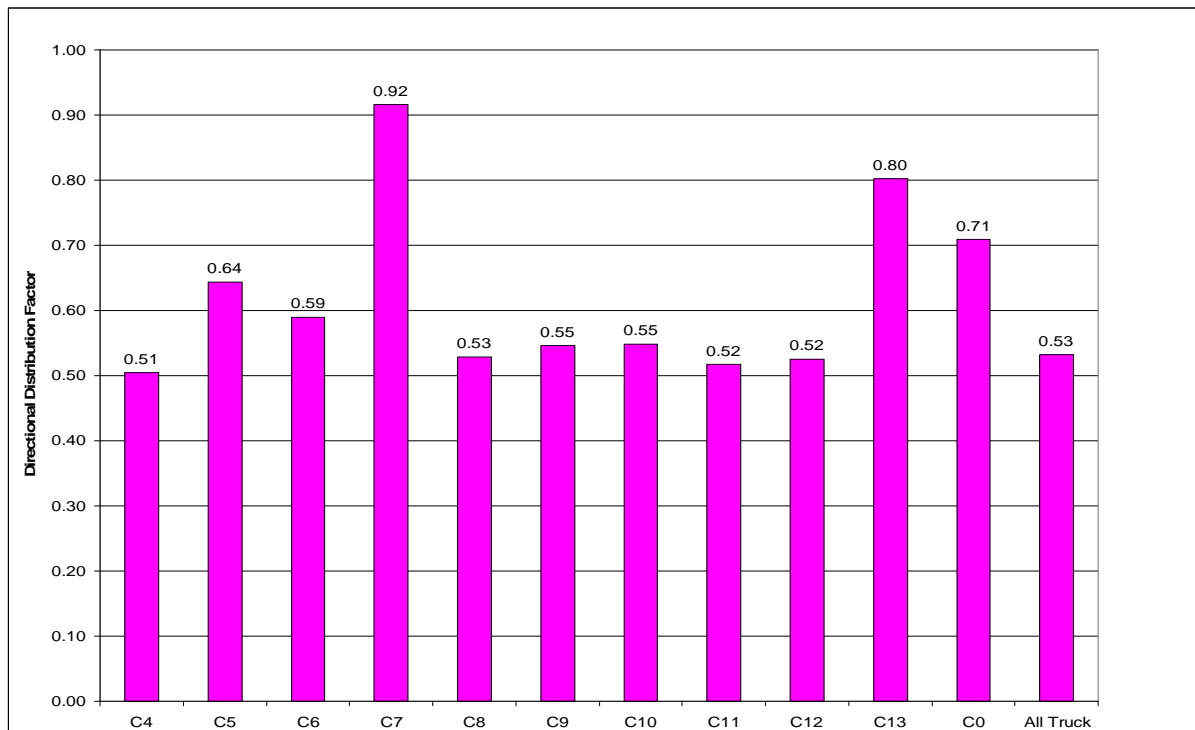


Figure 8: Truck Traffic Directional Distribution Factors

Through processing the WIM data files, the values of average axle weights, average axle spacing, and average numbers of axle types were obtained as part of the requirements for the MEPDG. Table 3 presents these values for the I-74 WIM station. In the table, W_i denotes the average weight of the i th axle of the vehicle class, S_{ij} is the average spacing between the i th and j th axles, and the low part of the table shows the average numbers of a particular type of axles (single, tandem, etc.) per vehicle. For example, from Table 3 the following values can be seen for the vehicles in Class 4:

- They have three axles with average weights of 14.70 kips (W_1), 13.88 kips (W_2), and 9.26 kips (W_3).
- The average axle spacing is 23.18 inches between the first and second axles (S_{12}) and 3.70 inches between the second and third axles (S_{23}).
- The average number of single axles is 1.78 per vehicle, and the average number of tandem axles is 0.22 per vehicle.

The number of average axle weights in the table implies the maximum number of axles in each class of trucks. As indicated in Table 3, the maximum number of axles of Class 5 vehicles is two because there are only two weights (W_1 and W_2), while the maximum number of axles of Class 13 vehicles is nine because there are nine weights (W_1 through W_9).

Table 3: Average Axle Weight (kips), Axle Spacing (inches), and Number of Axle Types by Vehicle Classes

Weight	Vehicle Classes									
	C4	C5	C6	C7	C8	C9	C10	C11	C12	C13
W1	14.70	5.33	7.78	9.44	8.51	8.44	8.08	8.60	9.62	6.66
W2	13.88	5.12	6.20	7.55	10.98	6.14	5.81	12.21	7.23	5.59
W3	9.26		6.20	7.51	10.03	6.00	5.71	12.88	7.66	5.77
W4				7.73	6.64	5.76	4.97	11.25	9.71	5.19
W5				4.39		5.73	4.90	11.31	11.35	5.57
W6							5.24		8.74	7.08
W7							2.47			6.31
W8										7.79
W9										4.20
Spacing										
S12	23.18	13.06	18.97	5.68	12.35	13.88	13.85	10.42	12.58	9.45
S23	3.70		3.24	20.55	18.41	3.93	3.64	17.62	4.05	5.28
S34				3.35	14.91	27.22	19.77	7.94	17.31	7.50
S45				1.85		4.21	5.67	17.98	8.78	10.96
S56							3.50		18.88	6.27
S67							1.88			5.62
S78										5.09
S89										3.58
Axle Type										
Single	1.78	2.00	1.00	1.75	2.36	1.27	1.05	4.74	3.72	2.10
Tandem	0.22		1.00	0.75	0.63	1.86	1.03	0.08	1.09	1.08
Tridem				0.12			0.92	0.03	0.02	0.45
Quad				0.12			0.02		0.01	0.15
Quinate										0.05
Hex							0.01			0.14

The magnitudes of axle loads are a major parameter for pavement design. To quantify axle loads, the MEPDG requires the axle load distributions for all classes of trucks. The axle load distributions are the percentages of axle loads in specified weight intervals, such as zero to three kips, three to four kips, and four to five kips. The axle load distributions include the axle weights for all-axle loads, single-axle loads, tandem-axle loads, tridem-axle load, quad-axle loads, quinate-axle loads, and hex-axle loads. It should be pointed out that the MEPDG does not require the information on axle load

distributions for quinate-axle and hex-axle loads. However, because the Indiana WIM data contain the values of quinate-axle and hex-axle loads, it would not require any extra effort to include these two types of axle loads in the computer program used in this study to extract and calculate axle load distributions. Thus, it was decided to generate the distributions for these axle loads as well for possible future use. The values of the all-axle load and single-load axle load distributions are shown in Tables 4 and 5, respectively. The values in the two tables are the percentages of the vehicle classes with axle loads within the given load ranges. For example, in Table 4, the value corresponding to vehicle class C4 and axle load range 0-3 is 3.82; meaning that 3.82% of Class 4 vehicles have axle loads less than 3 kips. Similarly, in Table 4 the value 5.37 (corresponding to C4 and axle load 3-4) indicates that 5.37% of Class 4 vehicles have axle load between 3 kips and 4 kips.

Traffic input information was obtained from the WIM recorded traffic data for all of the 47 WIM stations. The complete traffic input for the MEPDG at the I-74 WIM site is included in the appendix of this report in order to show the format and information on the truck traffic. Because of the large size of the files, the traffic input information from other WIM stations is not included in the appendix.

Table 4: All-Axle Load Distribution (Percentages) for Each Truck Class

Axle Load Range (kips)	Vehicle Classes									
	C4	C5	C6	C7	C8	C9	C10	C11	C12	C13
0-3	3.82	26.47	42.37	20.17	18.02	28.43	25.52	9.90	5.83	7.05
3-4	5.37	12.00	15.60	17.67	9.92	21.70	13.50	13.65	14.10	18.47
4-5	7.62	7.12	12.37	14.33	8.98	14.45	11.82	14.30	16.78	14.75
5-6	9.40	5.87	9.37	10.83	7.40	10.30	10.58	13.42	13.37	14.67
6-7	14.87	5.45	6.33	7.20	6.67	6.92	7.68	10.45	9.83	8.52
7-8	14.33	7.15	3.93	6.27	6.27	4.50	5.83	7.87	6.60	5.97
8-9	11.18	2.88	2.77	5.07	5.22	2.90	4.83	6.28	5.32	7.83
9-10	7.53	2.43	2.07	4.10	4.37	2.02	3.85	4.90	4.12	4.55
10-11	6.12	1.18	1.53	2.67	3.42	1.52	3.28	3.55	3.03	3.30
11-12	4.12	4.63	1.00	1.80	3.10	1.15	2.72	3.05	2.43	3.48
12-13	2.18	2.17	0.57	1.37	2.40	0.88	1.85	2.47	1.98	2.12
13-14	2.13	2.17	0.33	1.37	1.98	0.65	1.42	1.68	1.50	1.67
14-15	1.22	4.88	0.27	1.37	1.80	0.50	1.22	0.90	1.22	1.47
15-16	1.58	1.53	0.13	0.97	1.63	0.38	0.95	1.17	1.13	1.00
16-17	1.32	0.65	0.20	0.90	1.43	0.30	0.65	0.63	0.90	1.18
17-18	1.32	1.28	0.07	1.10	1.05	0.22	0.50	0.98	0.80	0.82
18-19	0.50	3.12	0.03	0.33	1.12	0.20	0.45	0.77	0.68	0.42
19-20	0.05	1.85	0.03	0.43	0.97	0.17	0.35	0.72	0.67	0.25
20-21	0.92	0.00	0.00	0.40	0.88	0.13	0.33	0.17	0.60	0.27
21-22	0.80	0.00	0.00	0.17	0.90	0.10	0.27	0.30	0.55	0.37
22-23	0.03	0.00	0.00	0.27	0.80	0.10	0.18	0.27	0.48	0.28
23-24	0.85	0.63	0.00	0.03	0.72	0.10	0.17	0.27	0.48	0.13
24-25	0.25	0.00	0.00	0.07	0.72	0.08	0.12	0.27	0.47	0.22
25-26	0.05	0.00	0.00	0.03	0.55	0.08	0.12	0.17	0.42	0.03
26-27	0.25	0.00	0.00	0.13	0.53	0.08	0.08	0.05	0.37	0.03
27-28	0.00	0.00	0.00	0.00	0.48	0.08	0.03	0.03	0.38	0.02
28-29	0.00	0.00	0.00	0.03	0.43	0.05	0.03	0.05	0.35	0.02
29-30	0.00	1.27	0.00	0.00	0.50	0.05	0.03	0.03	0.35	0.07
30-31	0.00	0.00	0.00	0.07	0.45	0.05	0.03	0.08	0.33	0.00
31-32	0.00	0.00	0.00	0.00	0.45	0.05	0.00	0.10	0.32	0.00
32-33	0.00	0.00	0.00	0.00	0.38	0.05	0.02	0.00	0.30	0.00
33-34	0.00	0.00	0.00	0.00	0.38	0.03	0.02	0.00	0.27	0.00
34-35	0.00	1.85	0.00	0.00	0.40	0.03	0.00	0.00	0.25	0.00
35-36	0.00	0.00	0.00	0.00	0.30	0.03	0.03	0.00	0.25	0.00
36-37	0.00	0.00	0.00	0.00	0.35	0.03	0.02	0.03	0.22	0.00
37-38	0.00	1.27	0.00	0.00	0.35	0.03	0.00	0.02	0.22	0.00
38-39	0.00	0.00	0.00	0.00	0.35	0.02	0.00	0.00	0.22	0.00
39-40	0.00	0.00	0.00	0.00	0.33	0.03	0.00	0.02	0.18	0.00
40-41	1.23	1.27	0.00	0.10	2.52	0.28	0.12	0.22	1.48	0.02

Table 5: Single-Axle Load Distribution (Percentages) for Each Truck Class

Axle Load Range (kips)	Vehicle Classes									
	C4	C5	C6	C7	C8	C9	C10	C11	C12	C13
0-3	0.59	51.34	14.72	2.07	5.61	3.52	2.31	0.14	0.23	0.20
3-4	0.38	20.56	3.28	4.30	12.30	3.34	2.17	4.30	4.08	7.08
4-5	0.47	10.23	4.11	3.48	10.63	3.79	3.15	6.14	6.09	9.96
5-6	0.89	5.09	4.65	3.44	9.59	4.60	4.61	7.67	8.62	9.76
6-7	8.06	3.22	5.25	3.42	9.13	5.92	7.22	8.84	9.55	9.18
7-8	14.35	2.27	6.81	4.00	9.24	8.29	10.22	10.38	11.30	9.07
8-9	14.31	1.69	9.18	4.83	8.52	11.77	14.19	11.28	12.01	9.43
9-10	12.70	1.25	11.13	5.96	7.00	15.83	17.16	10.33	11.71	9.59
10-11	10.64	0.90	10.00	6.34	5.27	15.00	15.03	8.87	9.89	9.43
11-12	8.58	0.64	7.18	7.19	3.88	10.13	10.29	6.93	7.74	6.24
12-13	6.45	0.46	4.95	7.59	2.93	5.77	5.41	5.45	5.50	4.64
13-14	4.74	0.34	3.42	7.78	2.32	3.00	2.42	4.60	4.00	3.24
14-15	3.54	0.27	2.56	7.16	1.93	2.04	1.55	3.69	2.72	2.05
15-16	2.64	0.22	2.03	6.75	1.63	1.68	1.09	2.95	1.90	1.81
16-17	2.07	0.18	1.75	5.92	1.33	1.40	0.79	2.27	1.31	2.13
17-18	1.59	0.15	1.52	5.48	1.12	1.09	0.58	1.64	0.99	2.18
18-19	1.25	0.13	1.29	4.35	0.92	0.79	0.43	1.18	0.65	1.35
19-20	0.97	0.11	1.04	3.00	0.75	0.54	0.30	0.84	0.49	0.54
20-21	0.87	0.10	0.90	1.74	0.64	0.37	0.23	0.59	0.27	0.43
21-22	0.65	0.09	0.73	1.11	0.52	0.25	0.17	0.38	0.25	0.32
22-23	0.50	0.08	0.61	0.72	0.45	0.18	0.12	0.26	0.13	0.29
23-24	0.43	0.07	0.51	0.61	0.39	0.13	0.11	0.17	0.10	0.21
24-25	0.38	0.07	0.41	0.42	0.35	0.10	0.08	0.13	0.08	0.17
25-26	0.31	0.06	0.34	0.35	0.31	0.08	0.07	0.11	0.05	0.14
26-27	0.25	0.06	0.29	0.27	0.28	0.07	0.05	0.08	0.04	0.07
27-28	0.25	0.05	0.24	0.21	0.26	0.05	0.05	0.09	0.04	0.08
28-29	0.20	0.05	0.21	0.28	0.24	0.04	0.04	0.08	0.04	0.09
29-30	0.22	0.05	0.17	0.17	0.22	0.04	0.03	0.07	0.03	0.05
30-31	0.14	0.04	0.14	0.14	0.21	0.03	0.03	0.04	0.03	0.05
31-32	0.16	0.04	0.11	0.16	0.19	0.02	0.02	0.05	0.02	0.05
32-33	0.18	0.03	0.08	0.13	0.18	0.02	0.02	0.04	0.02	0.03
33-34	0.11	0.03	0.06	0.13	0.17	0.02	0.01	0.05	0.02	0.03
34-35	0.12	0.03	0.05	0.08	0.16	0.02	0.01	0.03	0.02	0.02
35-36	0.11	0.02	0.04	0.07	0.15	0.01	0.01	0.04	0.02	0.01
36-37	0.10	0.01	0.04	0.06	0.13	0.01	0.01	0.03	0.02	0.02
37-38	0.10	0.01	0.03	0.09	0.12	0.01	0.01	0.03	0.01	0.01
38-39	0.12	0.01	0.03	0.05	0.12	0.01	0.00	0.03	0.01	0.01
39-40	0.10	0.01	0.03	0.04	0.11	0.01	0.01	0.02	0.01	0.01
40-41	0.54	0.06	0.15	0.15	0.72	0.05	0.03	0.17	0.03	0.03

CHAPTER 4: EFFECTS OF UNCLASSIFIED VEHICLES

As previously mentioned, the WIM data contained vehicles that could not be classified by the WIM device. The possible reasons for this include vehicle tailgating, lane changing, irregular vehicle size, and WIM equipment problems. These unclassified vehicles could be any types of vehicles, including passenger cars, buses, and trucks. How to deal with these vehicles will undoubtedly affect pavement designs because it will result in different truck traffic inputs. For instance, if all of the unclassified vehicles are treated as trucks, the total axle loads will be overestimated. On the other hand, if they are not included in the truck traffic, the total axle loads will be underestimated. One reasonable way to deal with this is to assign them to different vehicle groups, but to do this one needs to know the proportions of the vehicle types in the unclassified vehicles. However, the proportions are currently not available.

In order to analyze the effects of unclassified vehicles, various amounts of unclassified vehicle volumes were added to the total truck volumes of the five-year WIM data to examine the patterns of the truck traffic. If all of the unclassified vehicles are disregarded, then the total truck volumes and the truck volumes of individual types of trucks are as shown in Figure 9. The regression equation of the total AADTT values is also shown in the figure. If 100% of the unclassified vehicles are vehicles, the total AADTT will be increased by the amount of unclassified vehicles (C_0). Similarly, analysis can be done by adding 50% and 25% of the unclassified vehicles to the truck volumes. The truck traffic patterns and regression equations with 100%, 50%, and 25% of included unclassified vehicles are plotted in Figures 10, 11, and 12, respectively.

It is apparent that the truck volumes, patterns, and regression equations are all significantly different when different amounts of unclassified vehicles are included in the truck traffic. Consequently, pavement designs with these different truck volumes will certainly be very different. Therefore, it is essential to obtain more accurate estimation of proportions of different types of vehicles in the unclassified vehicle category. To determine the components of unclassified vehicles, research is being undertaken using image processing techniques to study the patterns of unclassified vehicles recorded by WIM devices. It is hoped that the study will yield useful results to improve the truck traffic inputs for the MEPDG.

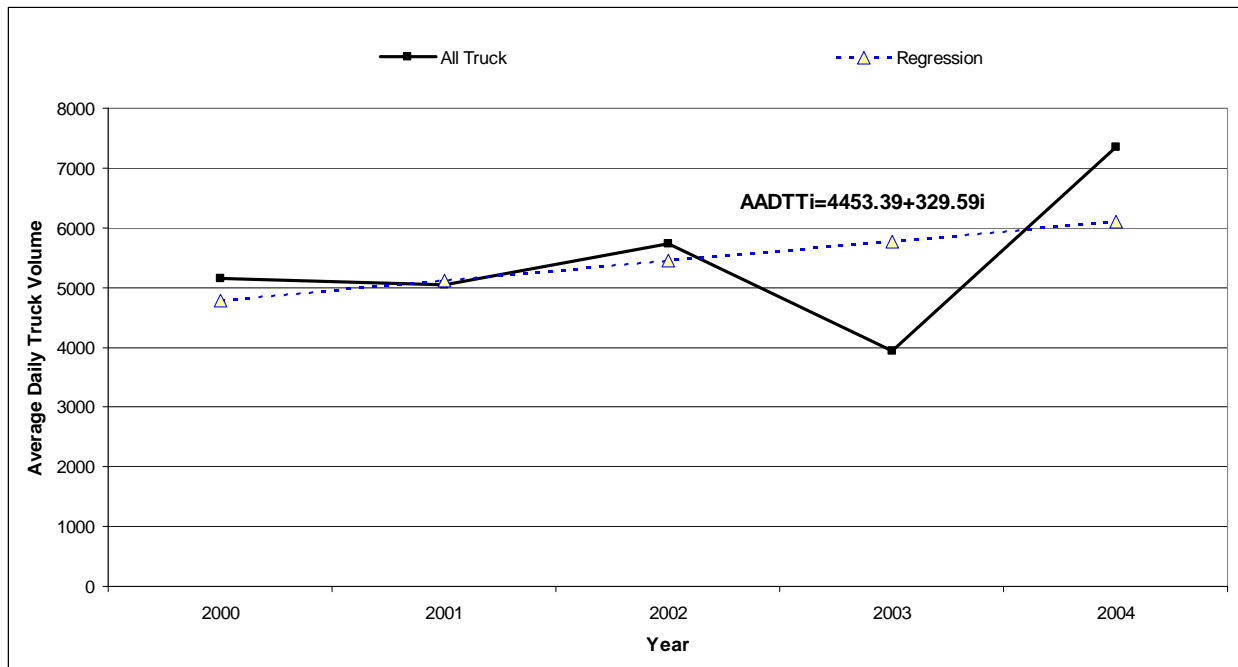


Figure 9: Average Daily Truck Traffic (no unclassified vehicles)

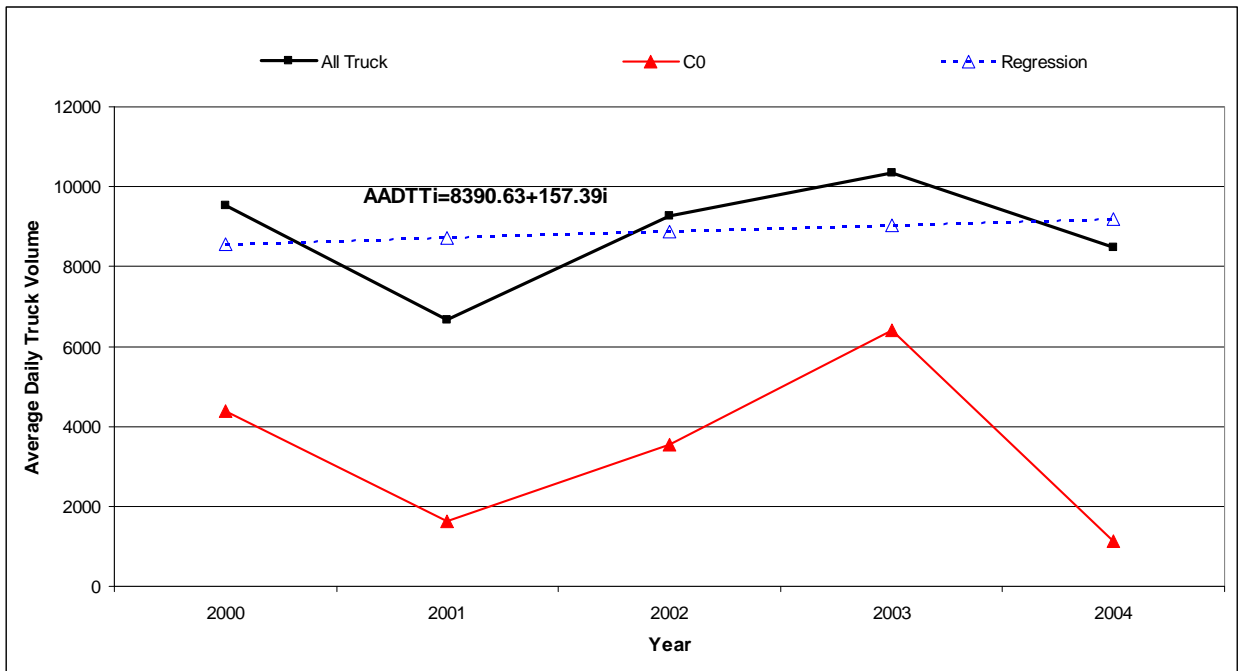


Figure 10: Average Daily Truck Traffic (including all unclassified vehicles)

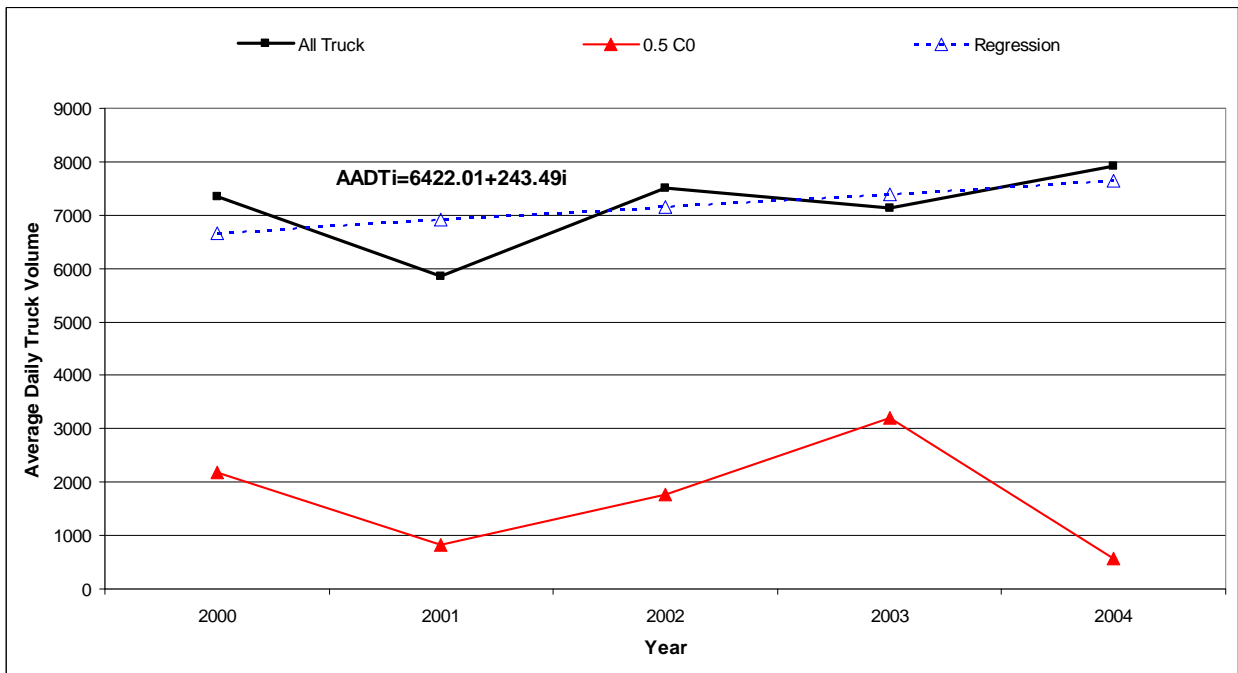


Figure 11: Average Daily Truck Traffic (including 50% unclassified vehicles)

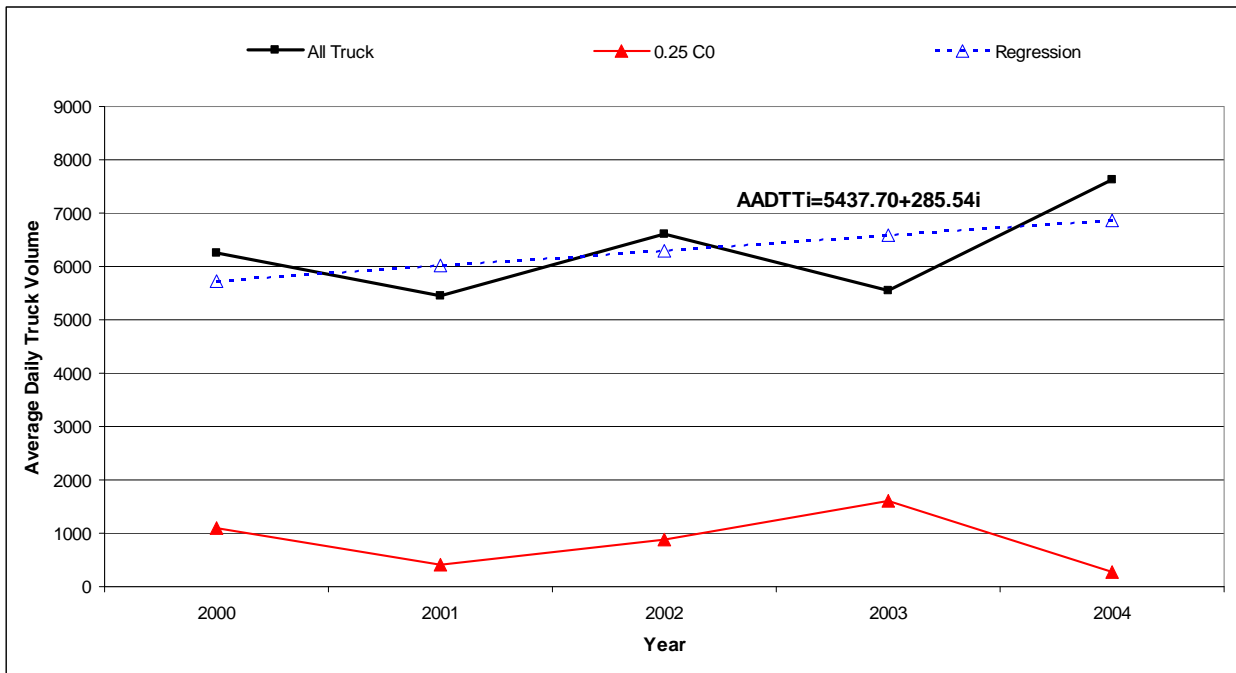


Figure 12: Average Daily Truck Traffic (including 25% unclassified vehicles)

CHAPTER 5: GEOSTATISTICAL ANALYSIS OF INDIANA TRAFFIC DISTRIBUTIONS

In addition to the WIM data analysis that resulted in the required truck traffic input for the MEPDG, the traffic volumes recorded by INDOT were analyzed using ArcGIS, a powerful GIS software, to examine the spatial distribution of traffic volumes over Indiana. The spatial distributions of traffic volumes were obtained to provide INDOT with (1) a 3-dimensional perspective of traffic volumes over entire Indiana; and (2) a basis for determining appropriate WIM locations. The Indiana highway GIS map was provided by the INDOT Traffic Monitoring Section. The INDOT GIS map contains Indiana's highway systems with traffic volumes at the traffic monitoring stations. ArcGIS 9.2 (ESRI 2007) was used in the analysis of the spatial distributions of traffic volumes. ArcGIS 9.2 applies the interpolation techniques in its Geostatistical Analyst. Geostatistical Analyst uses sample points taken at different locations in a landscape and creates (interpolates) a continuous surface. The sample points in this study are the traffic volumes at the INDOT traffic monitoring stations. Geostatistical Analyst derives a surface using the traffic volume values from the traffic monitoring stations to predict values for each location in the landscape. Geostatistical techniques rely on both statistical and mathematical methods that can be used to create surfaces and assess the uncertainty of the predictions. Geostatistical Analyst, in addition to providing various interpolation techniques, also provides many supporting tools. For example, prior to mapping, Exploratory Spatial Data Analysis (ESDA) Tools can be used to assess the statistical properties of the data. After exploring the data, one can create a variety of

output map types (prediction, error of prediction, probability and quantile) using various geostatistical algorithms and associated tools.

5.1: Exploring AADT Data

The traffic volume data contained in the INDOT GIS map are the average annual daily traffic (AADT) in 2004. In order to conduct geostatistical analysis, the traffic data should be examined to determine their characteristics. The geostatistical methods that are used to generate a 3-D surface give the best results if the data is normally distributed (a bell-shaped curve). If the data is skewed (lopsided), one may choose to transform the data to make it normal. Thus, it is important to understand the distribution of the AADT data before conducting geostatistical analysis. The Histogram tool in ArcGIS plots frequency histograms for the attributes in the dataset. Therefore, the histograms of INDOT traffic volume data were plotted to examine if the AADT data satisfy the normal distribution requirement. The Indiana AADT dataset contains a great deal of data points. It was found that the large amount of AADT data often overloaded the ArcGIS software and caused operational problems for the software. To reduce the amount of data for ArcGIS to run properly, only the AADT at the middle point of a segment of highway was selected to represent the AADT of the highway. This is reasonable because the AADT values are generally similar along a section of highway.

5.1.1: Histogram

The Histogram tool in ESDA provides a univariate (one-variable) description of the data. The tool displays the frequency distribution for the dataset of interest and

calculates summary statistics that describe the distribution's location, spread, and shape. The frequency distribution is a bar graph that displays how often observed values fall within certain intervals or classes. The number of classes of equal width must be specified first for the histogram. The relative proportion of data that falls in each class is represented by the height of each bar. The important features of a distribution can be summarized by the following summary statistics that describe its location, spread, and shape (ESRI 2007).

- **Measures of location:** Measures of location provide you with an idea of where the center and other parts of the distribution lie. The mean is the arithmetic average of the data. The mean provides a measure of the center of the distribution. The median value corresponds to a cumulative proportion of 0.5. If the data was arranged in increasing order, 50 percent of the values would lie below the median, and 50 percent of the values would lie above the median. The median provides another measure of the center of the distribution. The 1st and 3rd quartiles correspond to the cumulative proportion of 0.25 and 0.75, respectively. If the data was arranged in increasing order, 25 percent of the values would lie below the first quartile, and 25 percent of the values would lie above the third quartile. The 1st and 3rd quartiles are special cases of quantiles.
- **Measures of spread:** The spread of points around the mean value is another characteristic of the displayed frequency distribution. The variance of the data is the average squared deviation of all values from the mean. The units are the square of the units of the original measurements and, because it involves squared differences, the calculated variance is sensitive to unusually high or low values.

The standard deviation is the square root of the variance. It describes the spread of the data about the mean in the same units as the original measurements. The smaller the variance and standard deviation, the tighter the cluster of measurements about the mean value.

- ***Measures of shape***: The frequency distribution is also characterized by its shape. The coefficient of skewness is a measure of the symmetry of a distribution. For symmetric distributions, the coefficient of skewness is zero. If a distribution has a long right tail of large values, it is positively skewed, and if it has a long left tail of small values, it is negatively skewed. The mean is larger than the median for positively skewed distributions and vice versa for negatively skewed distributions. The kurtosis is based on the size of the tails of a distribution and provides a measure of how likely the distribution will produce outliers. The kurtosis of a normal distribution is three. Distributions with relatively thick tails are “leptokurtic” and have kurtosis greater than three. Distributions with relatively thin tails are “platykurtic” and have a kurtosis less than three.

The histogram of INDOT AADT data generated by ArcGIS is shown in Figure 13. The AADT distribution has a skewness of 4.7651 and a kurtosis of 35.47. Moreover, the distribution is obviously not a symmetric bell shaped distribution. Therefore, the AADT data are not normally distributed.

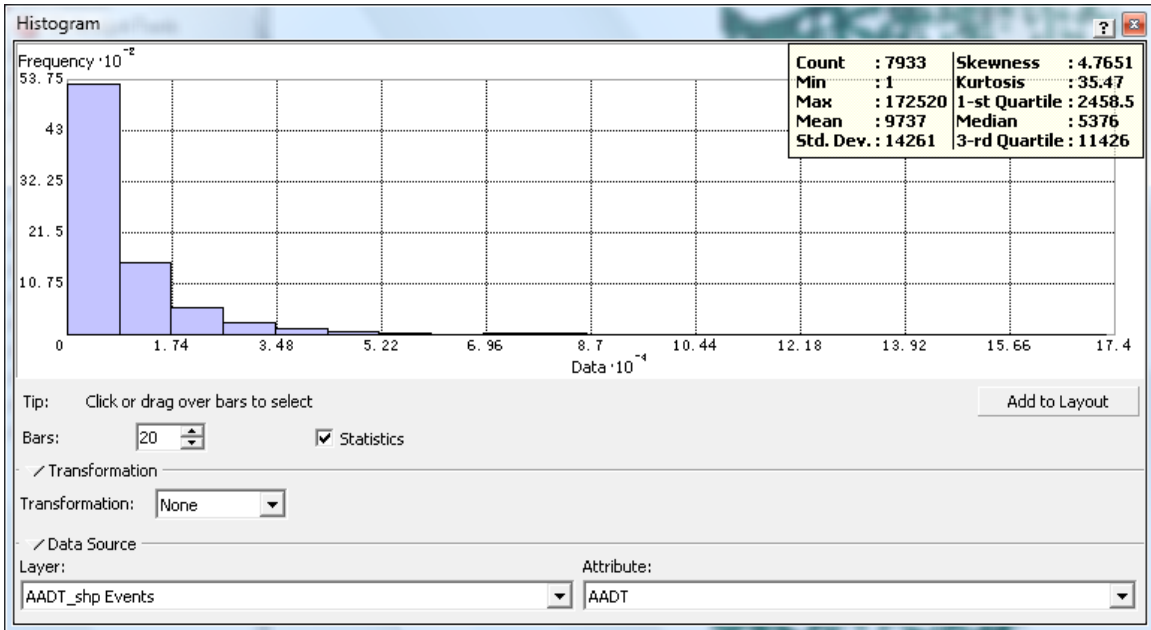


Figure 13: Histogram of INDOT AADT

5.1.2: Normal QQ Plot

To further examine the pattern of the AADT distribution, the Normal QQ Plot to analyze the AADT data. The QQ Plot is used to compare the distribution of the data to a standard normal distribution. The closer the points are to creating a straight line, the closer the distribution is to being normally distributed. Figure 14 shows the QQ Plot of the AADT data. As can be seen, the right hand side of the AADT line is far from the normal distribution straight line. This indicates again that the AADT data is not normally distributed.

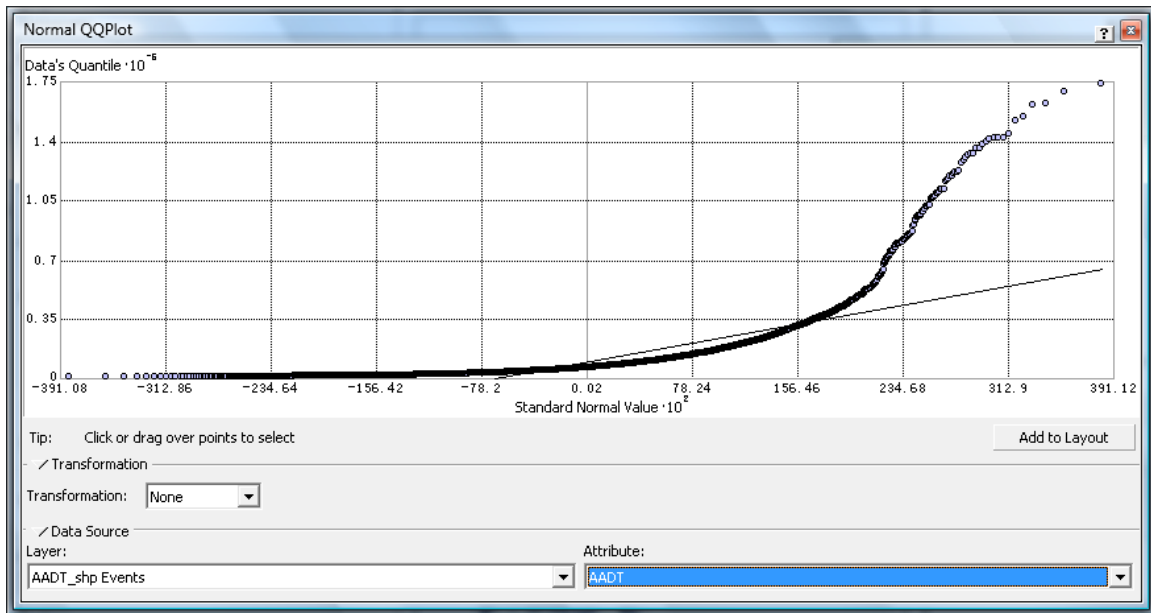


Figure 14: QQ Plot of INDOT AADT

5.1.3: Data Transformation

Some geostatistical methods are critically dependent on the data coming from a normal distribution. In statistics, the power transform is a family of transformations that map data from one space to another using power functions. This data processing technique is used to reduce data variation, make the data more normal distribution-like, and improve the correlation between variables and for other data stabilization procedures. Through data transformations, an original dataset that is not normally distributed can be transformed into a dataset that is normally distributed. Two types of data transformations were performed in this study in order to make the INDOT AADT data more normally distributed. They are log transformation and Box-Cox transformation (ESRI 2007). In ArcGIS, the log transformation is expressed as:

$$Y(s)=\ln(Z(s)), \text{ for } Z(s)>0 \quad (2)$$

where $Z(s)$ is the original dataset and $Y(s)$ is the transformed dataset.

The Box-Cox transformation (Box & Cox, 1964, and Myers and Montgomery, 2002) is a commonly used power transformation method. In ArcGIS, the Box–Cox transformation is expressed as:

$$Y(s)=(Z(s)^\lambda-1)/\lambda, \text{ for } \lambda \neq 0. \quad (3)$$

The log transformation is actually a special case of the Box–Cox transformation when $\lambda = 0$. The AADT was transformed through log transformation. For each AADT value, the transformed data is $\ln(\text{AADT})$. That is, the transformed data is the natural logarithm of the original data. The histogram of the log transformed data is shown in Figure 15. As can be seen, the shape of the new histogram shown in Figure 15 is more normally distributed than the one shown in Figure 13. The new kurtosis is 5.844 and the skewness is -0.5568, which are much improved compared to the values in Figure 13 (kurtosis of 35.47 and skewness of 4.7651). The improved normal distribution is also illustrated in the Normal QQ Plot in Figure 16. As shown in the Figure 16, the transformed data is almost on the normal distribution line with some exceptions at the two ends. This indicates that the distribution of the log transformed data is very close to the normal distribution.

The Box-Cox transformation, $Y(s)=(Z(s)^\lambda-1)/\lambda$, for $\lambda \neq 0$, is a distribution with a power parameter λ . For a given dataset, the value of the power parameter, λ , must be determined so that the transformed dataset will have a highest degree of normal distribution. Using the Box-Cox data transformation functions in ArcGIS, the AADT data were transformed with different λ values. For the selected λ values, the corresponding values of kurtosis and skewness can be compared to determine the distributions of the transformed datasets. Figures 17 through 20 are the histograms of the transformed AADT data with different λ values.

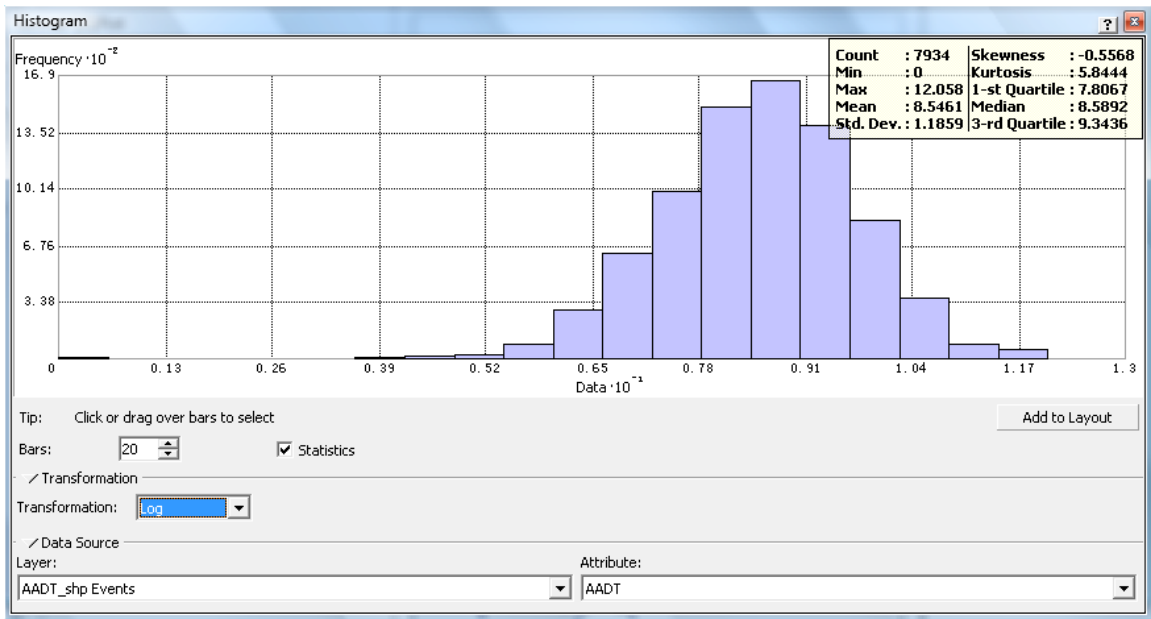


Figure 15: Histogram of Log Transformed AADT

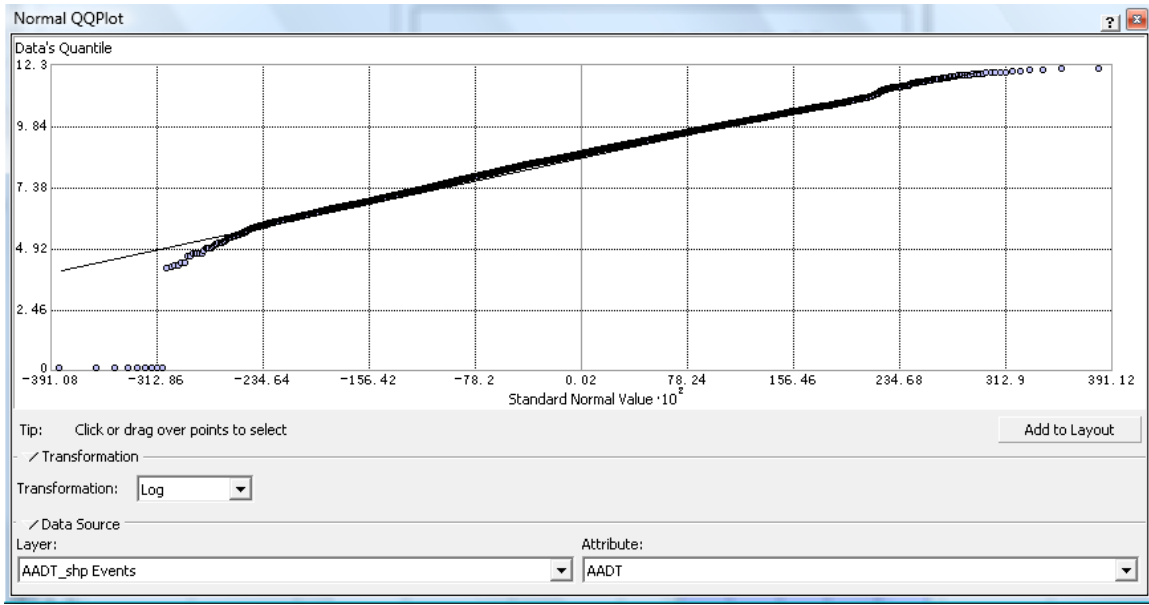


Figure 16: QQ Plot of the Log Transformed AADT

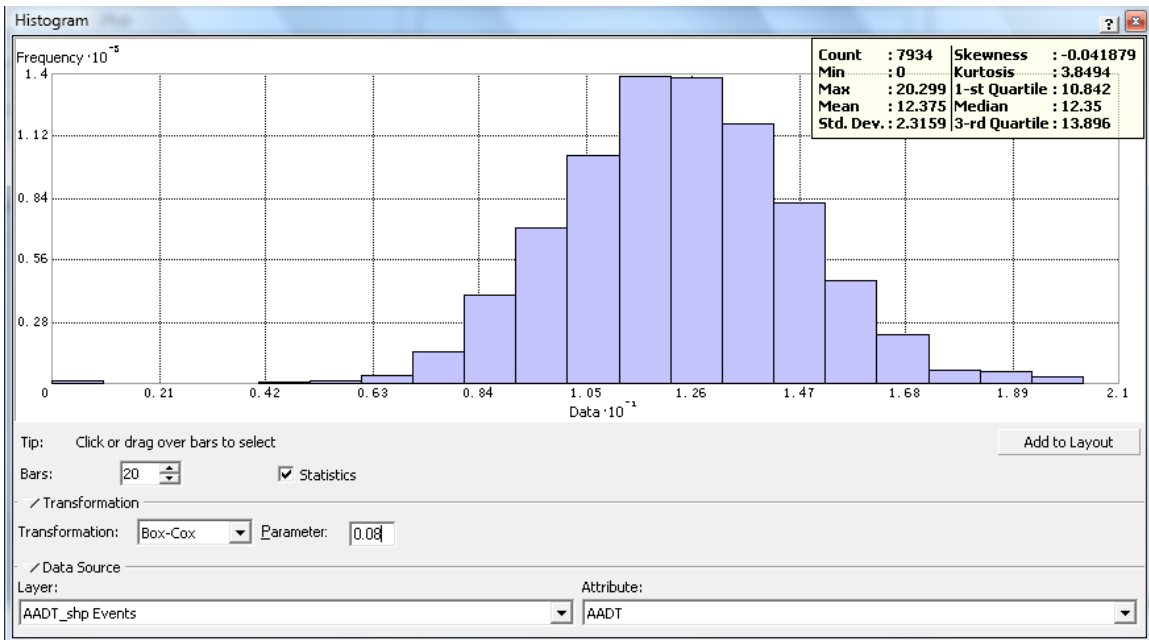


Figure 17: Histogram of the Box-Cox Transformed AADT ($\lambda=0.08$)

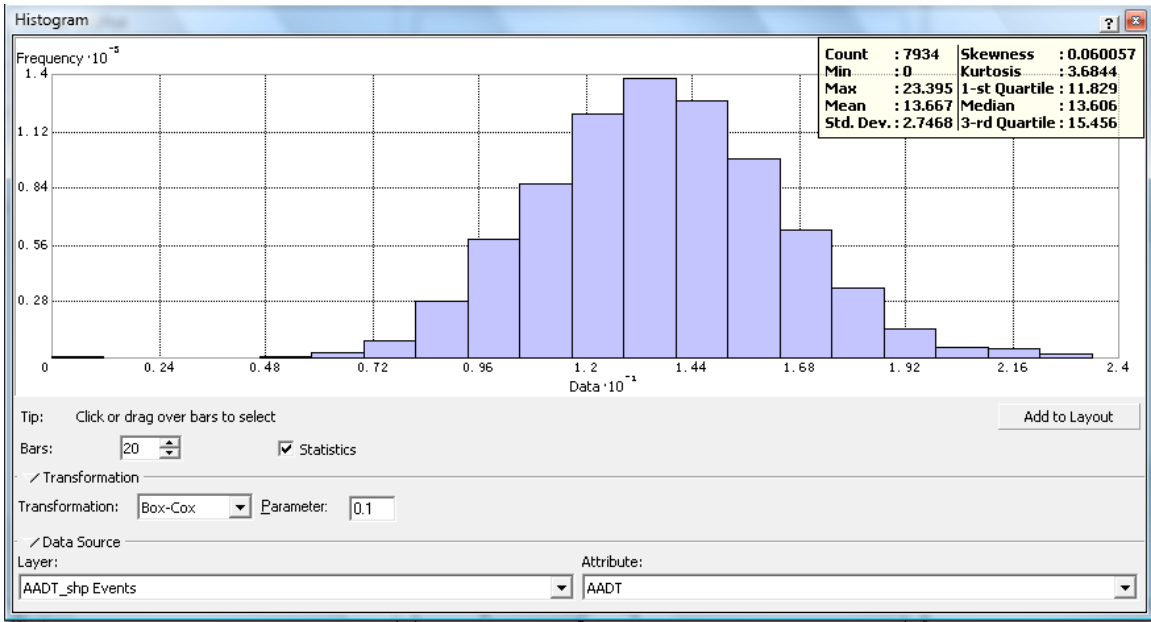


Figure 18: Histogram of the Box-Cox Transformed AADT ($\lambda=0.10$)

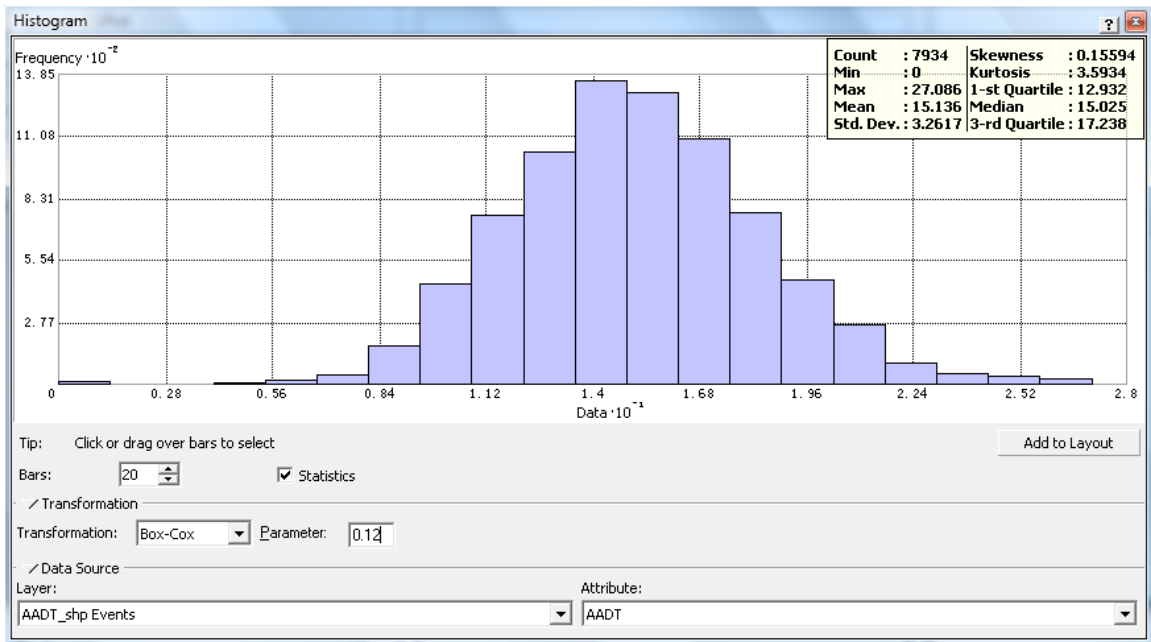


Figure 19: Histogram of the Box-Cox Transformed AADT ($\lambda=0.12$)

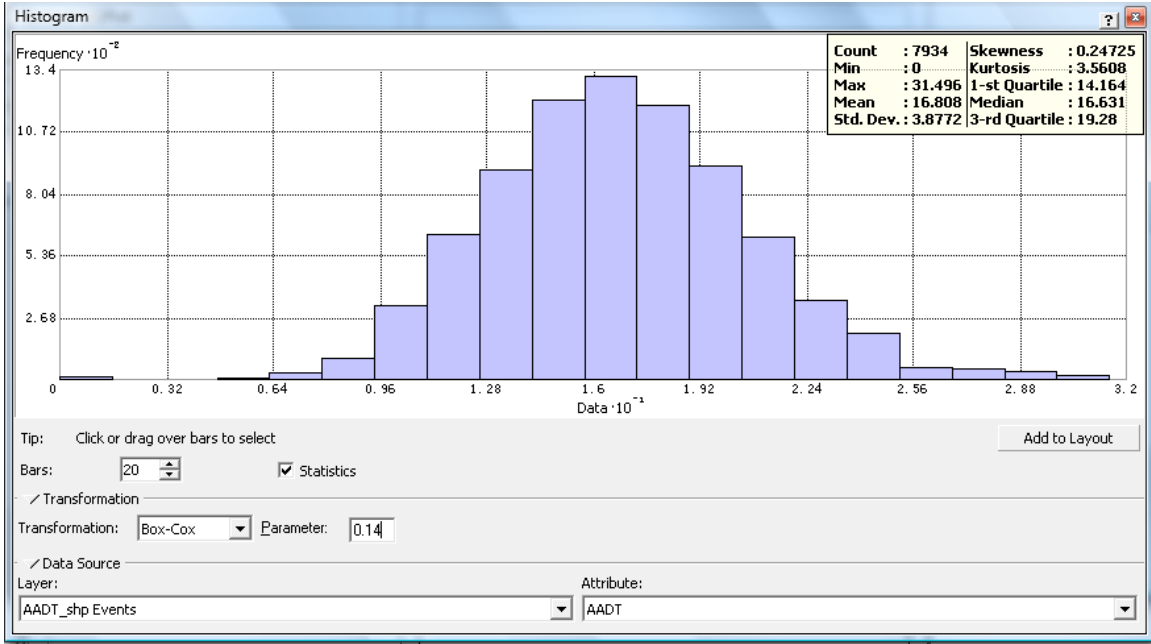


Figure 20: Histogram of the Box-Cox Transformed AADT ($\lambda=0.14$)

The histograms show that values of skewness and kurtosis vary with λ values. The values of skewness and kurtosis are listed in Table 6 for λ values ranging from 0.080 to 0.145. As previously discussed, the coefficient of skewness is a measure of the symmetry of a distribution. For a normal distribution, the histogram should be symmetric and the coefficient of skewness should be 0. If a distribution has a long right tail of large values, it is positively skewed, and if it has a long left tail of small values, it is negatively skewed. The kurtosis is based on the size of the tails of a distribution and provides a measure of how likely the distribution will produce outliers. The kurtosis of a normal distribution should be 3.

Table 6: Skewness and Kurtosis of Transformed AADT for Different λ values

λ	0.080	0.085	0.090	0.095	0.100	0.105	0.110	0.115	0.120	0.125	0.130	0.135	0.140	0.145
Kurtosis	3.8494	3.8009	3.7572	3.7186	3.6850	3.6560	3.6313	3.6107	3.5939	3.5808	3.5711	3.5647	3.5613	3.5610
Skewness	-0.0421	-0.0159	0.0098	0.0350	0.0599	0.0844	0.1085	0.1323	0.1558	0.1790	0.2019	0.2246	0.2471	0.2694

The log transformed AADT has a skewness of -0.5568 and a kurtosis of 5.8444 as shown in Figure 15. The values of kurtosis and skewness for the Box-Cox transformed AADT shown in Table 6 are improved compared to the log transformed AADT in terms of normal distribution, because the kurtosis values are closer to 3 and the skewness values are closer to 0. Among the many λ values, it was desirable to choose a λ value that would generate the transformation data with highest degree of normal distribution. The relationship between skewness and λ and the relationship between kurtosis and λ were obtained through regressions as shown in Figure 21 and Figure 22, respectively. The regression equations of the relationships are expressed as the following:

$$\text{Skewness} = 4.7816 \lambda - 0.4201 \quad (4)$$

$$\text{Kurtosis} = 80.239 \lambda^2 - 22.396 \lambda + 5.1244 \quad (5)$$

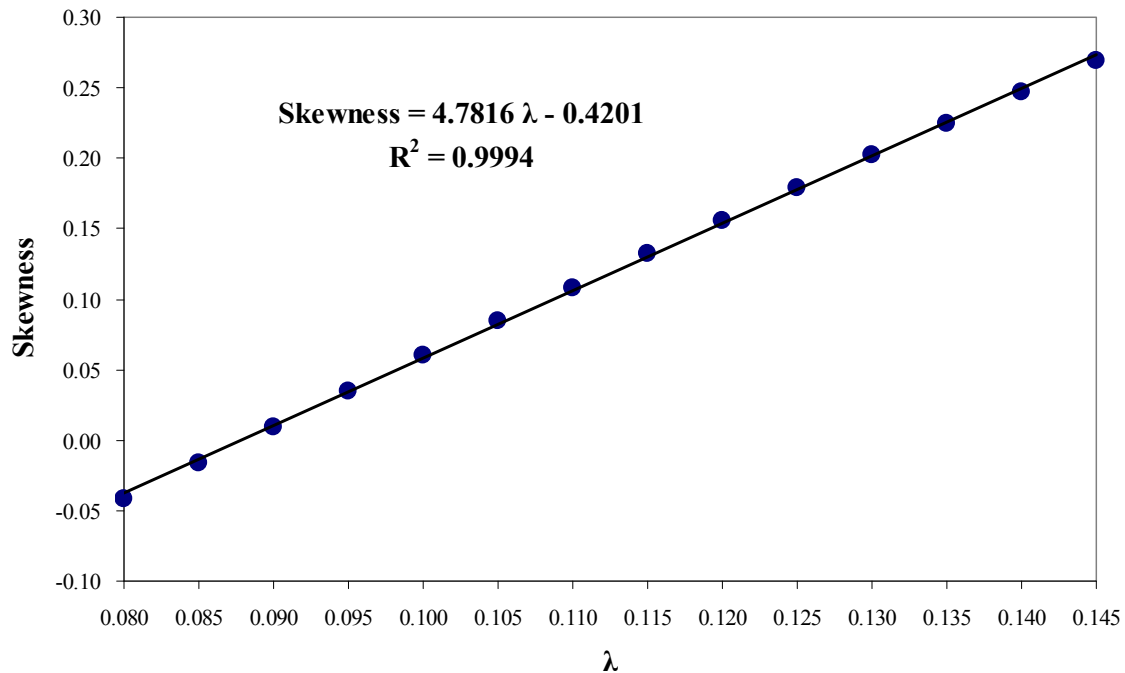


Figure 21: Relationship between Skewness and λ

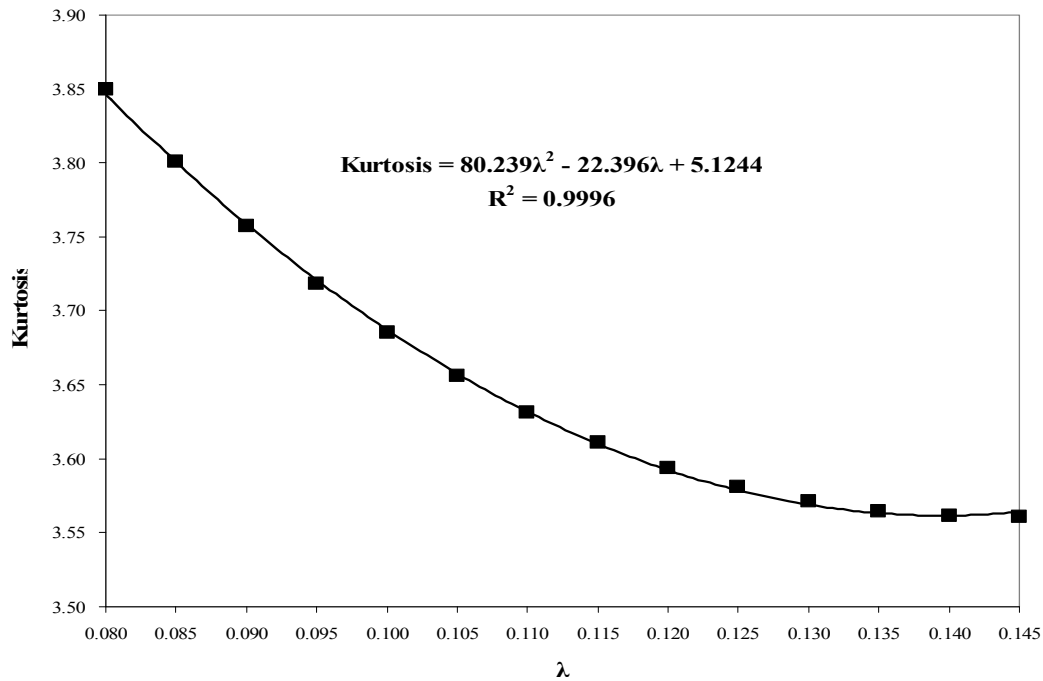


Figure 22: Relationship between Kurtosis and λ

From Equation 4, it can be obtained that when λ is 0.0878576 the skewness is 0. The histogram of the transformed AADT with a λ value of 0.0878576 is presented in Figure 23. From Equation 5, the minimum kurtosis can be computed as 3.561629 when λ is 0.139558. The histogram corresponding to λ of 0.139558 is shown in Figure 24. It should be pointed out that the values of skewness and kurtosis are slightly different from the expected values from the regression equations. This is because regression values are usually not a perfect fit of the data used in regression.

Since a true normal distribution has a skewness of 0 and a kurtosis of 3, a proper value of λ should be chosen so that the transformed data would be as normally distributed as possible. Such a λ should yield a Box-Cox transformed dataset with reasonably balanced skewness and kurtosis. In order to identify a good λ value, the QQ Plots

(Figures 25 through 30) were used to examine the degrees of normal distributions of the transformed datasets. Based on these QQ Plots, it can be seen that the Box-Cox transformation with a λ of 0.0878576 generated the data points that are closest to the straight line of the normal distribution. Therefore, in addition to the log transformation, the Box-Cox transformation of the AADT with a λ of 0.0878576 was also selected for geostatistical analysis in this study.

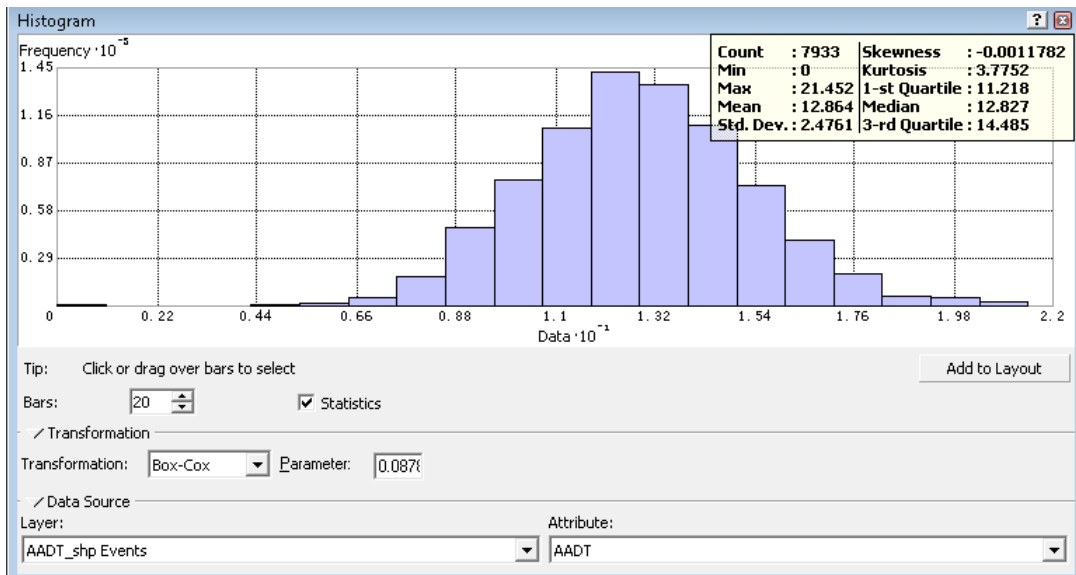


Figure 23: Histogram of Transformed AADT ($\lambda = 0.0878576$)

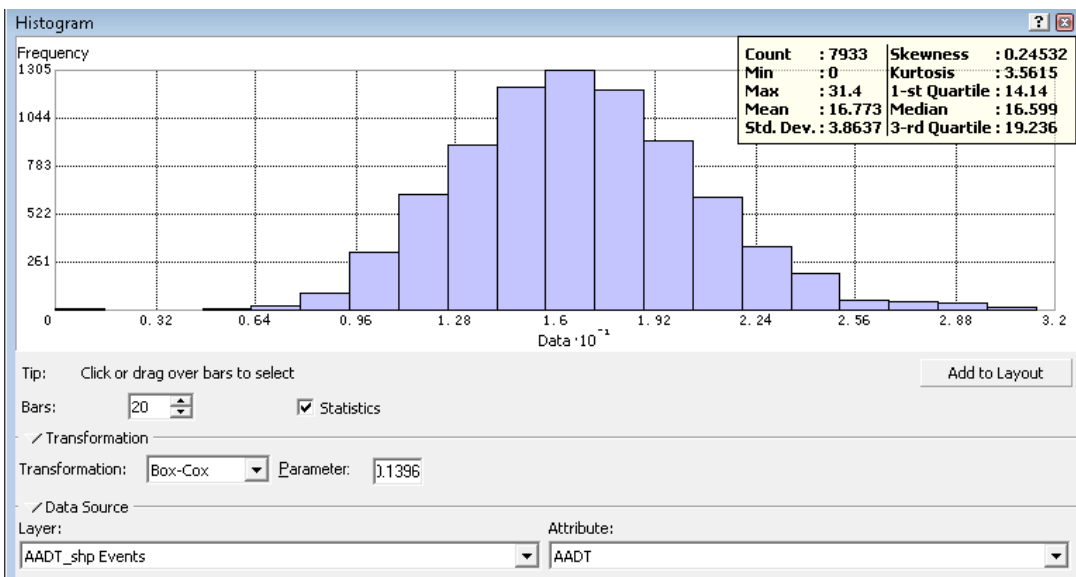


Figure 24: Histogram of Transformed AADT ($\lambda = 0.139558$)

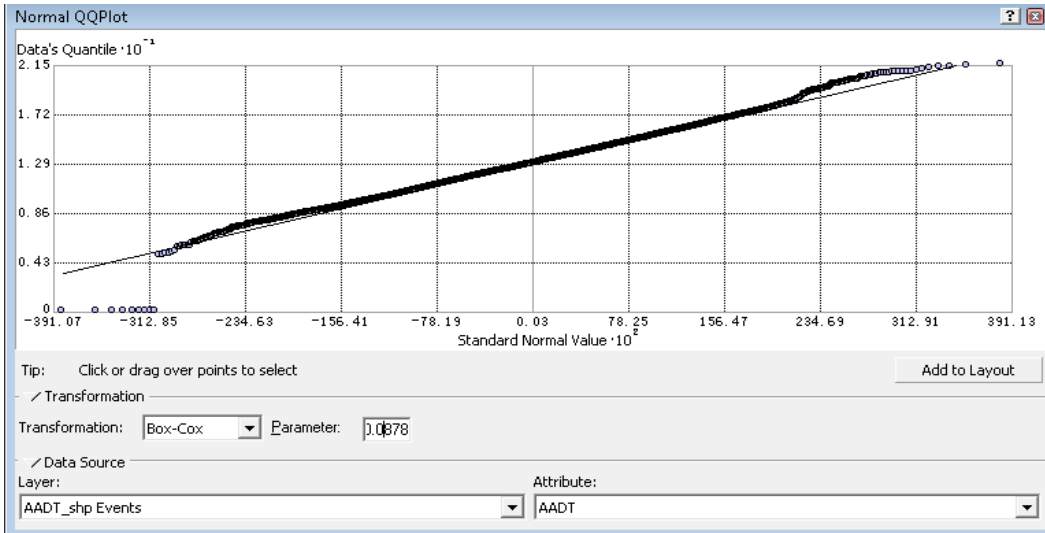


Figure 25: QQ Plot of Transformed AADT ($\lambda = 0.878576$)

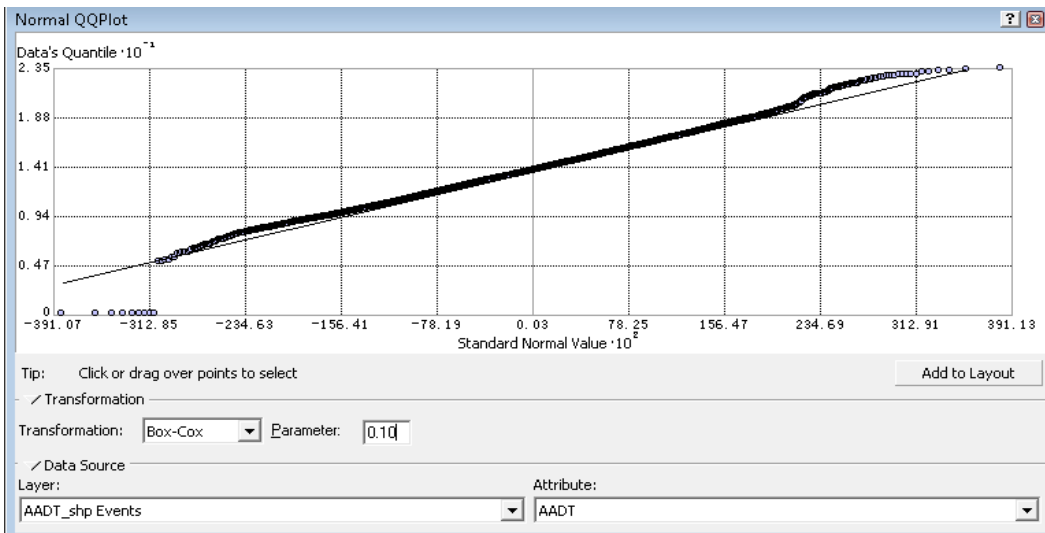


Figure 26: QQ Plot of Transformed AADT ($\lambda = 0.10$)

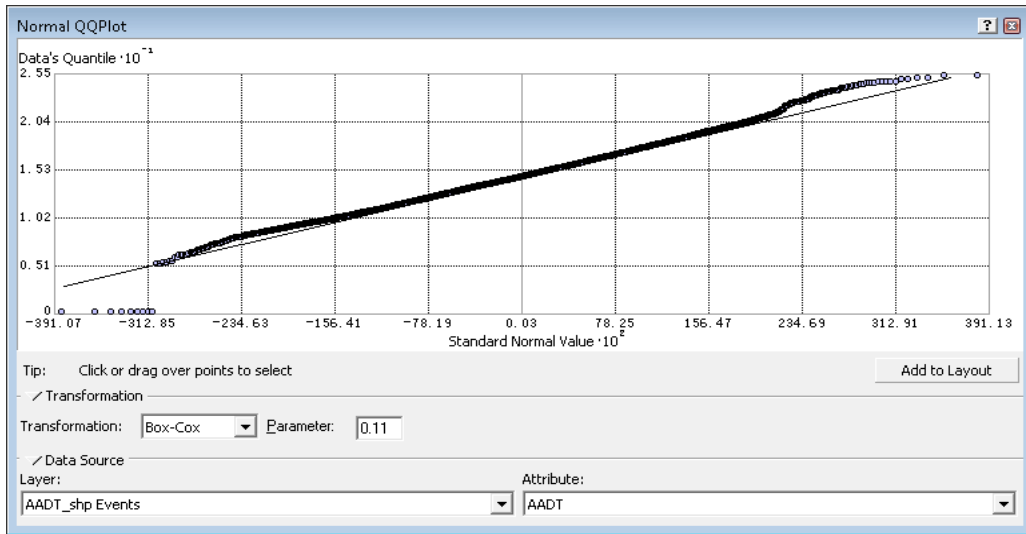


Figure 27: QQ Plot of Transformed AADT ($\lambda = 0.11$)

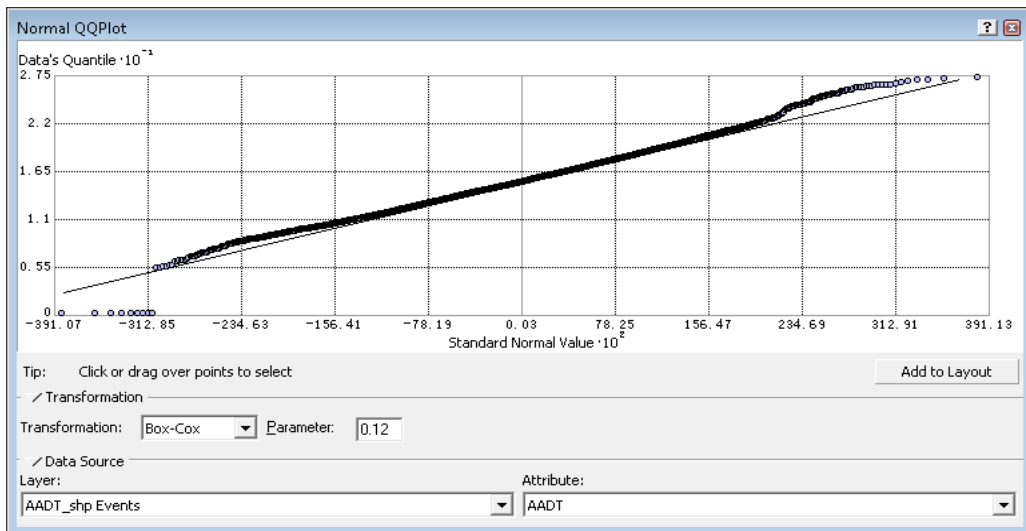


Figure 28: QQ Plot of Transformed AADT ($\lambda = 0.12$)

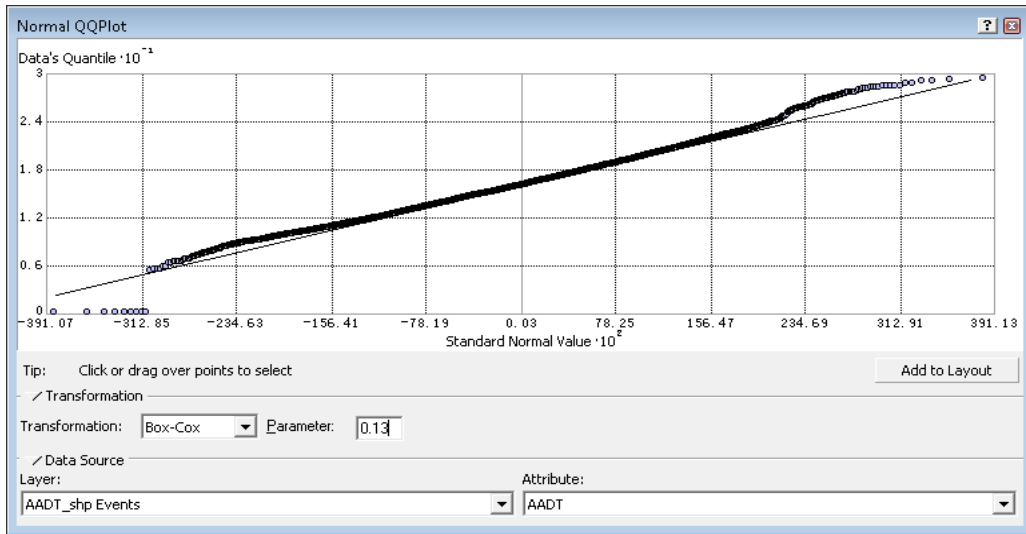


Figure 29: QQ Plot of Transformed AADT ($\lambda = 0.13$)

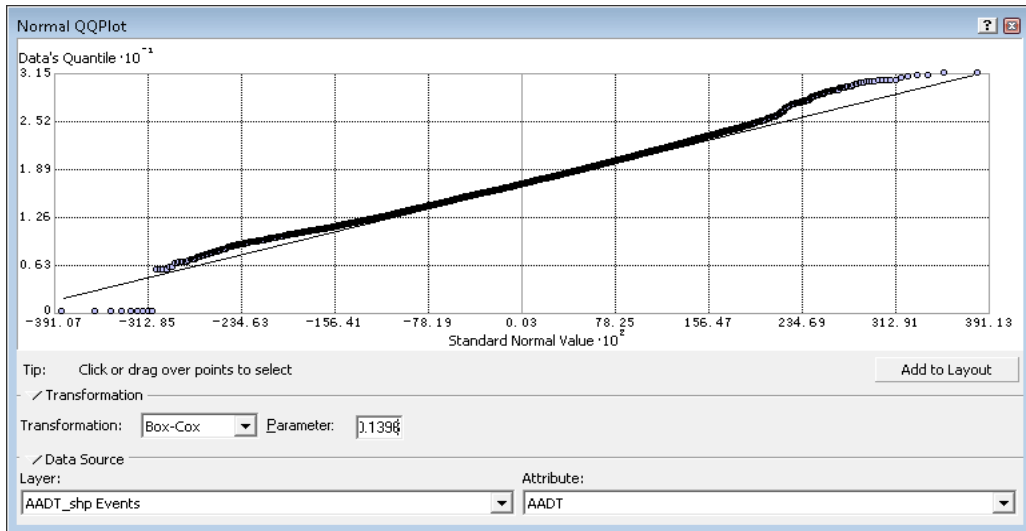


Figure 30: QQ Plot of Transformed AADT ($\lambda = 0.1396$)

5.2: Variograms

One of the most important concepts in geostatistics is called variogram. If the measurement of a sample at location x is $Z(x)$ and the measurement of another sample at location $x+h$, then the variogram (Clark, 1979), $2\gamma(h)$, is defined as:

$$2\gamma(h) = \frac{1}{n} \sum [Z(x) - Z(x+h)]^2 \quad (4)$$

The term $\gamma(h)$ is called semi-variogram:

$$\gamma(h) = \frac{1}{2n} \sum [Z(x) - Z(x+h)]^2 \quad (5)$$

The distance between the two samples, h , is called lag. As h changes, γ changes. The relationship between the semi-variogram γ and h are shown in Figure 31. The figure shows that the value of γ at which the graph levels off is called the sill of the semi-variogram; the h value corresponding to the start of sill is called range; and the value of γ at $h=0$ is called nugget. The partial sill is the sill minus the nugget. Sample locations separated by distances closer than the range are spatially autocorrelated, whereas locations farther apart than the range are not. Theoretically, at zero separation distance ($h = 0$), the semi-variogram value is zero. However, at an infinitesimally small separation distance, the semi-variogram often exhibits a nugget effect, which is some value greater than zero. The nugget effect can be attributed to measurement errors or spatial sources of variation at distances smaller than the sampling interval (or both) (ESRI 2007). An ideal shape for a semi-variogram should have a nugget value of 0. The ideal shape for the semi-variogram is to geostatistics as the normal distribution is to statistics. There are

many mathematical models for semi-variograms. The commonly used models are listed in Table 7.

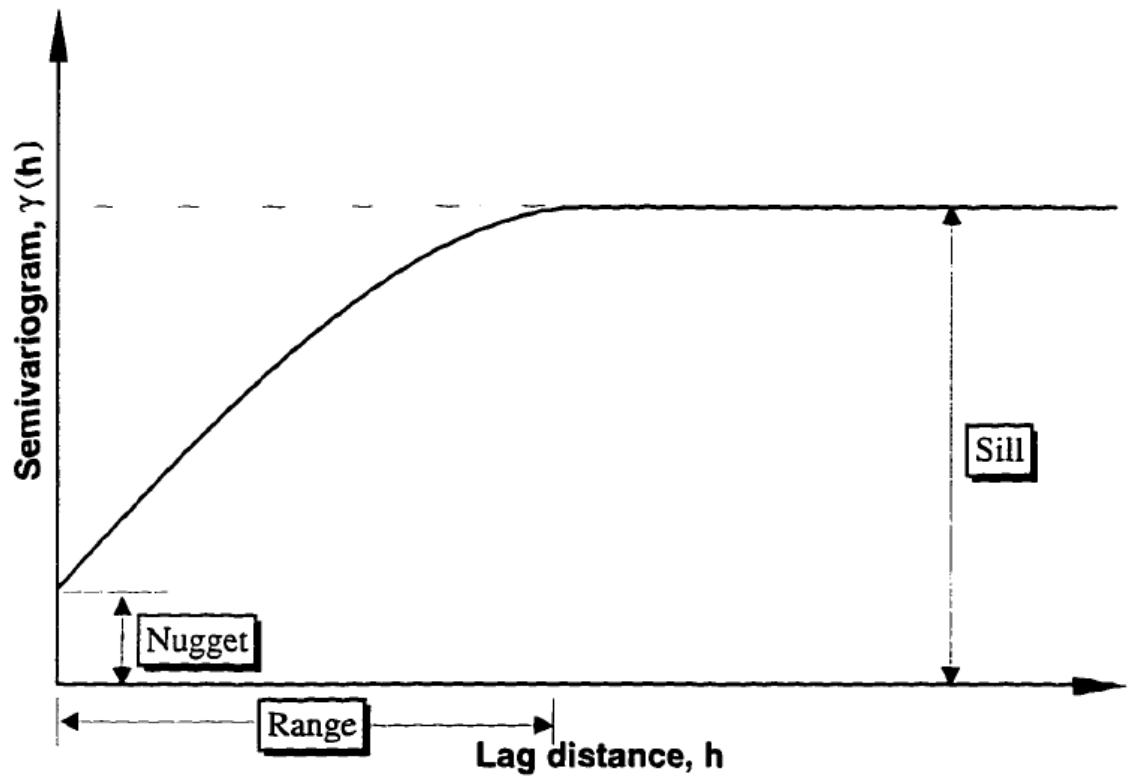


Figure 31: Semi-Variogram graph

Table 7: Commonly Used Semi-Variogram Models

Model	$\gamma(h)$	h value
Circular Model	$c[\frac{2h}{\pi a} \sqrt{1 - (\frac{h}{a})^2} + \frac{2}{\pi} \arcsin \frac{h}{a}]$	$0 \leq h \leq a$
	c	$h > a$
Spherical Model	$c[\frac{3h}{2a} - \frac{1}{2}(\frac{h}{a})^3]$	$0 \leq h < a$
	c	$h \geq a$
Penta-spherical Model	$c[\frac{15h}{8a} - \frac{5}{4}(\frac{h}{a})^3 + \frac{3}{8}(\frac{h}{a})^5]$	$0 \leq h < a$
	c	$h \geq a$
Exponential Model	$c[1 - \exp(-\frac{h}{a})]$	$h \geq 0$
Gaussian Model	$c[1 - \exp(-\frac{h^2}{a^2})]$	$h \geq 0$
K-Bessel Model	$c[1 - \frac{h}{a} K_1(\frac{h}{a})]$	$h \geq 0$
Linear Model with No Still	ch	$h \geq 0$
Power Model	ch^a	$h \geq 0, 0 < a \leq 2$
Nugget Model	0	$h = 0$
	c	$h > 0$
Linear Model with Still	$c(\frac{h}{a})$	$0 \leq h < a$
	c	$h \geq a$
Logarithmic Model	0	$h = 0$
	$c[\log(h + a)]$	$h > 0$
Periodic Model	$c[1 - \cos(\frac{2\pi h}{a})]$	$h \geq 0$

When modeling the semi-variogram, the autocorrelation can be examined and quantified. In geostatistics this is called spatial modeling, also known as structural

analysis or variography. In spatial modeling of the semi-variogram, the empirical semi-variograms are computed using the following formula:

$$\gamma(h) = \frac{1}{2} \sum [Z(x) - Z(x + h)]^2 \quad (6)$$

A graph based on the calculated values from Equation 6 is called the semi-variogram cloud. It shows the empirical semi-variogram for all pairs of locations within a dataset and plots them as a function of the distance between the two locations. The semi-variogram cloud can be used to examine the local characteristics of spatial autocorrelation within a dataset and look for local outliers. If all pairs are plotted on a graph, the number of pairs will become unmanageable. Instead of plotting each pair, the pairs are grouped into lag bins. Lag bins are the specified ranges of lag (h) values. For example, the average semi-variograms can be computed for all pairs of points that are within 3 miles apart. The values in the semi-variogram cloud are put into bins based on the direction and distance between a pair of locations. These bin values are then averaged and smoothed to produce a surface of the semi-variogram. The extent of the semi-variogram surface is controlled by selected lag size and number of lags.

The INDOT AADT data is depicted in the three dimensional graph in Figure 32. It is desirable to utilize geostatistics to express the AADT distribution mathematically. Figure 33 shows the semi-variogram cloud of the original INDOT AADT. Similarly, Figure 34 shows the semi-variogram cloud of the transformed INDOT AADT with the Box-Cox method. Both cloud graphs in Figures 33 and 34 do not show clear patterns of relationships between the semi-variograms and the lag distances. Therefore, it is needed to select a semi-variogram model that will best fit the INDOT AADT data.

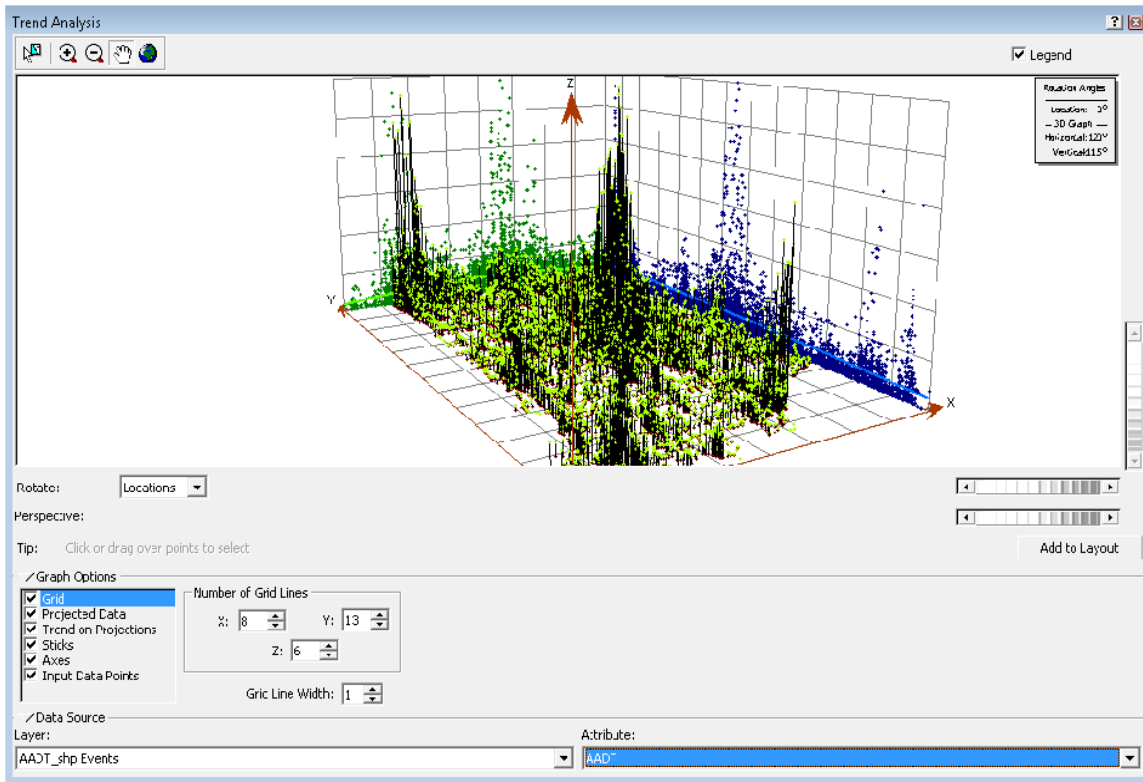


Figure 32: Three Dimensional Graph of INDOT AADT

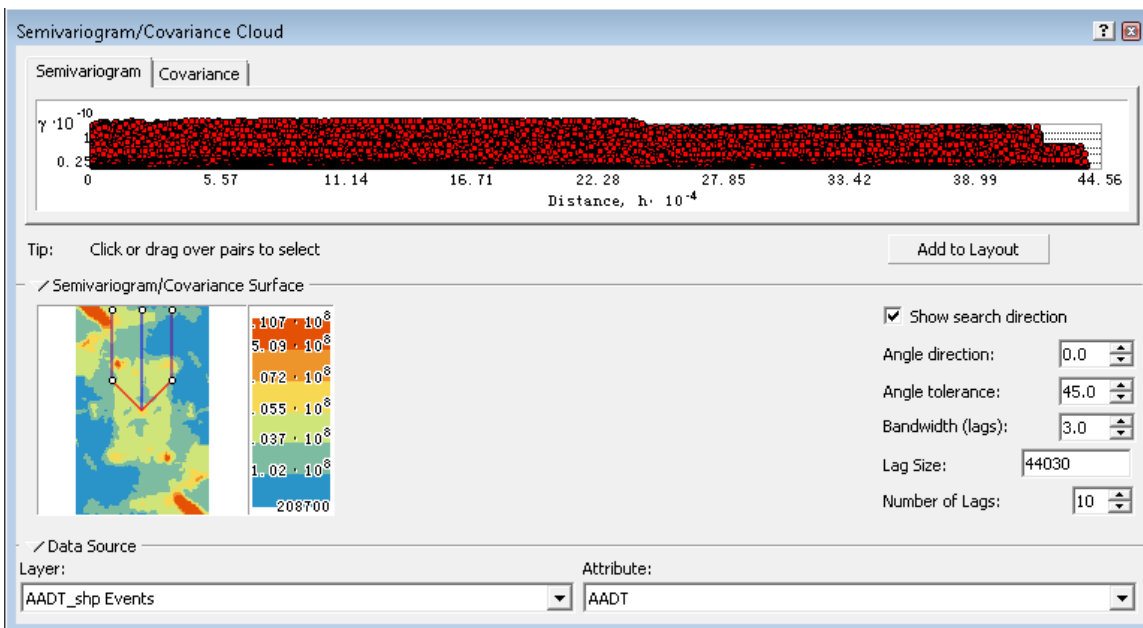


Figure 33: Semi-Variogram Cloud of INDOT AADT

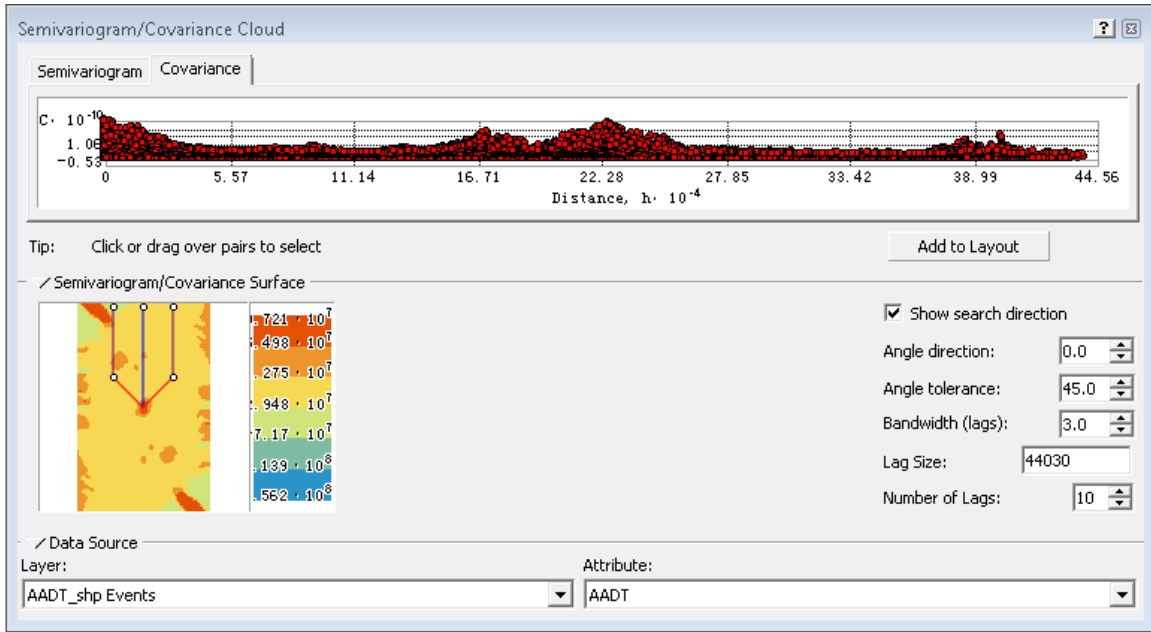


Figure 34: Semi-Variogram Cloud of Box-Cox Transformed INDOT AADT

5.3: Geostatistical Modeling

5.3.1: Kriging Methods:

In this study, it is desired to fit the best model of semi-variogram functions to the INDOT AADT measurements. The model will then be used to predict the AADT values at the locations without AADT measurements in Indiana. Semi-variogram modeling is a key step between spatial description and spatial prediction. A powerful method of geostatistical modeling is called kriging. Kriging is an advanced geostatistical procedure that generates an estimated surface from a scattered set of points with z values. For the AADT data, the x and y values represent locations of the data points and z values are the observed AADT at these locations. Kriging involves an interactive investigation of the

spatial behavior of the phenomenon represented by the z values before the user selects the best estimation method for generating the output surface.

Kriging offers two types of surface estimators: Ordinary Kriging and Universal Kriging. Ordinary Kriging assumes the constant mean is unknown. Universal Kriging assumes that there is an overriding trend in the data. Universal Kriging should only be used when there is a trend in the data (ESRI 2007). As previously discussed, the INDOT AADT data do not show any trend, thus Universal Kriging method is not suitable. Ordinary Kriging method was used in this study to analyze INDOT AADT data. Also as previously discussed, the original AADT data are not normally distributed, but can be transformed into near normal distribution data through log transformation and Box-Cox transformation. Therefore, the log and Box-Cox transformed AADT data were used in Ordinary Kriging modeling.

Kriging assumes that the distance or direction between sample points reflects a spatial correlation that can be used to explain variations in the surface. Kriging fits a mathematical function to a specified number of points, or all points within a specified radius, to determine the output value for each location. Kriging is a multi-step process; it includes exploratory statistical analysis of the data, variogram modeling, creating the surface, and (optionally) exploring a variance surface (ESRI 2007). The general formula for Kriging interpolator is formed as a weighted sum of the data:

$$\hat{Z}(s_j) = \sum_{i=1}^N \lambda_i Z(s_i) \quad (7)$$

where:

$\hat{Z}(s_j)$ = the predicted value at location j.

$Z(s_i)$ = the measured value at location i.

λ_i = an unknown weight for the measured value at location i.

N = the number of measured values.

The Geostatistical Analyst in ArcGIS (ESRI 2007) provides the following 11 Ordinary Kriging functions to model the empirical semi-variogram:

- Circular
- Spherical
- Tetraspherical
- Pentaspherical
- Exponential
- Gaussian
- Rational Quadratic
- Hole Effect
- K-Bessel
- J-Bessel
- Stable

The selected model influences the prediction of the unknown values, particularly when the shape of the curve near the origin differs significantly. The steeper the curve near the origin, the more influence the closest neighbors will have on the prediction. As a result, the output surface will be less smooth. Each model is designed to fit different types of phenomena more accurately.

In this study, ArcGIS was used for the geostatistical modeling. The Ordinary Kriging was used to process the log and Box-Cox transformed AADT data. All of the 11 functions in the ArcGIS Geostatistical Analyst (ESRI 2007) were used to develop the prediction models. Then the Prediction Errors from the generated models were compared to choose a best model. A good model should have a Mean Standardized value close to 0, a small Root-Mean-Square value, an Average Mean-Error value close to the Root-Mean-Square value, and a Root-Mean-Square Standardized value close to 1.

Using log transformed AADT, the prediction errors of the 11 models are shown in Figures 35 through 45. These figures are from the ArcGIS's Geostatistical Analyst

functions. The prediction errors in the figures are listed in Table 8 to compare the models. As indicated in the table, the Exponential model has a Mean Standardized value closest to 0, a smallest Root-Mean-Square value, and a Root-Mean-Square Standardized value closest to 1. In addition, the difference between the Average Standard Error and the Root-Mean-Square of the Exponential model are the smallest among the 11 models. Therefore, with log transformed AADT, the Exponential model is the best one among the 11 models.

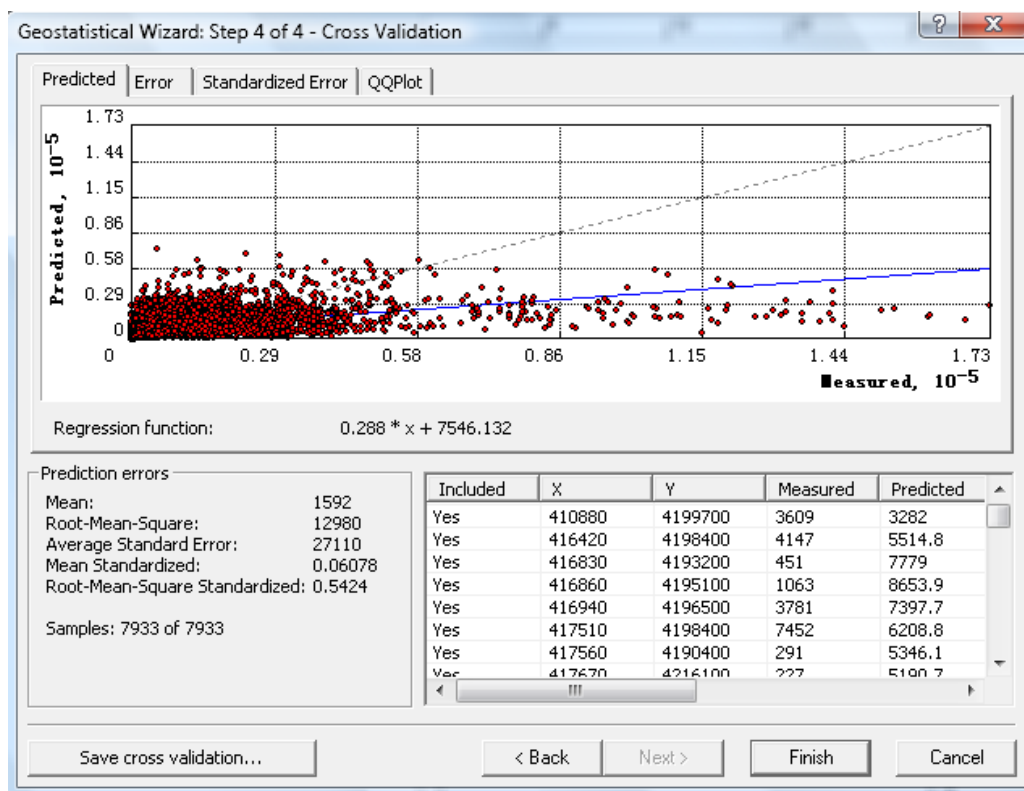


Figure 35: Prediction Errors of Circular Model with Log Transformed AADT

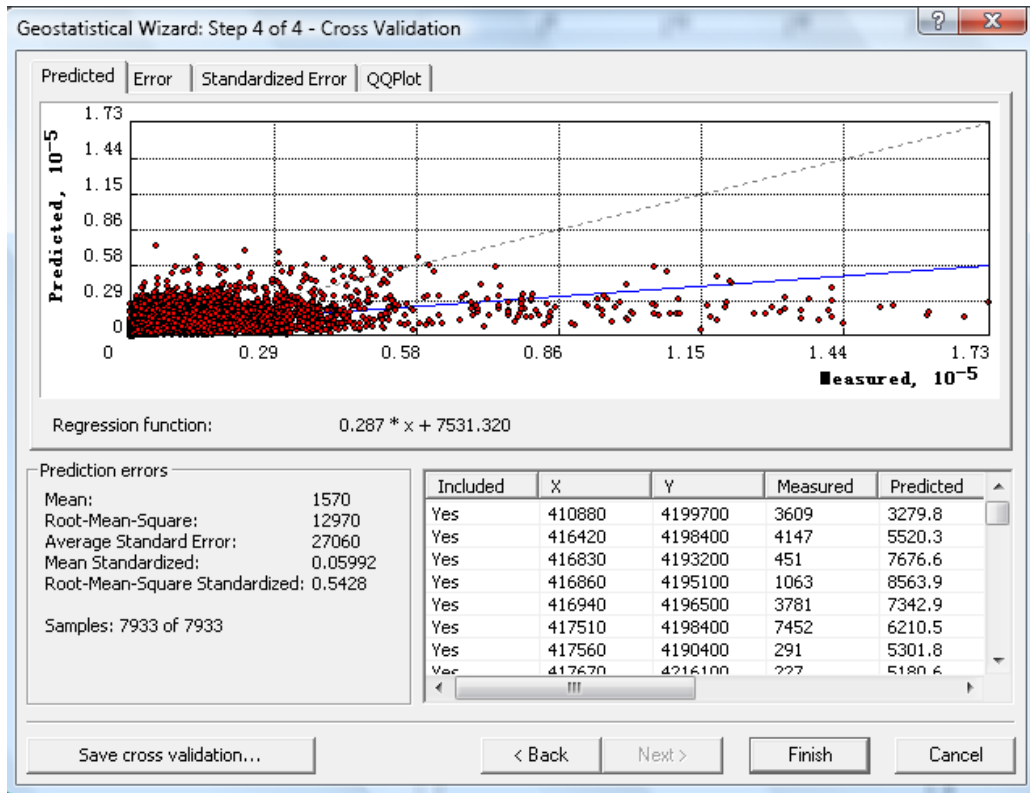


Figure 36: Prediction Errors of Spherical Model with Log Transformed AADT

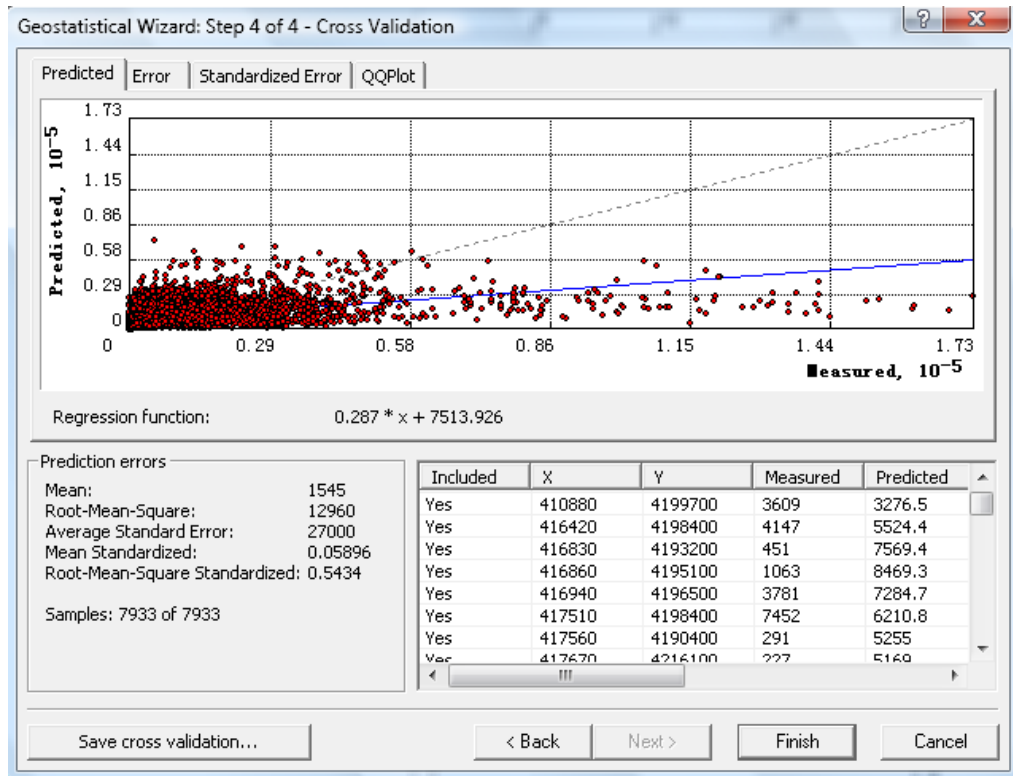


Figure 37: Prediction Errors of Tetraspherical Model with Log Transformed AADT

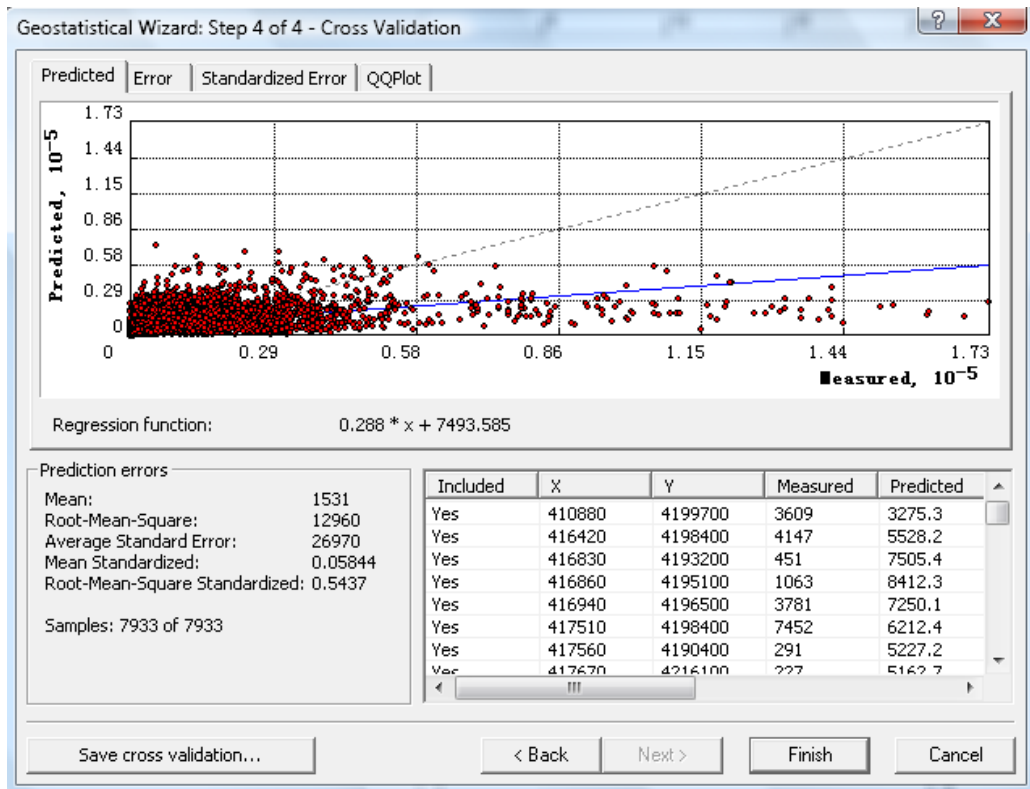


Figure 38: Prediction Errors of Pentaspherical Model with Log Transformed AADT

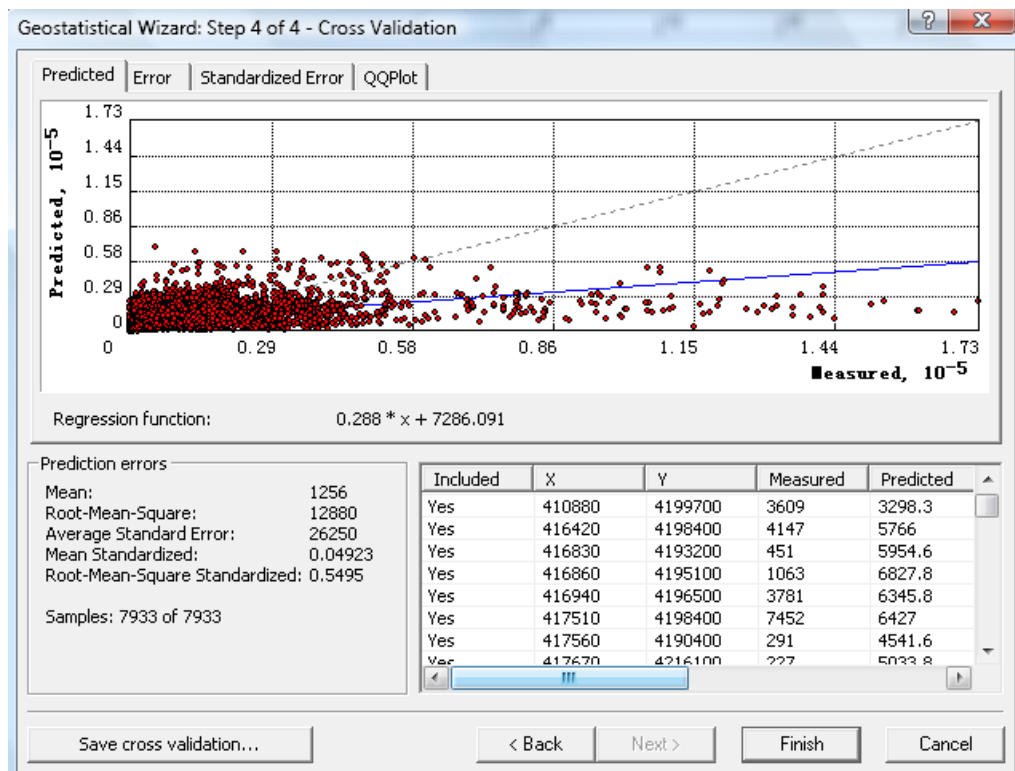


Figure 39: Prediction Errors of Exponential Model with Log Transformed AADT

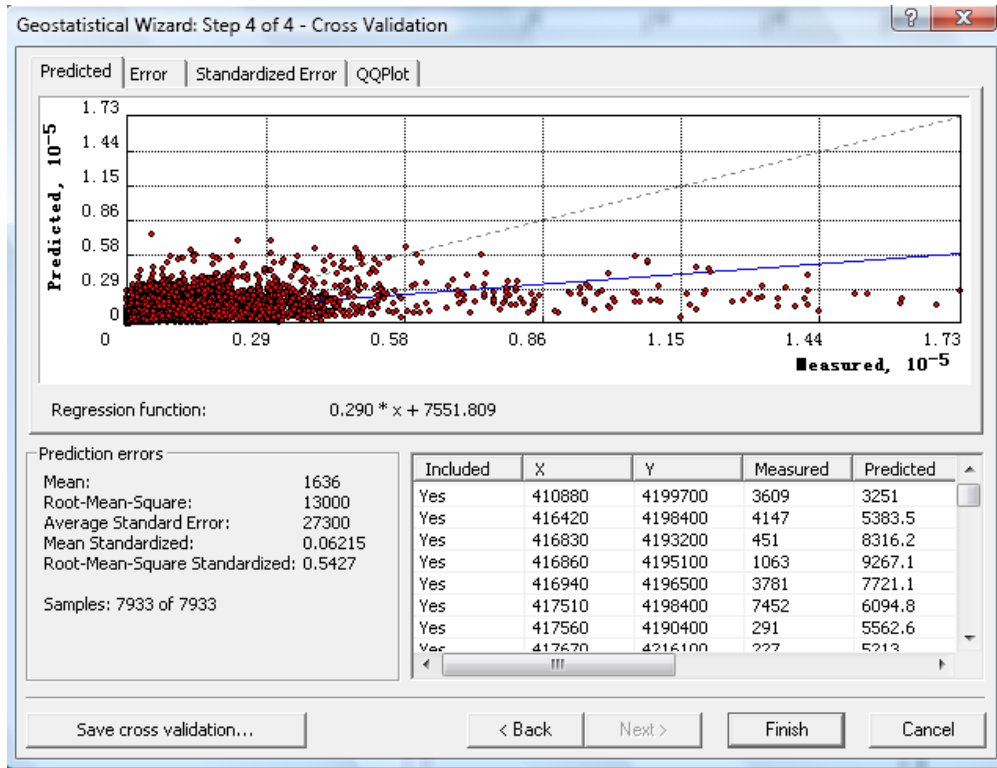


Figure 40: Prediction Errors of Gaussian Model with Log Transformed AADT

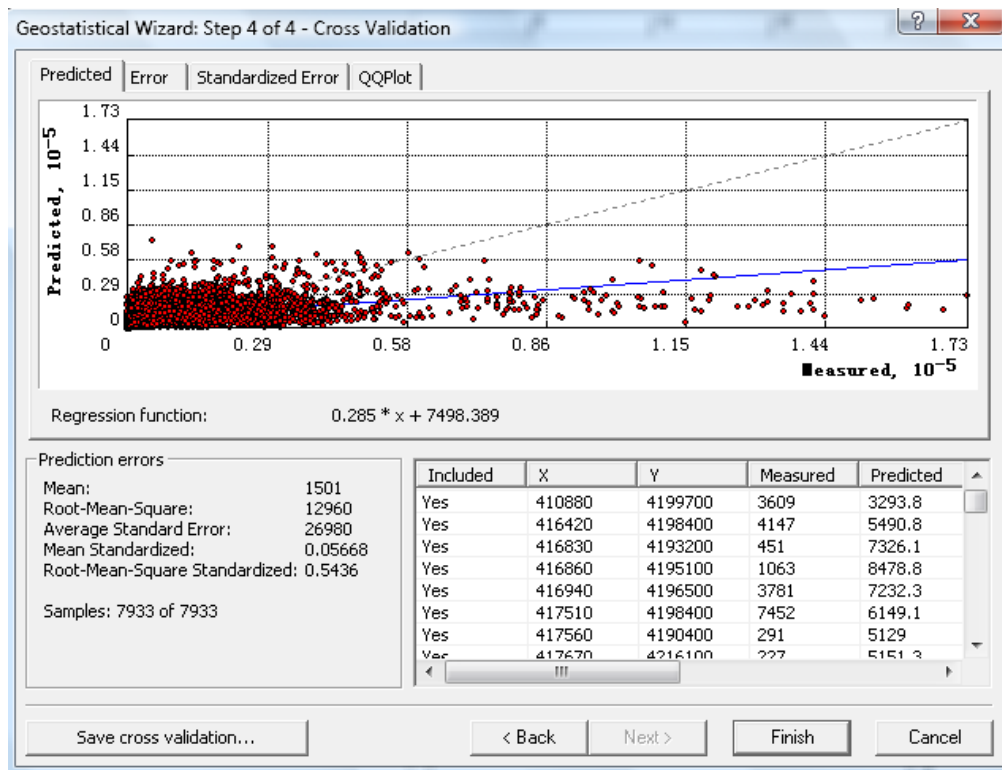


Figure 41: Prediction Errors of Rational Quadratic Model with Log Transformed AADT

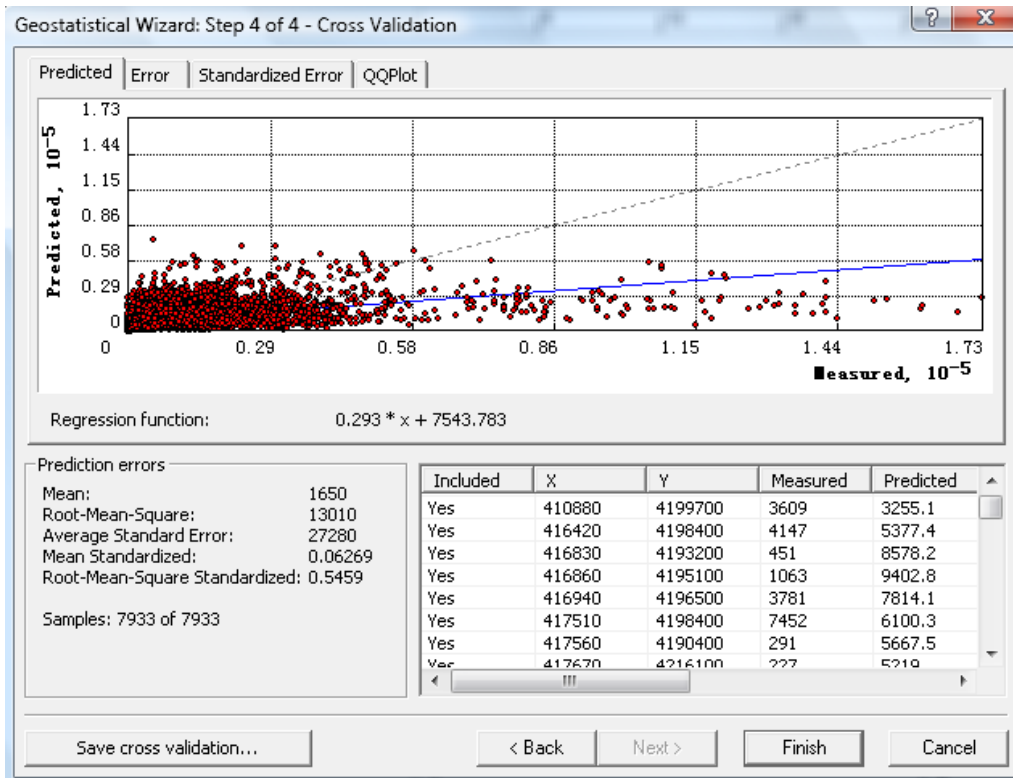


Figure 42: Prediction Errors of Hole Effect Model with Log Transformed AADT

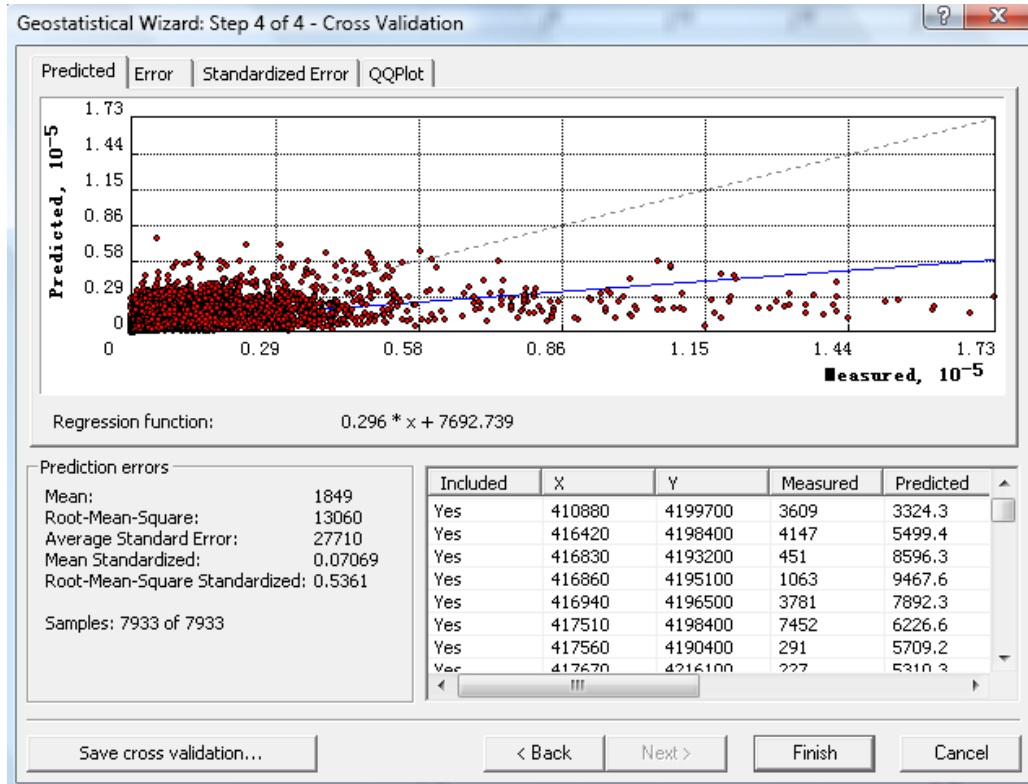


Figure 43: Prediction Errors of K-Bessel Model with Log Transformed AADT

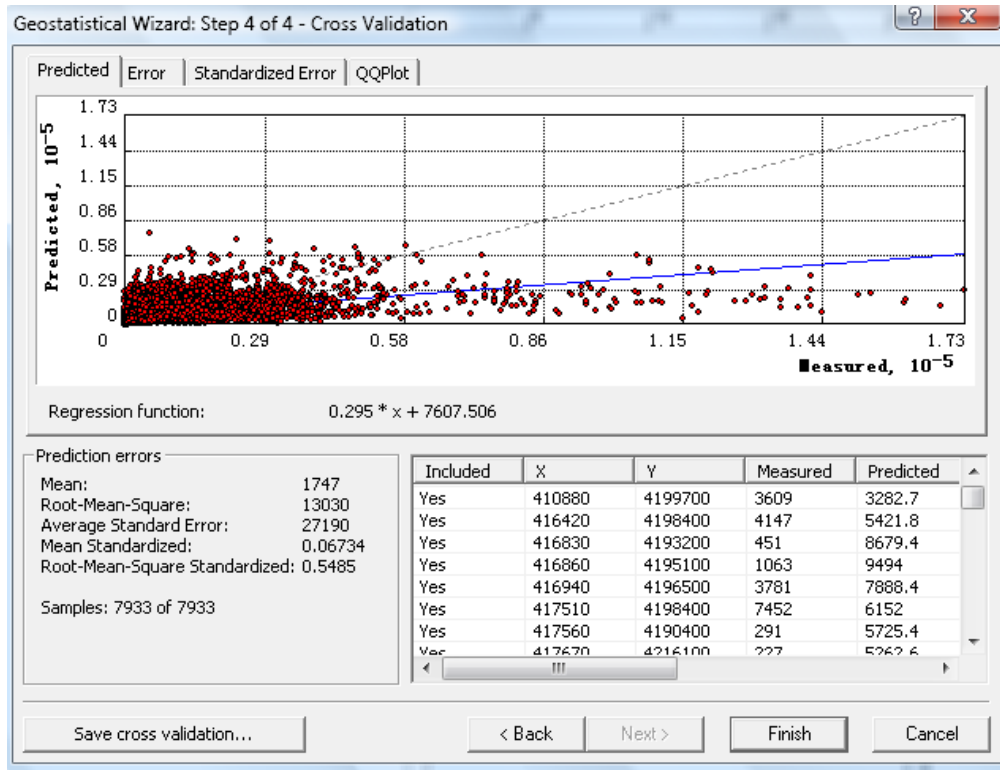


Figure 44: Prediction Errors of J-Bessel Model with Log Transformed AADT

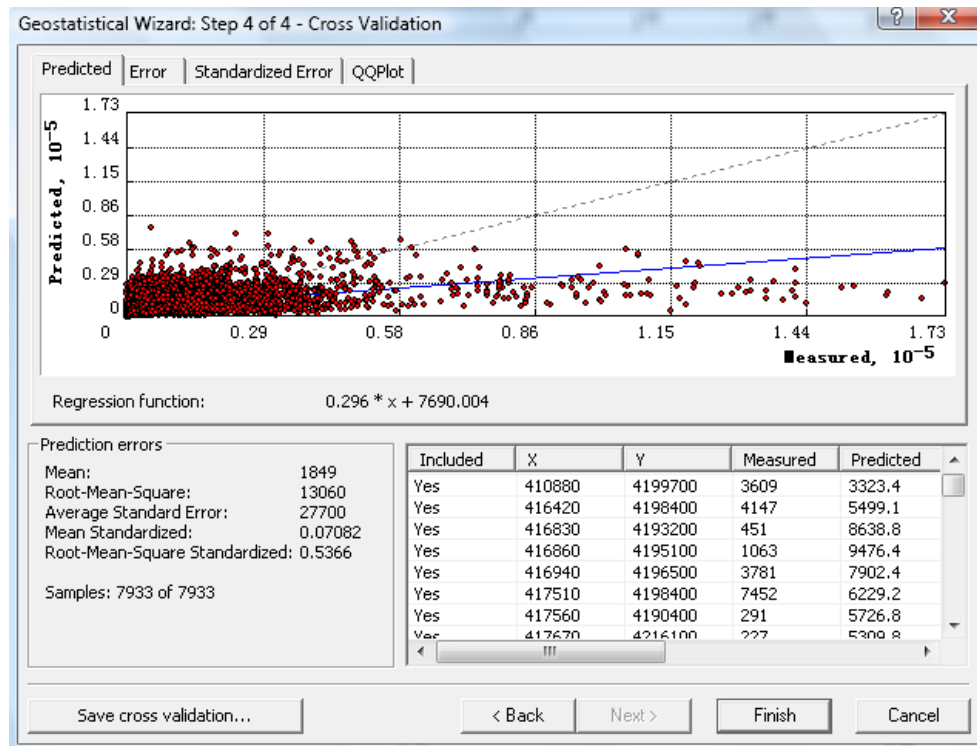


Figure 45: Prediction Errors of Stable Model with Log Transformed AADT

Table 8: Prediction Errors of Different Models with Log Transformed AADT

Model	Mean	Root-Mean-Square	Average Standard Error	Mean Standardized	Root-Mean-Square Standardized
Circular	1592	12980	27110	0.06078	0.5424
Spherical	1570	12970	27060	0.05992	0.5428
Tetraspherical	1545	12960	27000	0.05896	0.5434
Pentaspherical	1531	12960	26970	0.05844	0.5437
Exponential	1256	12880	26250	0.04923	0.5495
Gaussian	1636	13000	27300	0.06215	0.5427
Rational Quadratic	1501	12960	26980	0.05668	0.5436
Hole Effect	1650	13010	27280	0.06269	0.5459
K-Bessel	1849	13060	27710	0.07069	0.5361
J-Bessel	1747	13030	27190	0.06734	0.5485
Stable	1849	13060	27700	0.07082	0.5366

Similarly, the prediction errors of the 11 models with Box-Cox transformed AADT were generated using the ArcGIS's Geostatistical Analyst functions. The results are shown in Figures 46 through 56. The prediction errors in the figures are listed in Table 9 to compare the models. As can be seen in the table, the Rational Quadratic model has a Mean Standardized value closest to 0; the Exponential model has a smallest Root-Mean-Square value; and the Stable model has a Root-Mean-Square Standardized value closest to 1 and a smallest difference between the Average Standard Error and the Root-Mean-Square. Therefore, with the Box-Cox ($\lambda=0.08786$) transformed AADT, the Rational Quadratic model, the Exponential model and the Stable model can be used for AADT predictions.

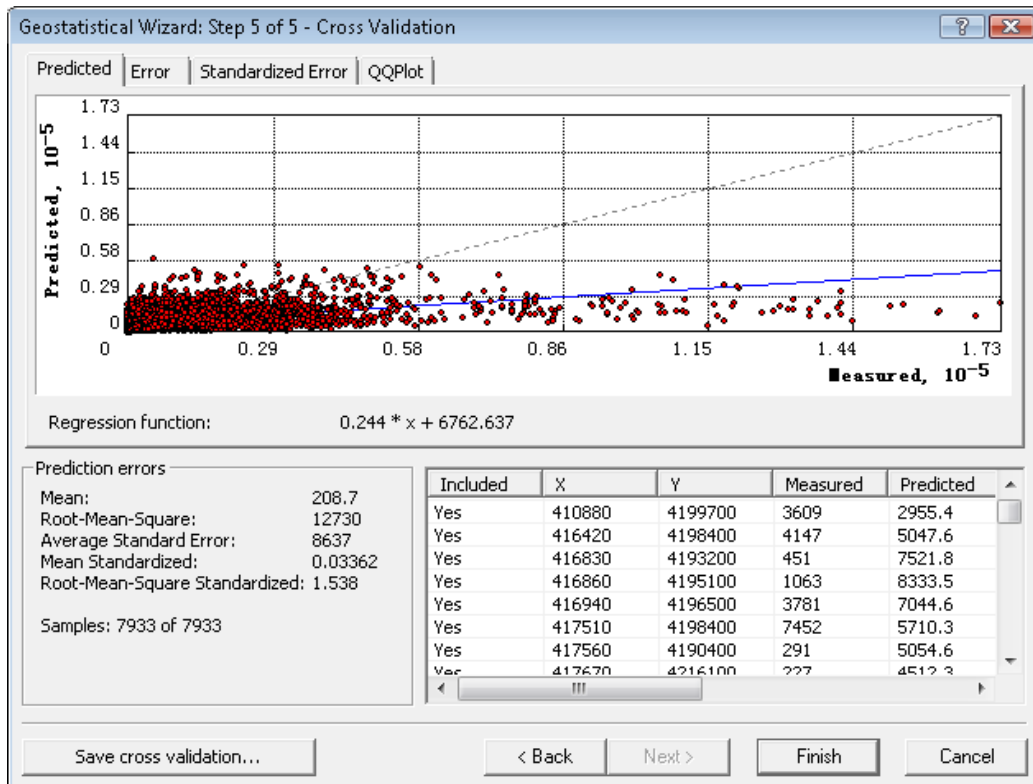


Figure 46: Prediction Errors of Circular Model with Box-Cox Transformed AADT

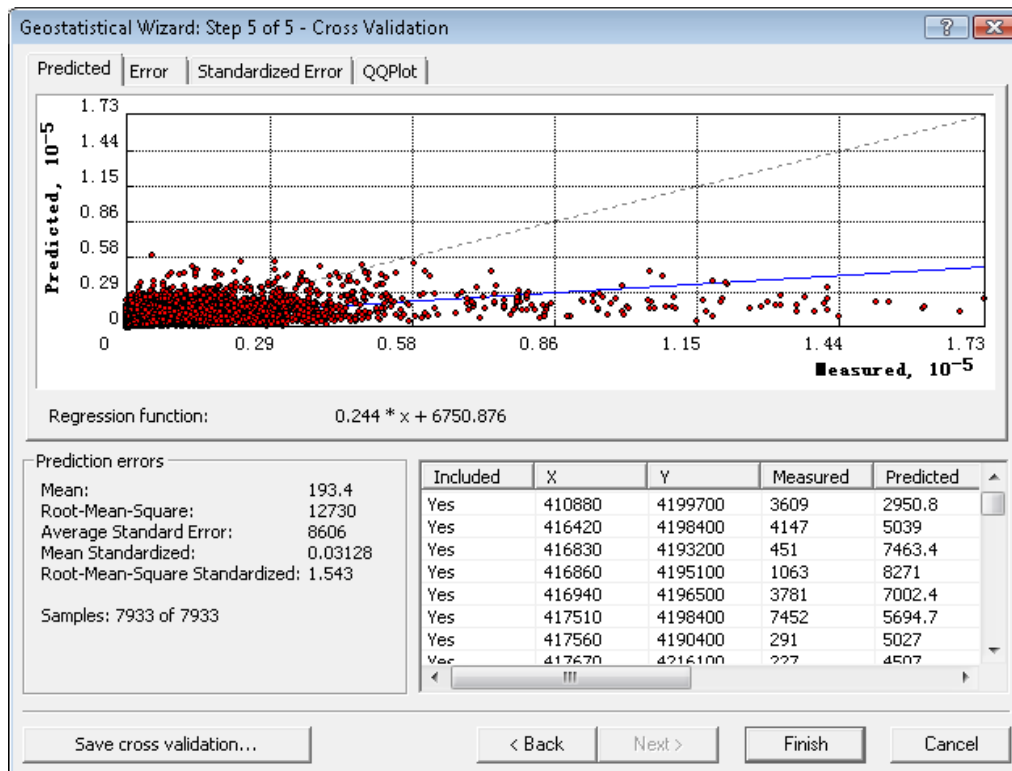


Figure 47: Prediction Errors of Spherical Model with Box-Cox Transformed AADT

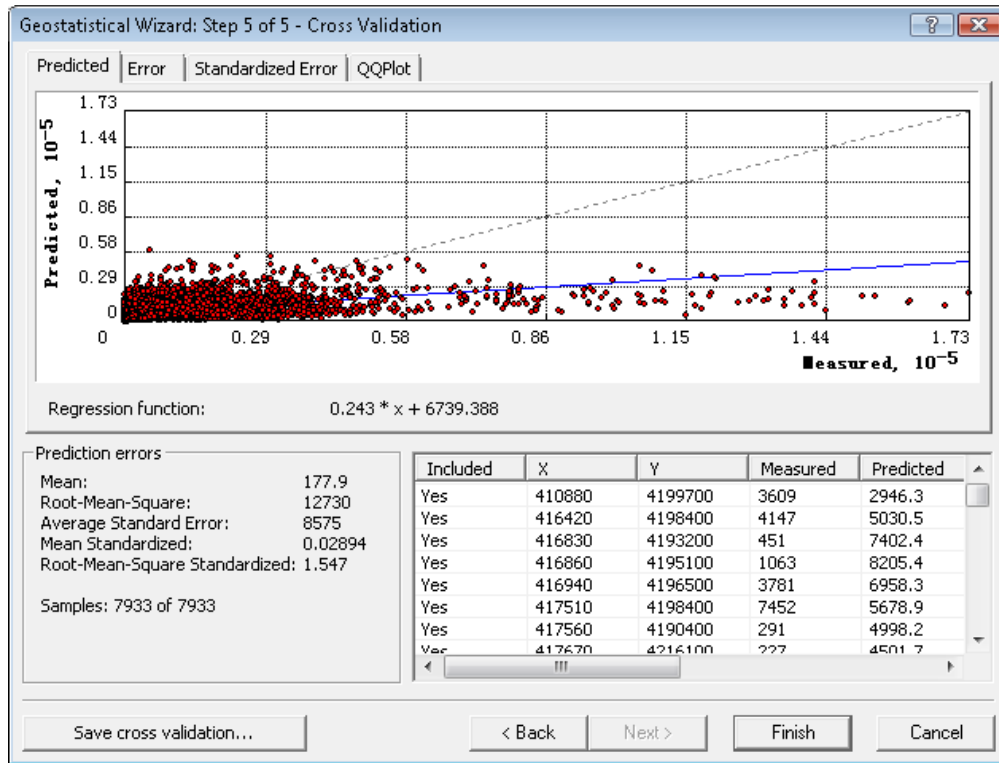


Figure 48: Prediction Errors of Tetraspherical Model with Box-Cox Transformed AADT

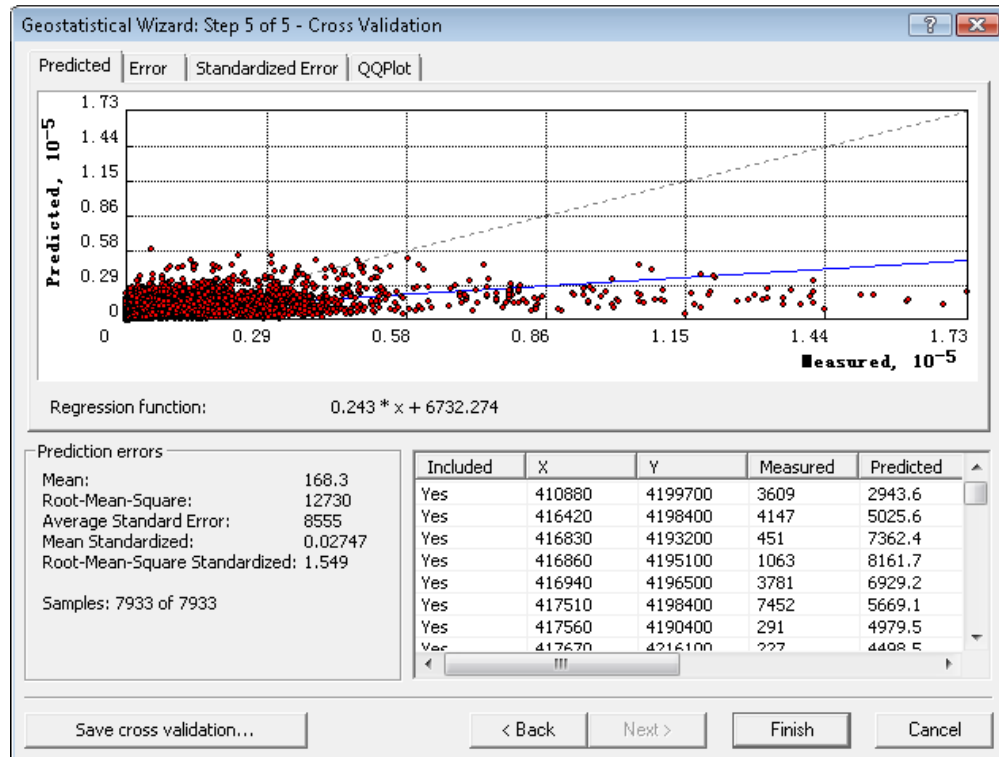


Figure 49: Prediction Errors of Pentaspherical Model with Box-Cox Transformed AADT

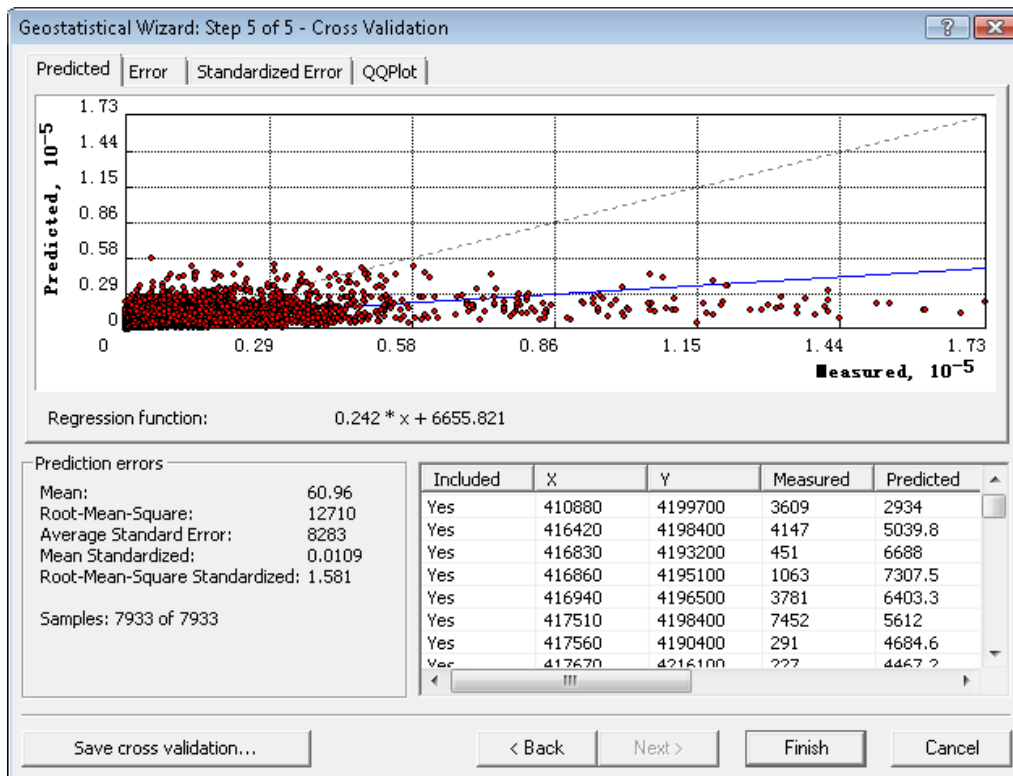


Figure 50: Prediction Errors of Exponential Model with Box-Cox Transformed AADT

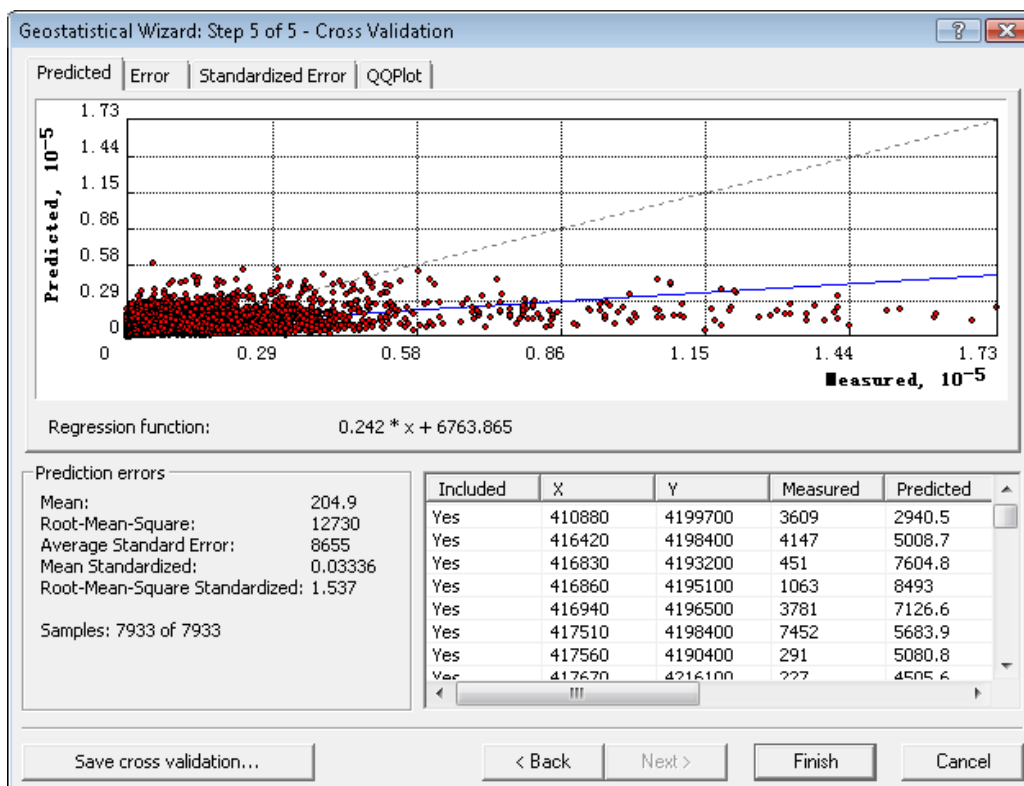


Figure 51: Prediction Errors of Gaussian Model with Box-Cox Transformed AADT

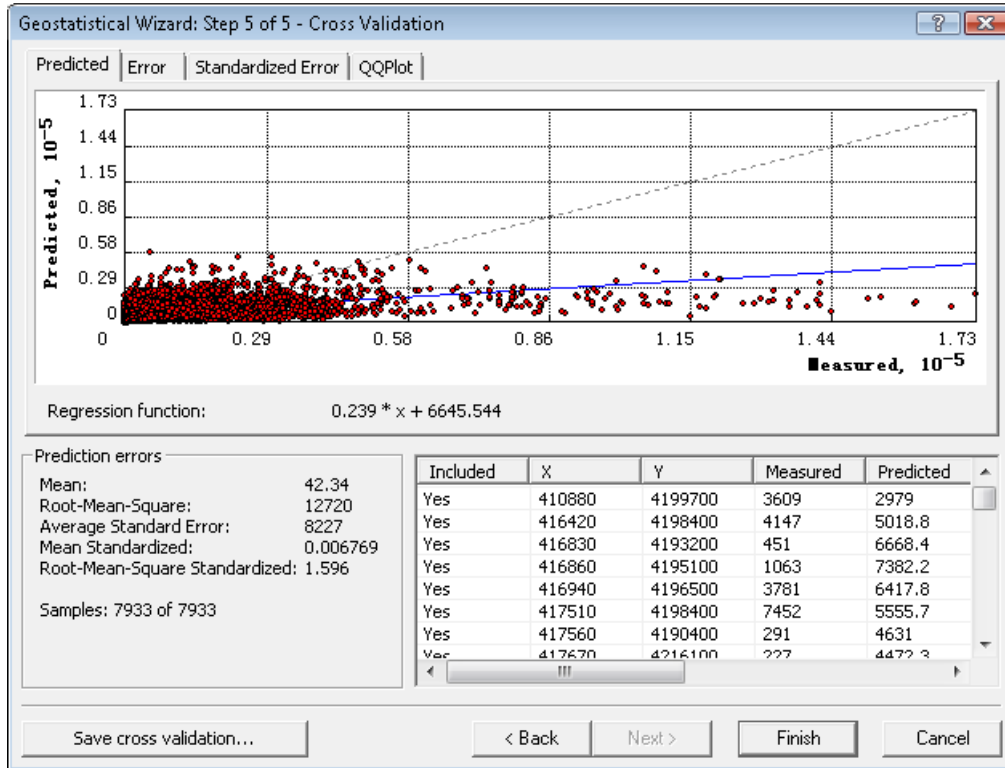


Figure 52: Prediction Errors of Rational Quadratic Model with Box-Cox Transformed AADT

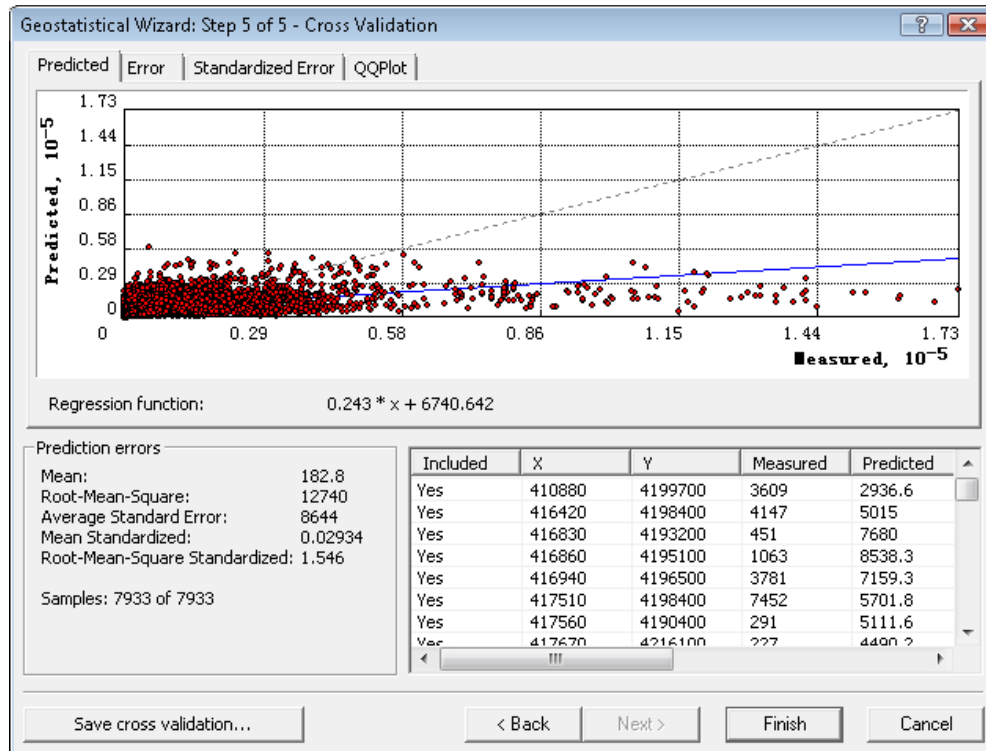


Figure 53: Prediction Errors of Hole Effect Model with Box-Cox Transformed AADT

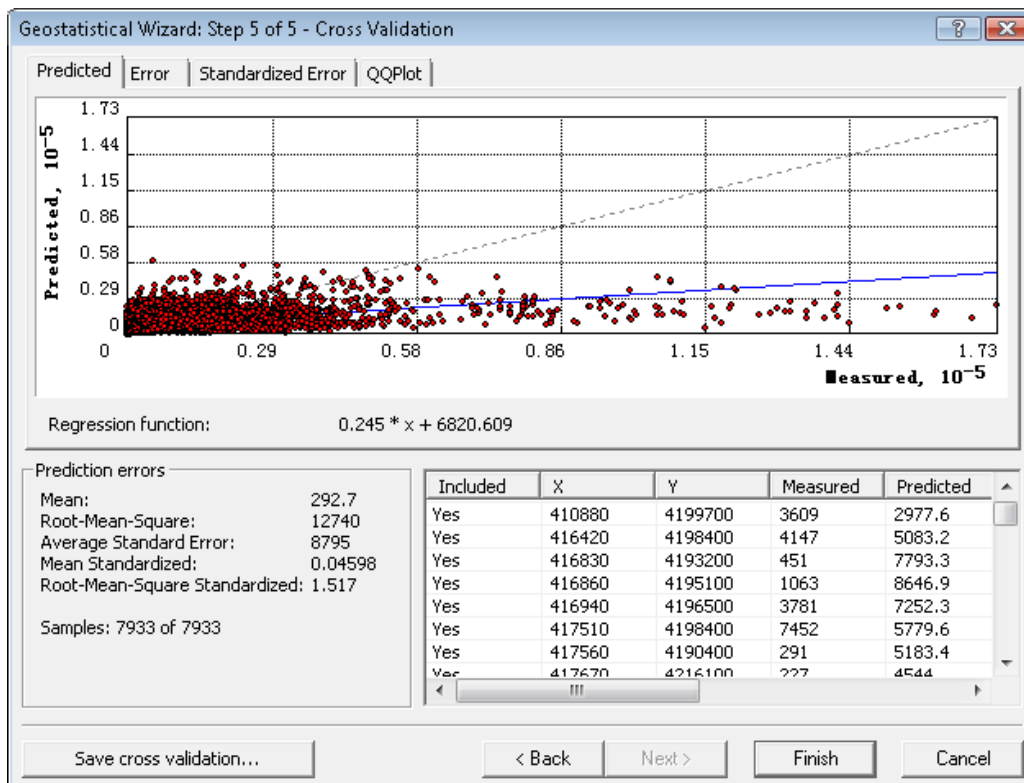


Figure 54: Prediction Errors of K-Bessel Model with Box-Cox Transformed AADT

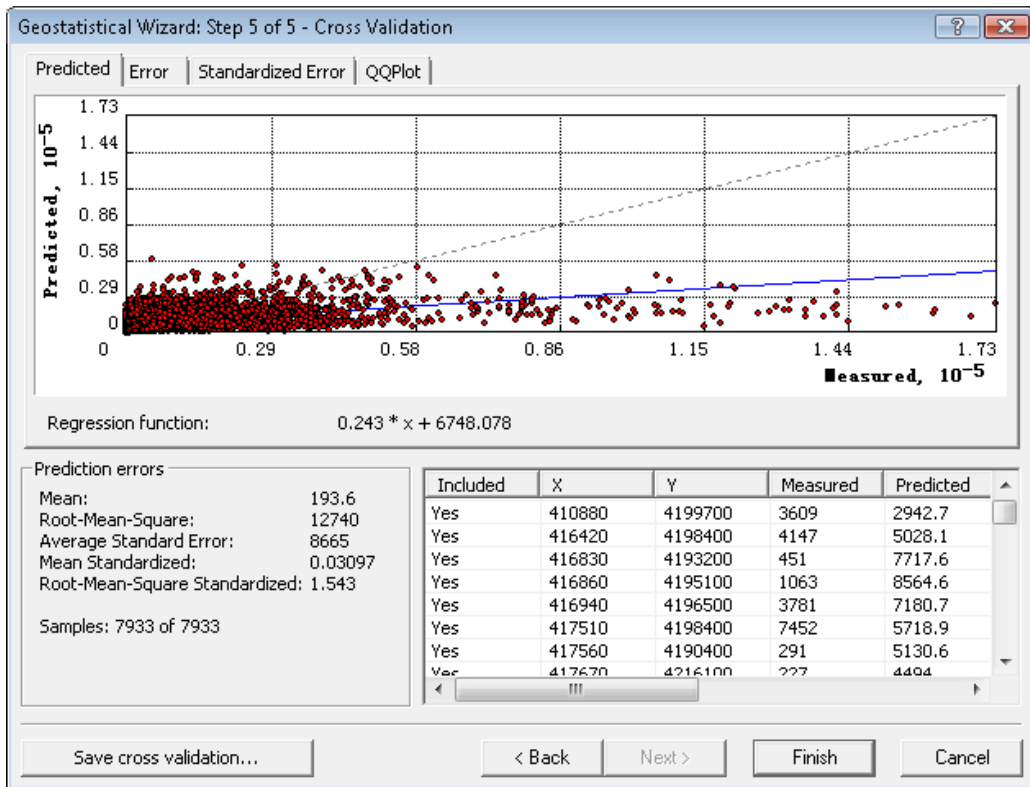


Figure 55: Prediction Errors of J-Bessel Model with Box-Cox Transformed AADT

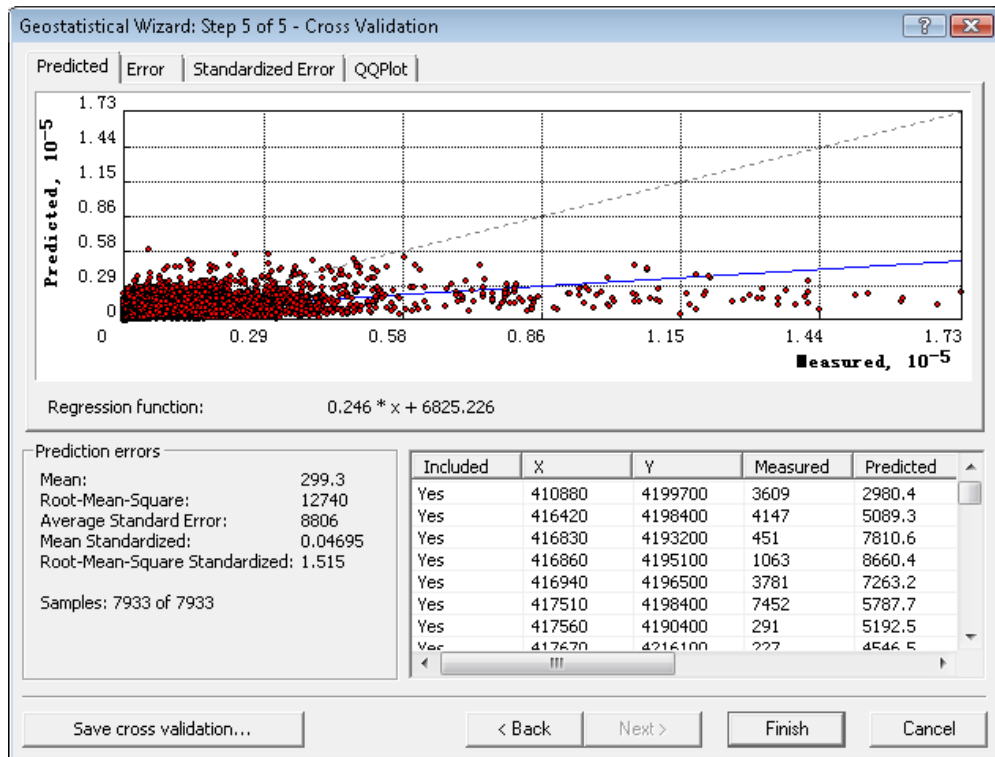


Figure 56: Prediction Errors of Stable Model with Box-Cox Transformed AADT

Table 9: Prediction Errors of Different Models with Box-Cox Transformed AADT ($\lambda=0.08786$)

Model	Mean	Root-Mean-Square	Average Standard Error	Mean Standardized	Root-Mean-Square Standardized
Circular	208.70	12730	8637	0.03362	1.538
Spherical	193.40	12730	8606	0.03128	1.543
Tetraspherical	177.90	12730	8575	0.02894	1.547
Pentaspherical	168.30	12730	8555	0.02747	1.549
Exponential	60.76	12710	8283	0.01090	1.581
Gaussian	204.90	12730	8655	0.03336	1.537
Rational Quadratic	42.34	12720	8227	0.006769	1.596
Hole Effect	182.80	12740	8644	0.02934	1.546
K-Bessel	292.70	12740	8795	0.04598	1.517
J-Bessel	193.60	12740	8665	0.03097	1.543
Stable	299.30	12740	8806	0.04695	1.515

5.3.2: Other Modeling Methods:

In addition to Kriging methods, there exist some other spatial interpolation methods for prediction of attribute values at unsampled locations. Under ArcGIS's Geostatistical Analyst, the interpolation methods include Inverse Distance Weighing (IDW), Global Polynomial Interpolation (GPI), Local Polynomial Interpolation (LPI), Radial Basis Functions (RBF), and Inverse Multiquadric Spline (IMS).

Inverse Distance Weighing interpolation explicitly implements the assumption that things that are close to one another are more alike than those that are farther apart. To predict a value for any unmeasured location, Inverse Distance Weighing will use the measured values surrounding the prediction location. Those measured values closest to the prediction location will have more influence on the predicted value than those farther

away. Thus, Inverse Distance Weighing assumes that each measured point has a local influence that diminishes with distance. It weights the points closer to the prediction location greater than those farther away. Weights are proportional to the inverse distance raised to the power value p . As a result, as the distance increases, the weights decrease rapidly. How fast the weights decrease is dependent on the value for p . If $p = 0$, there is no decrease with distance, and because each weight λ_i will be the same, the prediction will be the mean of all the measured values. As p increases, the weights for distant points decrease rapidly. If the p value is very high, only the immediate few surrounding points will influence the prediction. Geostatistical Analyst in ArcGIS uses power functions greater than 1 (ESRI 2007).

An example of Inverse Distance Weighing using ArcGIS's Geostatistical Analyst is depicted in Figures 57 through 60. The example shows the steps and results for predicting an AADT at a given location.

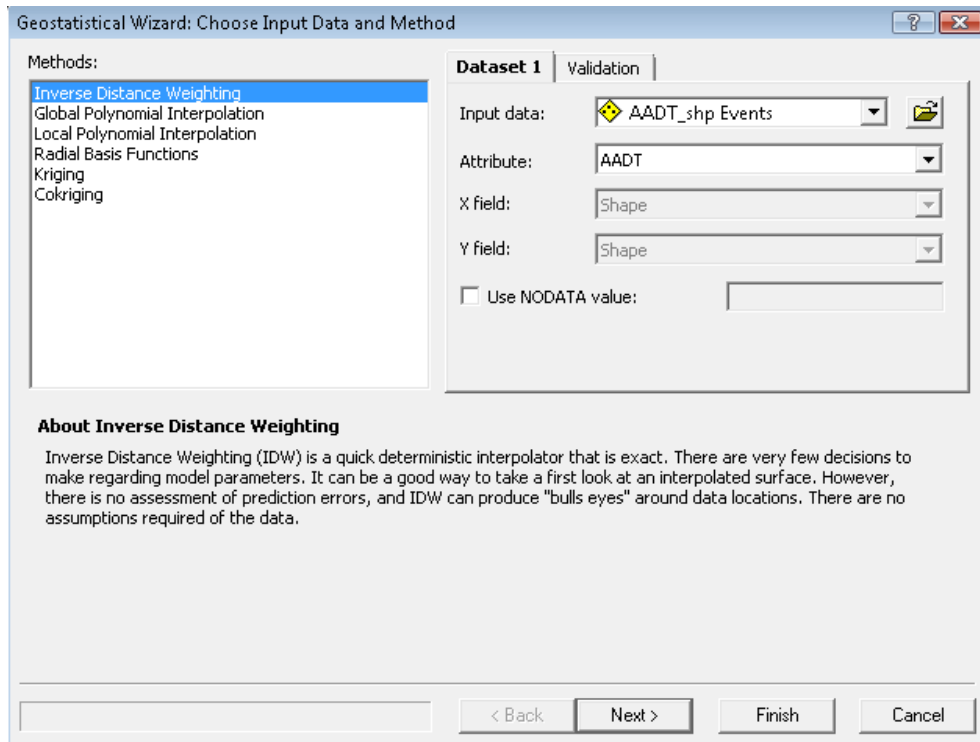


Figure 57: AADT Prediction Using Inverse Distance Weighting Method – Data Input

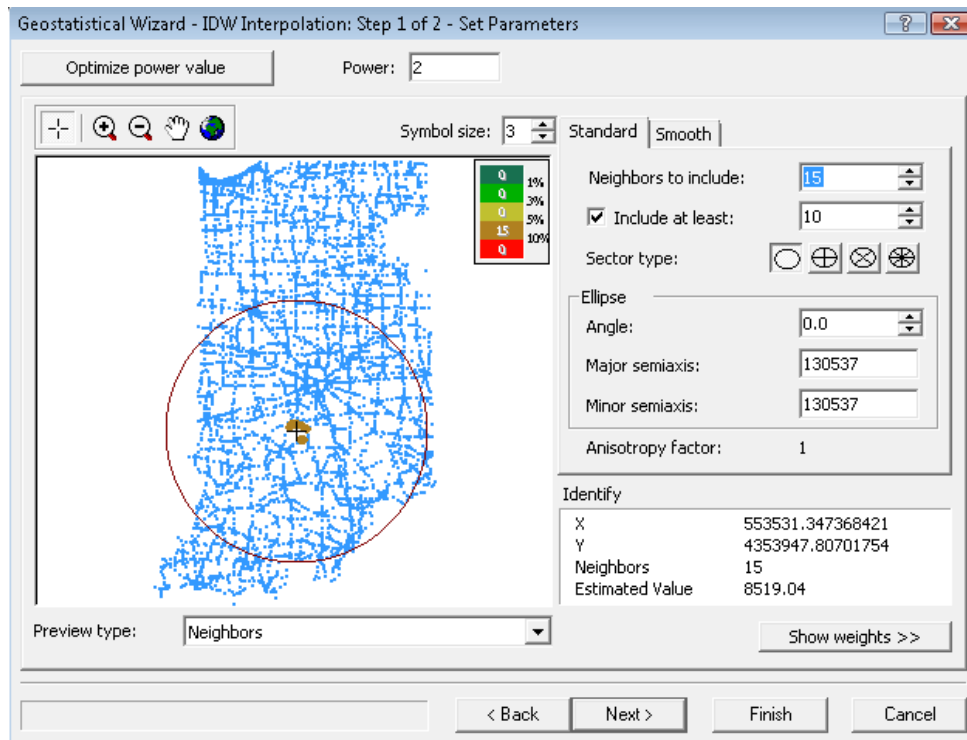


Figure 58: AADT Prediction Using Inverse Distance Weighting Method – Set Parameters

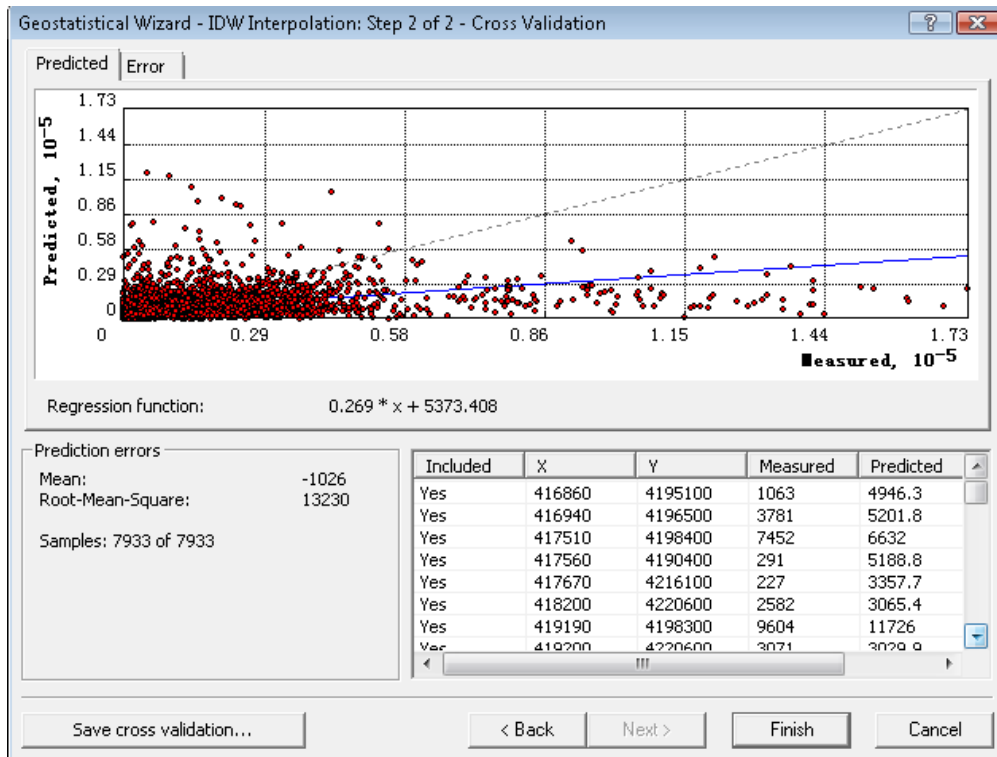


Figure 59: Inverse Distance Weighing AADT Prediction Results

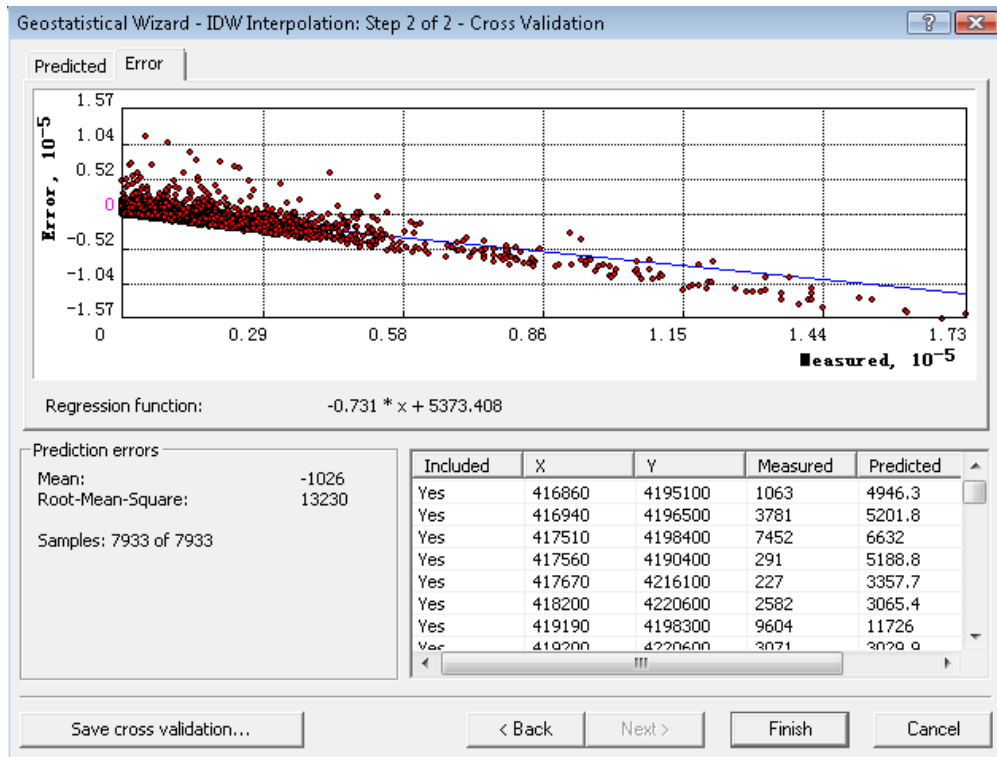


Figure 60: Inverse Distance Weighing AADT Prediction Errors

Global Polynomial interpolation fits a smooth surface that is defined by a mathematical function (a polynomial) to the input sample points. Global interpolation is used for fitting a surface to the sample points when the surface varies slowly from region to region over the area of interest. Since the INDOT AADT varies greatly from region to region as indicated in Figure 32, it was determined that this method was not suitable for the AADT analysis. Therefore, this method was not used in this study.

While Global Polynomial interpolation fits a polynomial to the entire surface, Local Polynomial interpolation fits many polynomials, each within specified overlapping neighborhoods. This method was tested with the INDOT AADT data, but it did not produce good results. Therefore, this method was excluded in this study.

Radial Basis Functions method includes a series of exact interpolation techniques; that is, the surface must go through each measured sample value. There are five different basis functions:

- Thin-Plate Spline (TPS)
- Spline with Tension (SWT)
- Completely Regularized Spline (CRS)
- Multiquadric Function (MF)
- Inverse Multiquadric Function (IMF)

The five basis functions are called kernel functions in ArcGIS. Each kernel function has a different shape and results in a slightly different interpolation surface. In ArcGIS, the steps to run the Radial Basis Functions are similar to those to run the Inverse Distance Weighing. Figures 61 through 64 show an example of AADT predictions with the kernel function of Completely Regularized Spline. Any of other kernel functions can be selected in the drop-down menu shown in Figure 62.

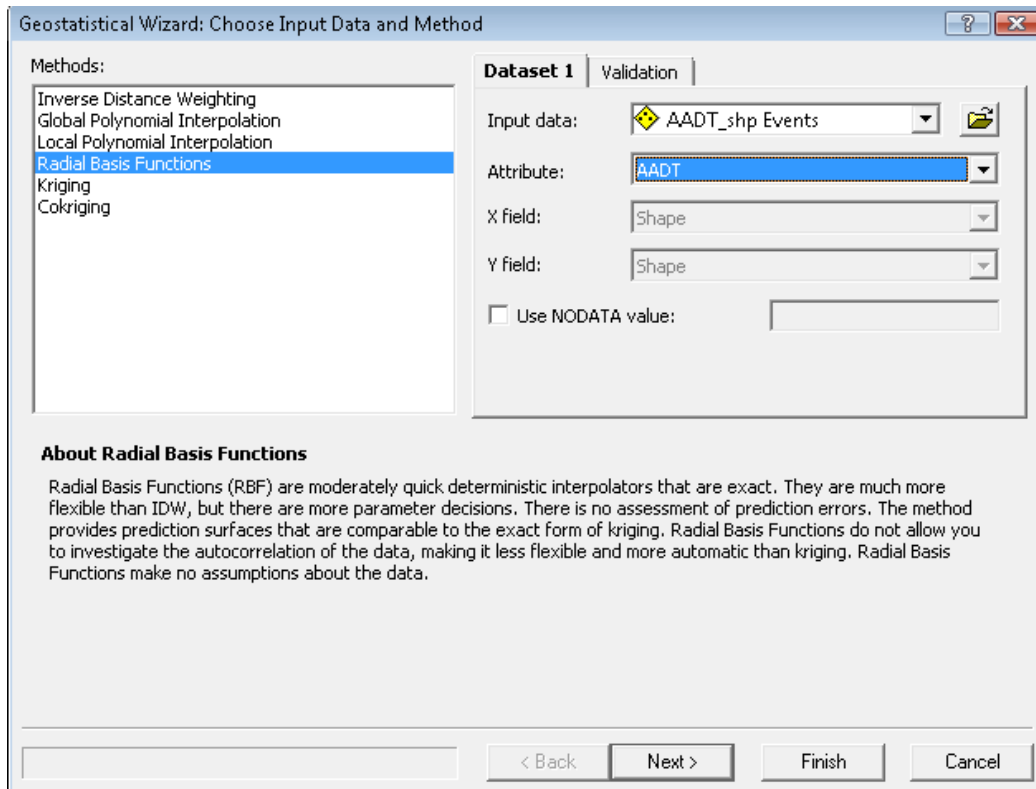


Figure 61: AADT Prediction Using Radial Basis Functions – Data Input

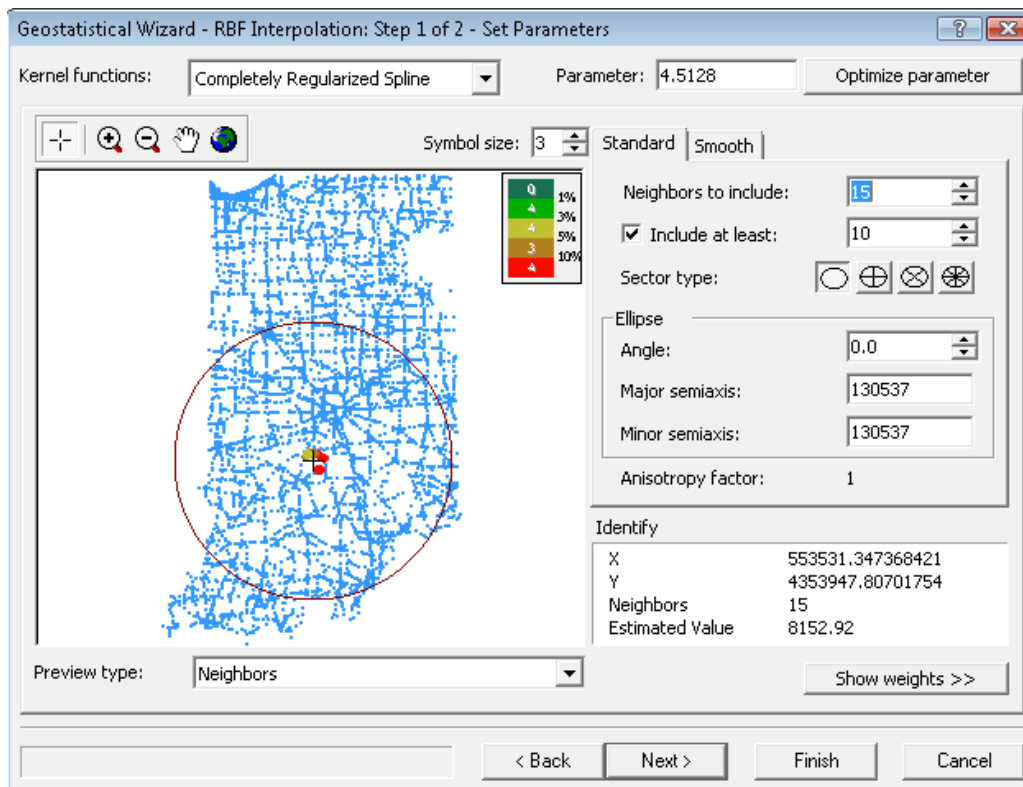


Figure 62: AADT Prediction Using Radial Basis Functions – Specify Functions

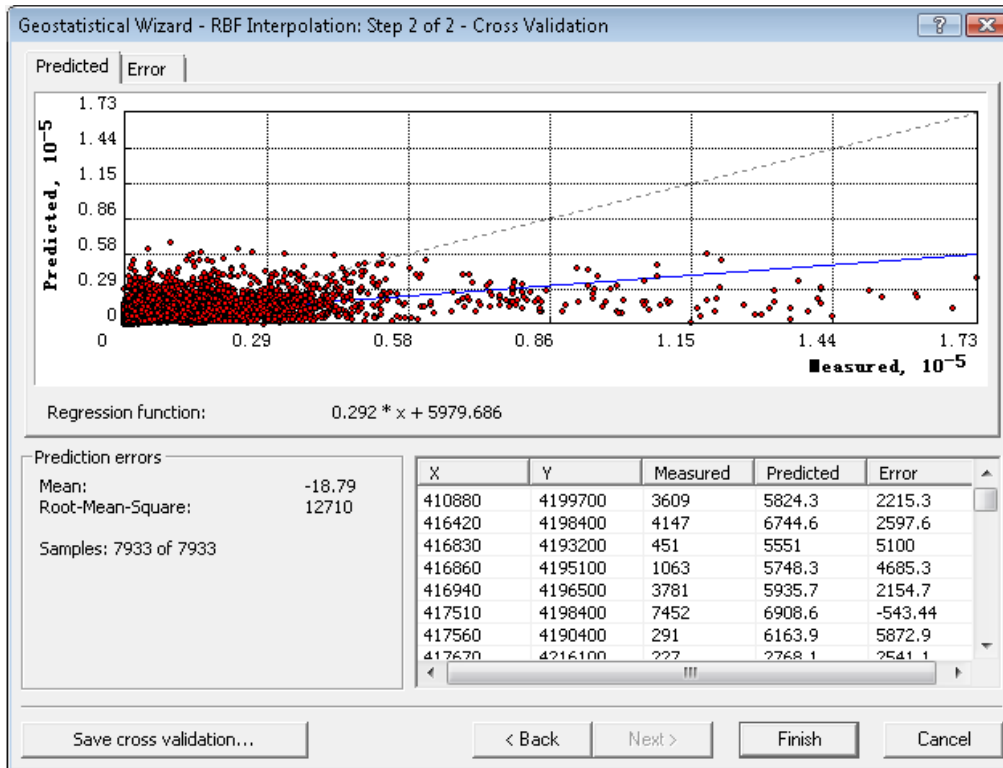


Figure 63: Radial Basis Functions Prediction Results

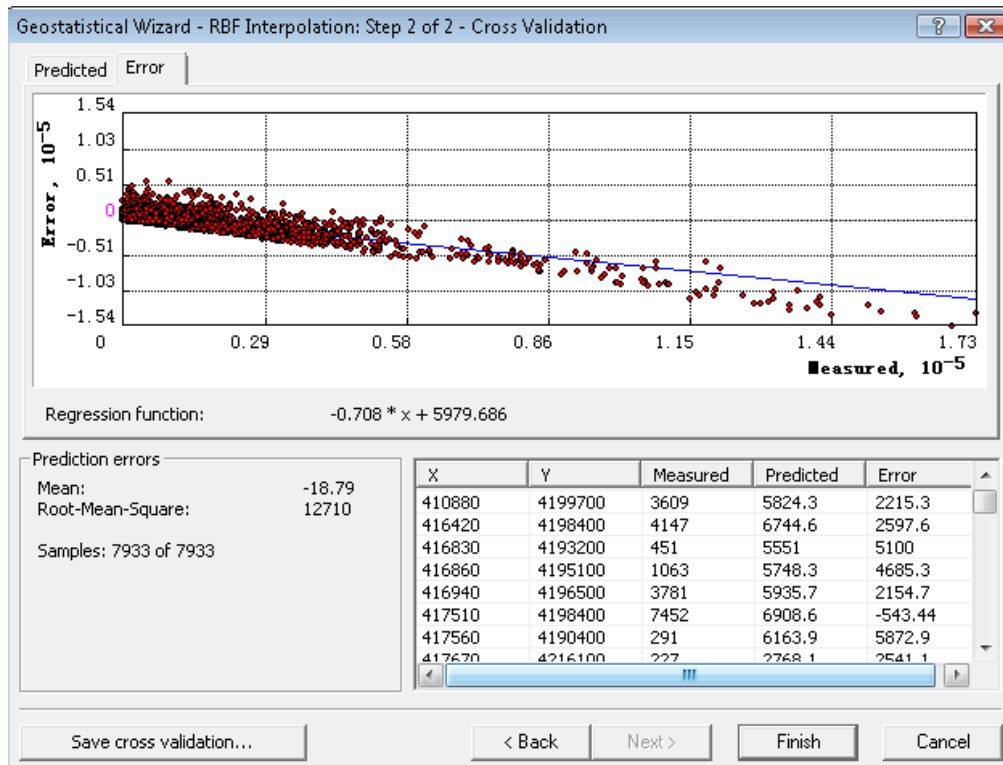


Figure 64: Radial Basis Functions Prediction Errors

5.3.3: Comparison of the Modeling Methods:

To compare the prediction accuracies of the above modeling methods, the recorded AADT values at 22 randomly selected locations were used. The locations in terms of x and y coordinate values were used as input of each of the 10 modeling methods to produce the predicted AADT values. The recorded and predicted AADT values are listed in Table 10. Also included in the last row of Table 10 are the prediction errors of the ten modeling methods. The prediction errors were calculated with the following formula:

$$\Delta = \sqrt{\frac{1}{n} \sum_{i=1}^n (\text{AADT}'_i - \text{AADT}_i)^2} \quad (8)$$

where:

AADT'_i = Predicted AADT at location i;

AADT_i = Recorded AADT at location i;

n = 22, number of locations.

As shown in Table 10 and Figure 65, the Inverse Distance Weighing (IDW) method generated the best AADT predictions among the ten modeling methods.

Table 10: AADT Predictions from Ten Modes

x	y	Recorded AADT	IDW	RBF					Ordinary Kriging			
				CRS	SWT	MF	IMS	TPS	Log Transformed	Box-Cox ($\lambda=0.08786$) Transformed		
									Exponential	Exponential	Stable	Rational Quadratic
474459	4605206	30703	30566	23437	22609	30422	10066	30928	12756	12507	12982	12504
471920	4606008	987	1270	4928	5220	1083	9473	814	14301	13684	13948	14467
471932	4605956	880	1048	4835	5256	1153	12111	892	14948	14303	14621	15179
688524	4301131	480	481	846	912	517	1632	506	1750	1858	1865	1920
551555	4417667	7953	7960	11982	12211	8001	14856	8030	10777	9744	9534	9946
478391	4485380	1888	1888	1886	1885	1880	1759	1881	2928	2212	2253	2195
480241	4485385	2932	2816	2035	2009	2759	1568	2803	2859	2449	2428	2487
672787	4493963	6460	6460	5775	5757	6432	6447	6445	5807	4902	4871	4774
682185	4515096	1160	1160	1329	1390	1160	2287	1160	3374	3876	3888	4123
664671	4502941	1820	1834	2132	2144	1825	2376	1830	3560	3499	3512	3612
457402	4610604	3394	3416	8917	9411	3988	14750	3746	16799	11327	11335	11717
457878	4610080	3038	3050	6387	6831	3140	13973	3036	17936	10428	10502	10879
457808	4609656	2594	2624	7089	7602	2696	13499	2252	16768	11381	11426	11832
457983	4610052	3647	3651	6471	6898	3595	13973	3647	17919	11128	11224	11625
456485	4482520	783	784	978	1002	785	1869	810	1006	883	874	900
460276	4485643	723	735	1334	1362	732	1948	724	1260	1054	1058	1088
465704	4485577	904	1019	2240	2262	1305	2493	1190	2435	3230	3259	3367
592572	4326130	33617	33579	21118	20374	33286	8102	33354	6874	5971	5582	5610
591108	4353216	31416	31339	22769	22128	31301	10506	31143	8641	7536	7278	7376
589280	4351187	3039	2927	5559	5852	2566	11405	2256	7443	7401	7524	7924
589291	4351111	4592	4524	5701	5930	4433	11405	4788	8336	8223	8364	8689
589314	4351230	745	766	3760	4234	880	11405	674	7365	7261	7385	7721
Prediction Error			91	4377	4741	226	10605	728	11355	10349	10434	10609

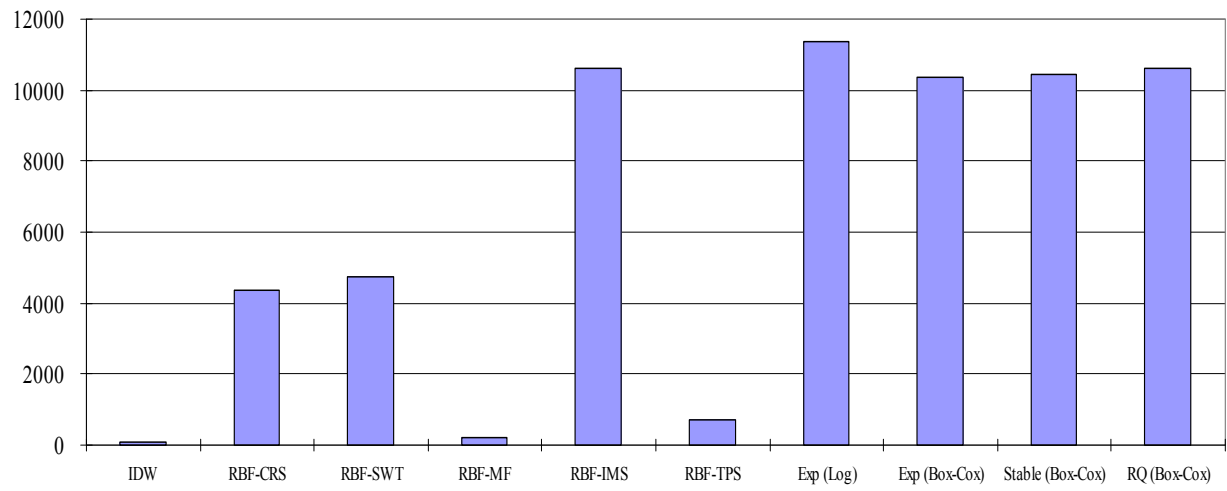


Figure 65: Prediction Errors of the Ten Models

CHAPTER 6: TRAFFIC VOLUME LEVELS AND WIM STATION DISTRIBUTIONS

6.1: Traffic Volume Levels and AADT Prediction

As discussed in the previous chapter, the Inverse Distance Weighing (IDW) method provided better AADT predictions than the other modeling methods. Consequently, the IDW method was used to analyze traffic volume levels. The traffic volume values were grouped into ten levels based on predicted AADT. Then the AADT distributions were depicted on the Indiana map using different colors. Using ArcGIS, traffic volume distribution can be obtained as follows:

1. Convert the AADT dataset from the format (x, y, AADT) to the ArcGIS shape file AADT_shp.ly;
2. Load the shape file in ArcMap.
3. Click Geostatistical Analyst and select Geostatistical Wizard, the window shown in Figure 66 will appear.
4. Select Inverse Distance Weighing under Method, select AADT under Attribute, and click Next, the window shown in Figure 66 will appear. If an AADT value is to be predicted at a location (x, y), input the coordinates, the predicted AADT will be generated as shown in Figure 67.
5. Click Next, the Cross Validation window shown in Figure 68 will appear.
6. Click Next, the prediction map as shown in Figure 69 will appear.

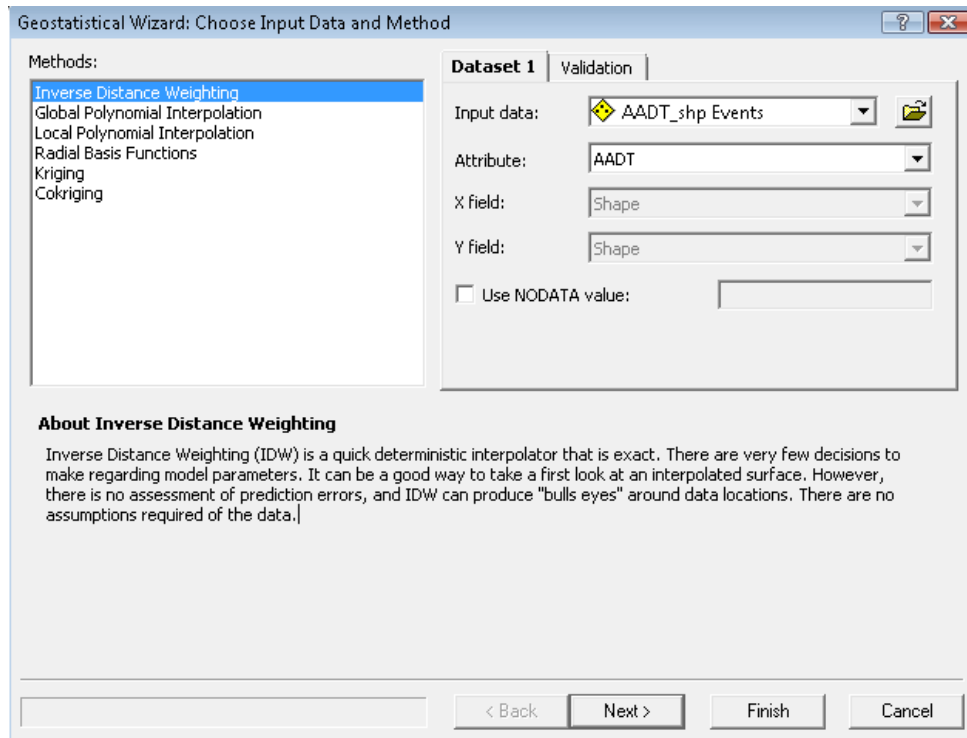


Figure 66: Method and Data Window in Geostatistical Wizard

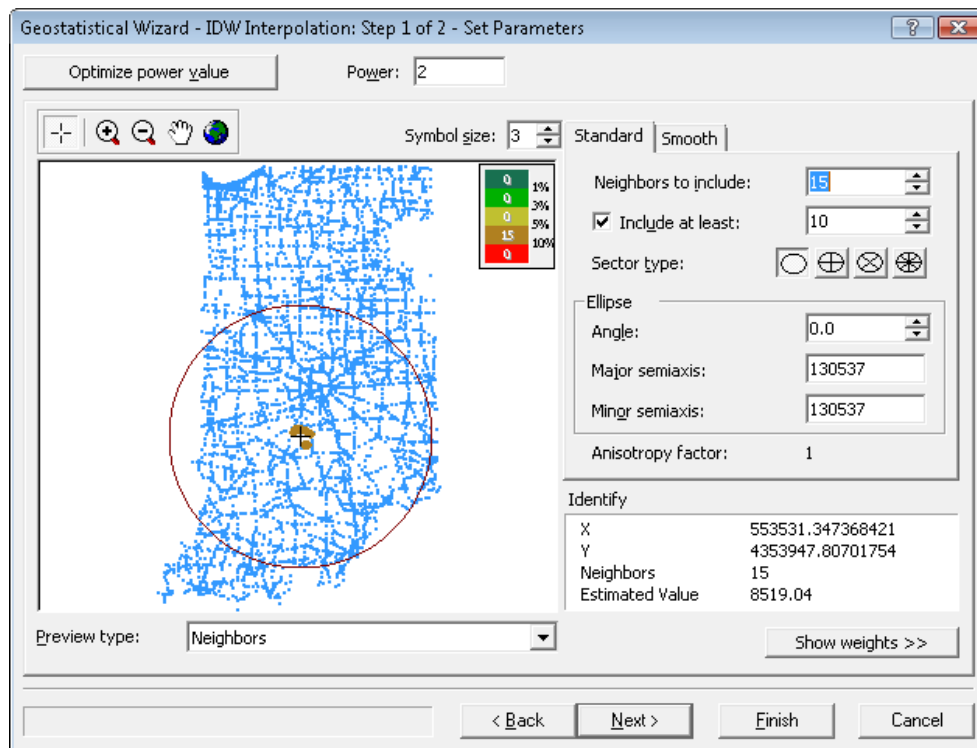


Figure 67: Set Parameters Window in Geostatistical Wizard

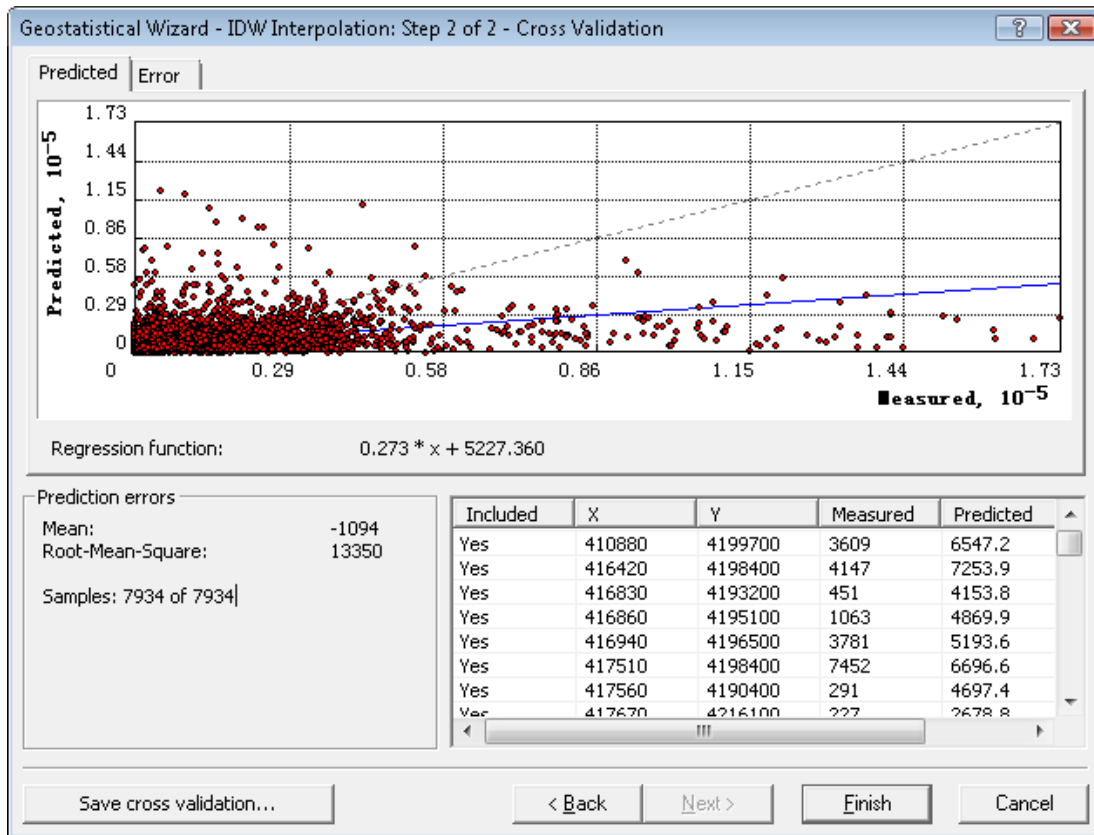


Figure 68: Cross Validation Window in Geostatistical Wizard

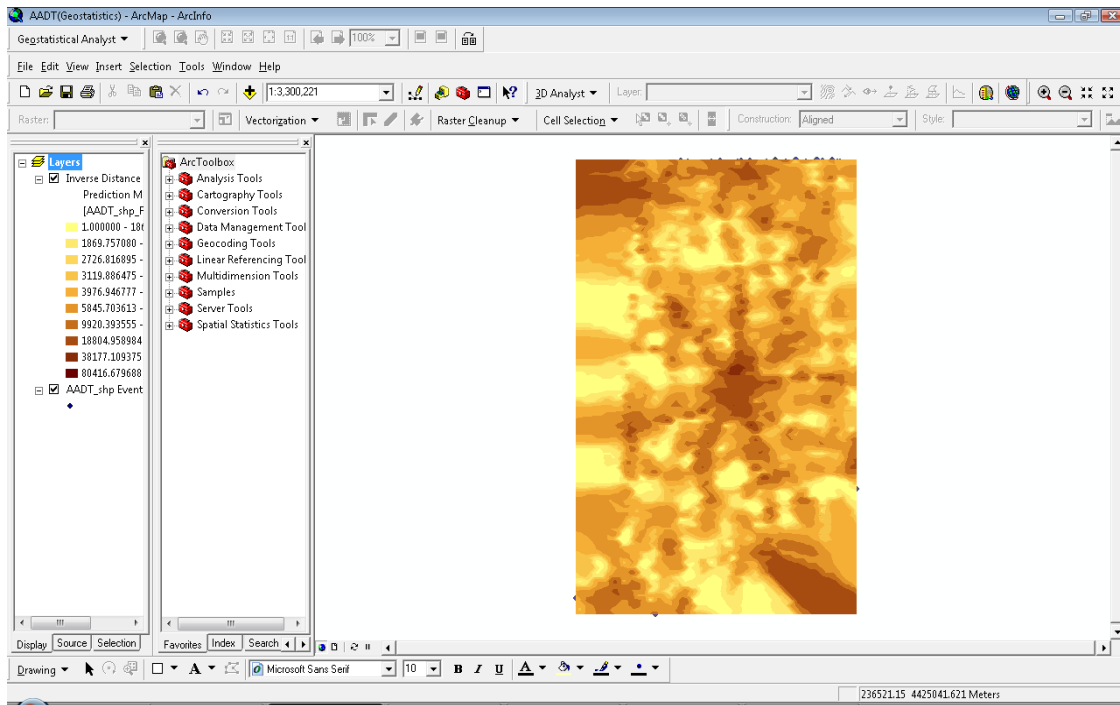


Figure 69: Prediction Map Generated by Inverse Distance Weighing Method

As can be seen in the prediction map shown in Figure 69, the AADT values in Indiana are grouped into ten levels as specified. The AADT levels are illustrated by the colors in the map, with the light colors for low AADT levels and the dark colors for high AADT levels.

6.2: Possible Locations of Future WIM Stations

There were 47 WIM stations in Indiana. It is likely that in the future more WIM stations will be needed to improve the coverage and quality of traffic data collections. Thus, an attempt was made in this study to reasonably determine the locations for the future WIM stations. If new WIM devices are ever to be installed, it is desired to install them at the locations so that the WIM stations would best reflect the patterns and characteristics of the traffic conditions in the state. In this study, the locations of the future WIM devices were determined on the basis of the spatial AADT map generated using various ArcGIS functions.

To show AADT distributions and the WIM stations on the same map, the triangulated irregular network (TIN) method in ArcGIS was selected. TINs are made up of triangular facets and the nodes and edges that make up the triangles. They may also contain breaklines—lines that follow sets of edges that play important roles in defining the shape of the surface. Examples of breaklines are ridgelines, roads, or streams (ESRI 2007). A 2D TIN map can be created with ArcGIS through the following steps.

1. Start ArcGIS and load AADT.shp.
2. In the 3D Analyst drop-down menu, select Create/Modify TIN.
3. In the window shown in Figure 70, select AADT in Layers and select AADT_COUNT in Height Source. The 2D TIN map is created as shown in Figure 71.

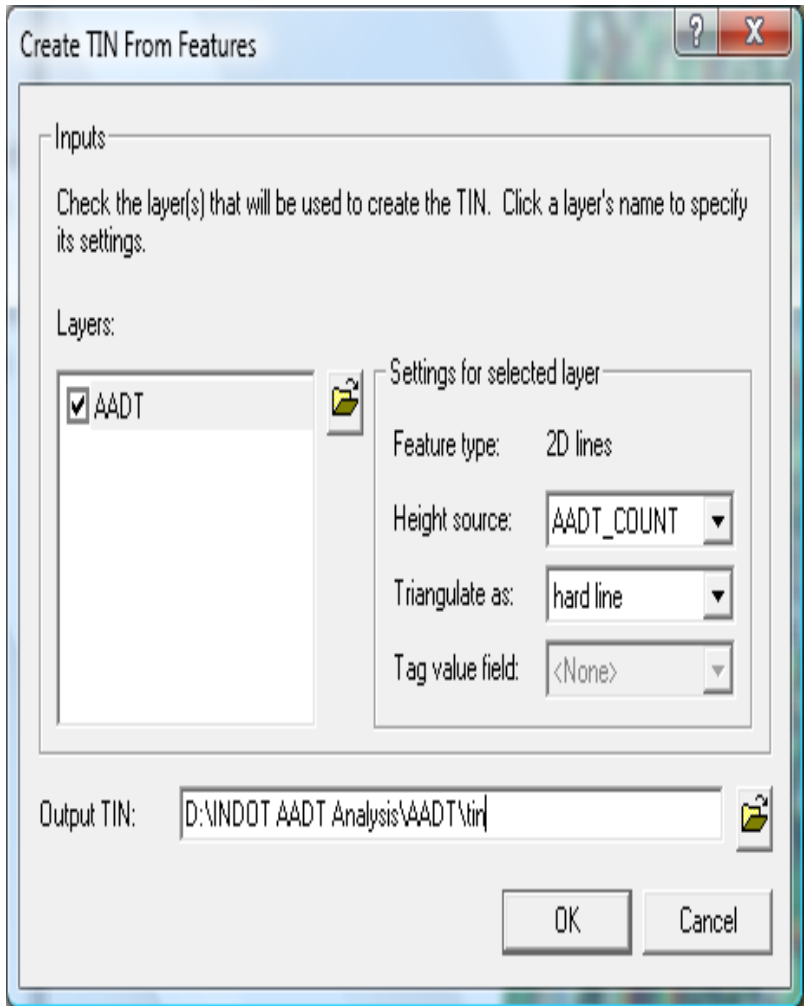


Figure 70: 2D TIN Map Input Window

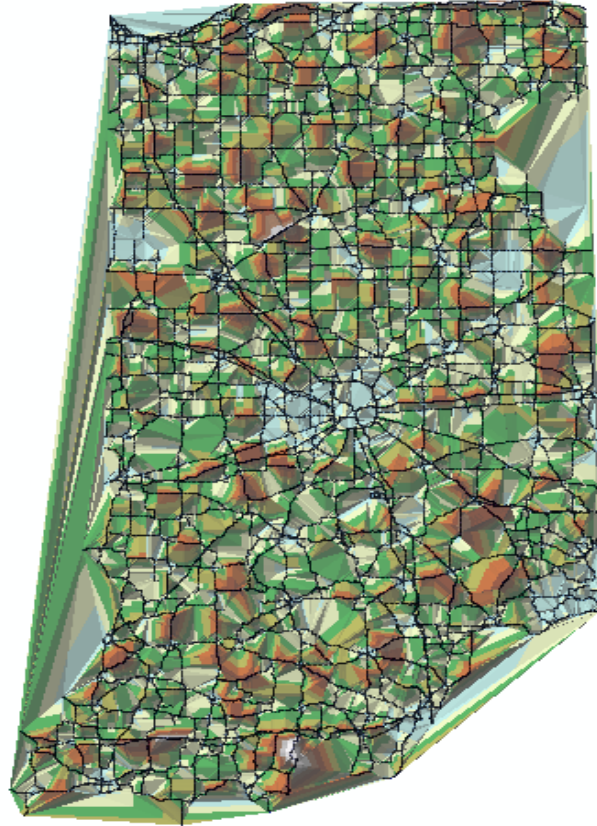


Figure 71: A 2D TIN Map of Indiana AADT

Although the map in Figure 71 shows the AADT values in different colors, the AADT distributions are not clear. To improve the map, the 2D TIN map can be changed to a 3D map by using ArcScene in ArcGIS. The following steps can be used to create a 3D AADT distribution map with WIM stations shown on the map.

1. Start ArcGIS and click ArcScene;
2. Load wim_sites, AADT, and TIN map;
3. Right click Properties, select Display, select 30% Transparent;
4. Click Navigate and select appropriate angle.

The 3D map with WIM stations is shown in Figure 72. In the 3D map, the heights of the z values represent AADT and the red dots are the WIM stations. The 3D map clearly shows the areas with high and low AADT values. However, when analyzing the AADT distributions, there

is a problem with the 3D map, i.e., the z values in high AADT areas block the views to the details behind these areas.

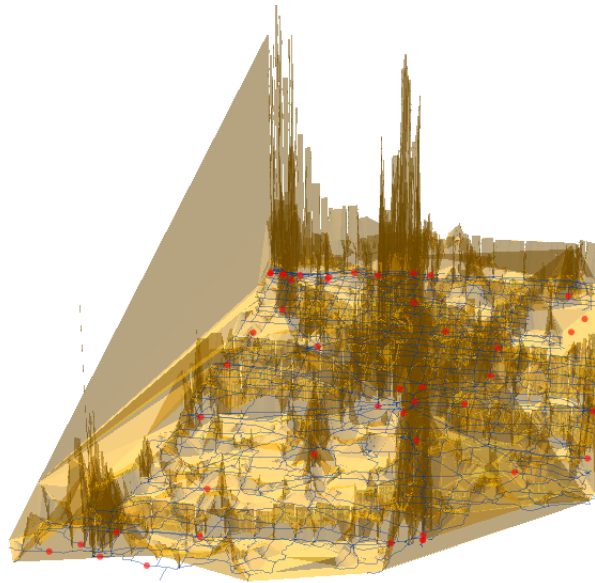


Figure 72: 3D AADT Map with WIM Stations

To convert the 3D map in Figure 72 to a 2D map, start ArcMap and load AADT to TIN map and the map in Figure 73 can be created. The AADT values were divided into 15 levels in the map. Because most of the AADT values are in the lowest level (1 to 11502), the color for this AADT level dominates in the 2D map and other AADT levels can not be clearly seen. To solve this problem, the AADT values were log transformed to make the divided levels more evenly spread. Figure 74 is the 2D map created with the log transformed AADT data.

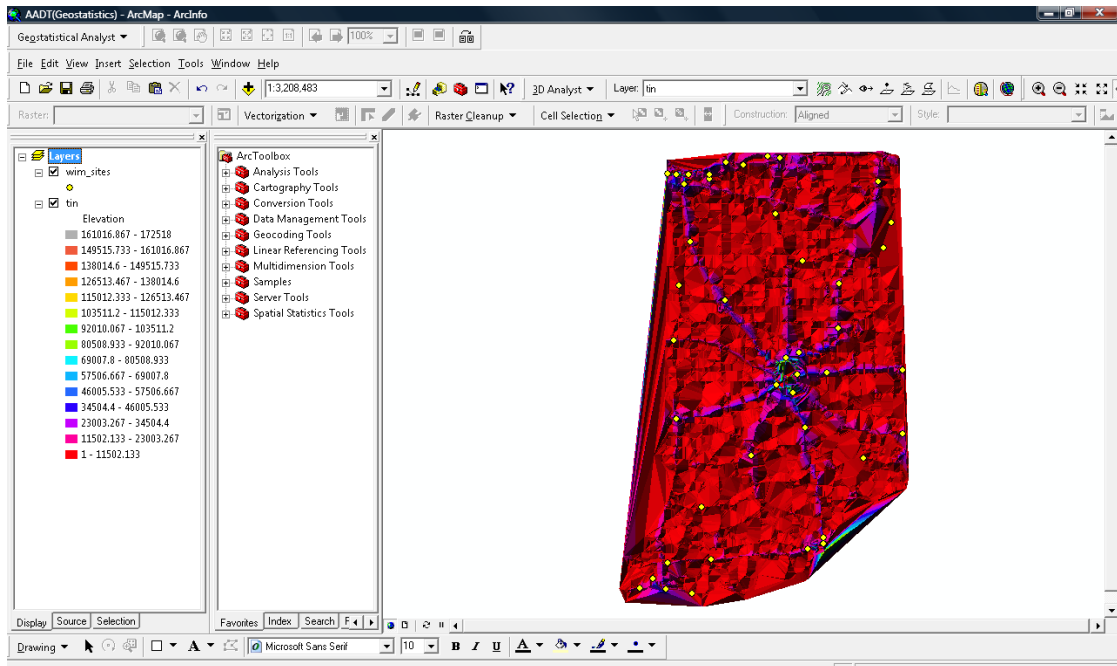


Figure 73: 2D Map of Original AADT with WIM Stations

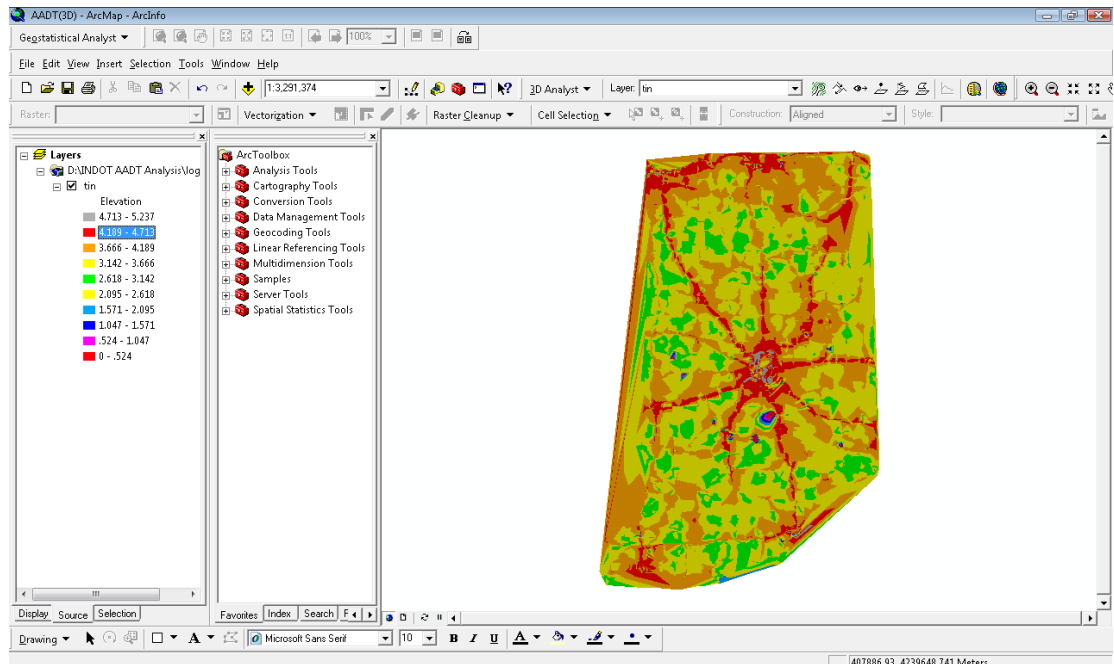


Figure 74: 2D Map of Log Transformed AADT

Figure 74 illustrates the AADT distributions on the highway system with 10 levels. As can be seen, on the interstate highways most of the AADT values are shown in red, which

corresponds to the level between 4.189 and 4.793 of the log transformed AADT or between 15452.14 and 62086.90 of the original AADT values. To examine the relationship between the AADT values and the WIM station locations, the WIM stations were added to the 2D map of the log transformed AADT by including WIM_sites file in ArcMap. Figure 75 shows the WIM stations as the black triangles on the AADT map.

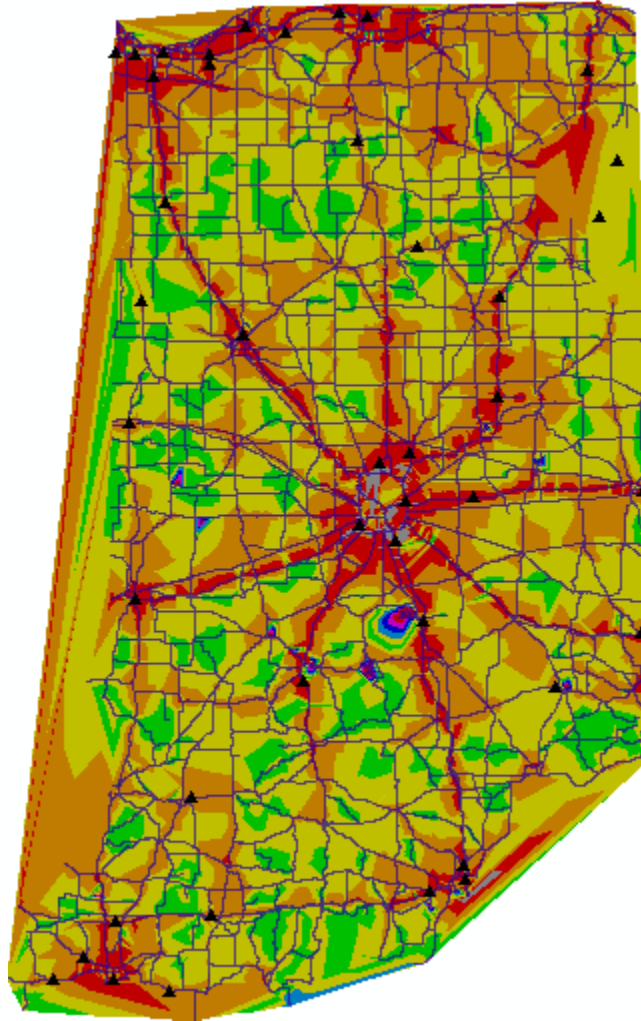


Figure 75: 2D Map of Log Transformed AADT with WIM Stations

The map in Figure 75 shows that most of the WIM stations are located on the interstate highways. That is, the high AADT areas are well covered by the WIM stations. However, there are only a few WIM stations on the relatively low AADT roads, such as on the state roads and

the US routes. Although it is appropriate to install more WIM stations on high volume roads, it should also be necessary to install some WIM stations in low volume roads in order to capture the main characteristics of AADT distributions in the state. With the map, it is possible to identify the locations that may need additional WIM stations.

If additional funds are available for new WIM stations, it is necessary to determine the reasonable locations of the new WIM stations. To reflect the traffic volume changes, the WIM stations should be distributed in such a way that they can cover as many levels of traffic volumes as possible. It is recommended that the following principles be considered to determine the locations for the new WIM stations:

1. A new WIM station should be placed at a location with a traffic level that is not covered by the existing WIM stations.
2. A new WIM station should be placed at a location where traffic volume changes from one level to another level.
3. Higher traffic areas should have higher priority for a new WIM stations.

The proposed location of a new WIM station can be determined by considering the above principles. To mark the coordinates of a proposed new WIM station location, first click Interpolate Point on the ArcMap menu as shown in Figure 76. The next step is to click the proposed location of the new WIM station and then right click at the location and select Properties. The coordinates of the new WIM station location is shown in the new window on the map as illustrated in Figure 77.

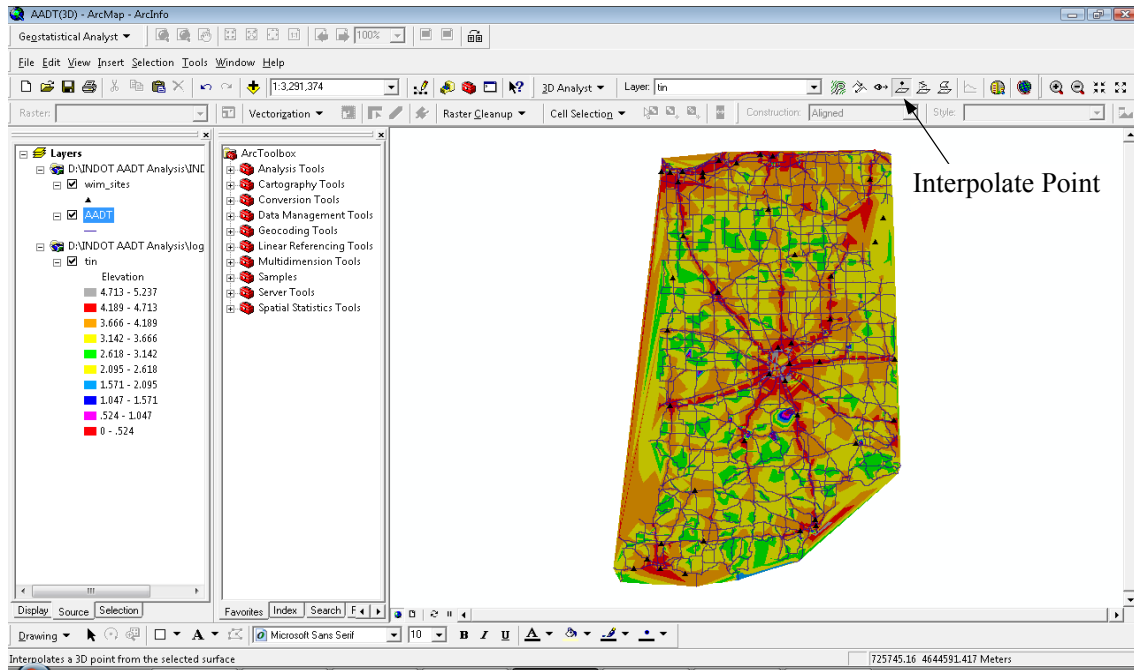


Figure 76: Interpolate Point in ArcMap

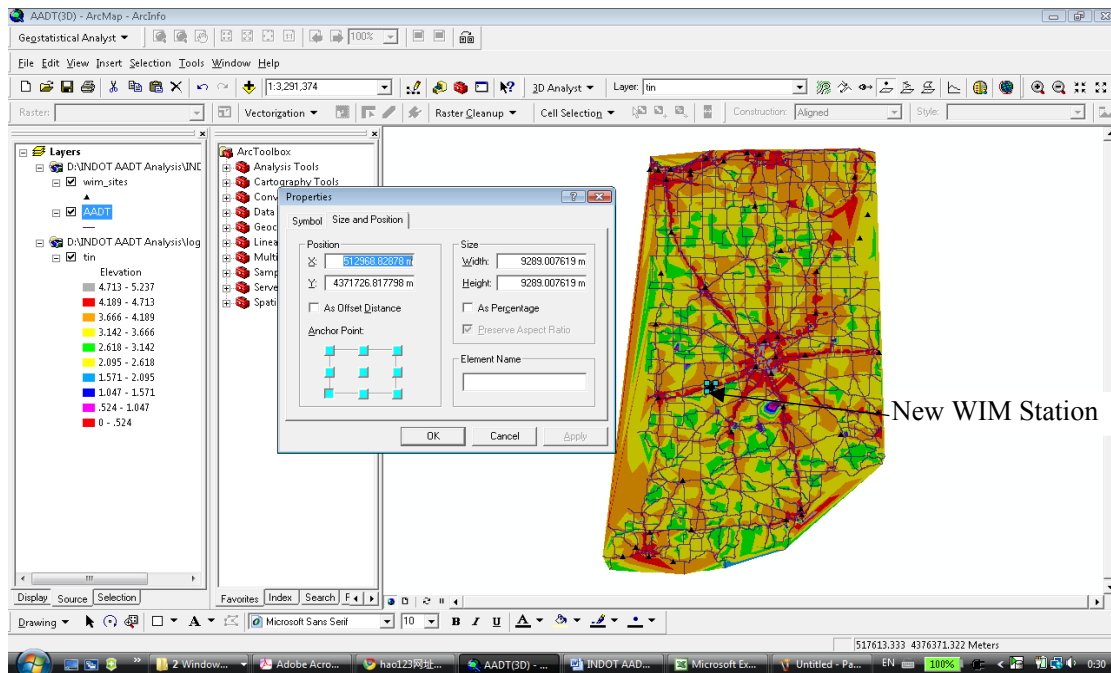


Figure 77: Coordinates of the Proposed New WIM Station

Based on these principles and procedures, the future WIM locations can be identified.

Table 11 lists the proposed coordinates of the future WIM locations. The coordinates in Table

11 are provided for INDOT to consider first if new WIM stations are to be installed in the future. In case all of the coordinates in Table 11 are used up, additional coordinates shown in Table 12 should be considered for new WIM station locations. The coordinates in Table 12 are provided as the secondary locations after the ones in Table 11.

Table 11: Proposed Locations of Future WIM Stations

Site	x	y	Site	x	y
1	570444.618005	4477969.676659	7	506292.336930	4430363.459028
2	512097.973226	4373468.223323	8	596860.263154	4308445.096803
3	557672.218153	4417300.777361	9	578572.508820	4394658.795805
4	626469.008266	4353729.0599916	10	602665.899450	4372597.377879
5	555930.527264	4576665.493698	11	623856.471932	4554894.357587
6	562897.290082	4541831.675920	12	492068.528003	4585954.511773

Table 12: Secondary List of Proposed Locations of Future WIM Stations

Site	x	y	Site	x	y
1	546931.791005	4506707.576326	15	516307.059541	4199589.416245
2	621243.935599	4526156.457919	16	570299.477098	4228327.315913
3	615148.017488	4587115.639032	17	539529.604727	4281158.606210
4	538513.618375	4298865.796914	18	479731.550873	4319766.087581
5	614277.172043	4315411.860359	19	666673.039618	4362147.232545
6	627920.417340	4381305.832324	20	666092.475989	4474776.576696
7	543303.268319	4264031.979136	21	514275.086837	4542412.239549
8	452735.342095	4277965.506247	22	627775.276432	4608886.775144
9	632710.067284	4288125.369766	23	569138.349838	4583341.975439
10	575524.549764	4270127.897247	24	486698.314429	4343278.914582
11	501502.686985	4246615.070246	25	614712.594765	4316282.705804
12	471893.941873	4256194.370136	26	629516.967321	4382466.959583
13	546931.791005	4506707.576326	27	516307.059541	4199589.416245
14	621243.935599	4526156.457919	28	570299.477098	4228327.315913

The locations listed in Table 11 and 12 can be shown in the 2D map. As shown in Figure 78, the coordinates in Table 11 were included in ArcMap as the file New_WIM(first_Class) Events. Similarly, the coordinates in Table 12 were included as the file New_WIM(Second_Class) Events. The two files were added as new layers in ArcMap. Figure 79 shows the existing WIM stations (black triangles), the first set of proposed future WIM stations (red circles), and the second set of proposed future WIM stations (black circles).

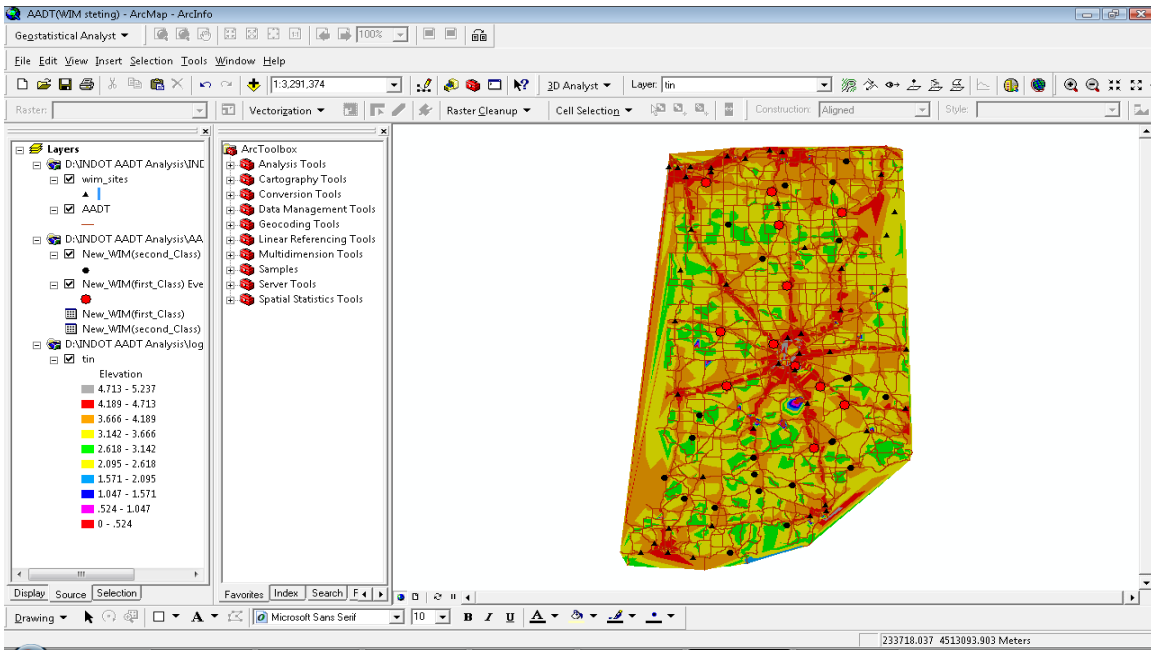


Figure 78: Adding Coordinates of the Proposed New WIM Station in the Map

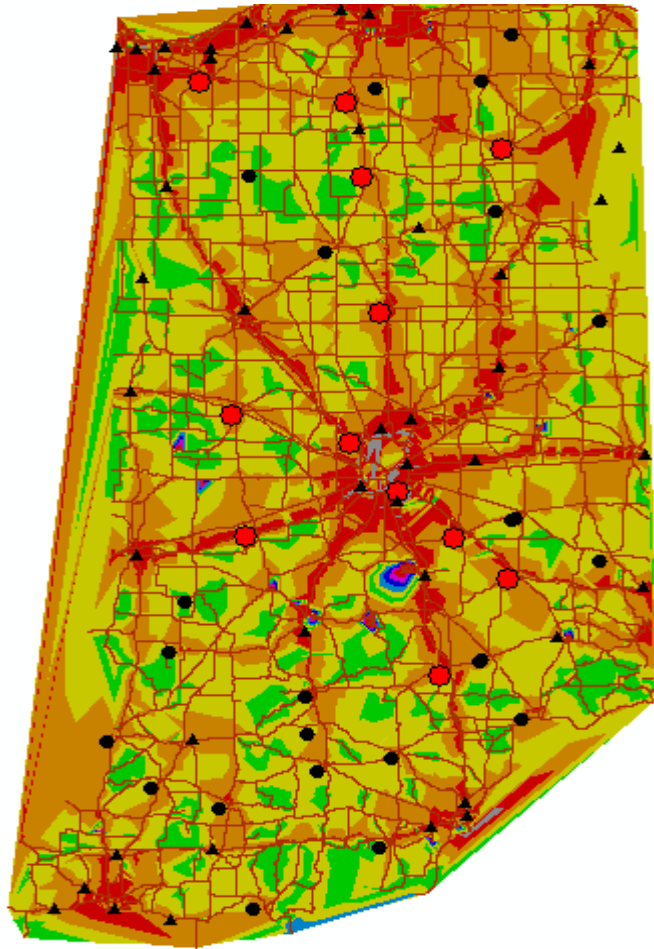


Figure 79: Locations of Existing and the Proposed WIM Stations

CHAPTER 7: CONCLUSIONS

In order to satisfy the requirements of the MEPDG, it is essential to prepare the truck traffic inputs because truck traffic is the most important requirement for the new design method. INDOT has made great effort to retrieve the required traffic information from the stored WIM data. As presented in this report, a Visual Basic computer program was developed and was successfully utilized to obtain the necessary traffic information for the new pavement design method from the WIM data. The truck traffic data include average annual daily truck traffic, average monthly and hourly truck traffic, adjustment factors, axle load spectra, and axle weight and spacing values. The truck traffic can be expressed in individual vehicle types as well as in combined truck traffic values. It was found that the WIM data contained a noticeable amount of unclassified vehicles, which would affect pavement designs if their patterns and components could not be reasonably identified.

Furthermore, the INDOT AADT data were used in this study to analyze the spatial distributions of the traffic volumes in Indiana. The spatial distributions of traffic volumes were obtained to provide INDOT with (1) a 3-dimensional perspective of traffic volumes over entire Indiana; and (2) a basis for determining appropriate WIM locations. ArcGIS 9.2 (ESRI 2007) was used in the analysis of the spatial distributions of traffic volumes. ArcGIS 9.2 applies the interpolation techniques in its Geostatistical Analyst. Geostatistical Analyst uses sample points taken at different locations in a landscape and creates a continuous surface. The sample points in this study are the traffic volumes at the INDOT traffic monitoring stations. It was found that the AADT data were not normally distributed. The data were transformed by log or Box-Cox techniques to make the data more normally distributed in order to satisfy the normal distribution

requirement of the geostatistics. Through various types of mathematical modeling techniques, it was concluded that the Inverse Distance Weighing (IDW) method generated the best AADT predictions among the ten modeling methods. The IDW method can be used to predict the AADT at any given location within Indiana.

Based on the IDW predictions of AADT, a prediction map can be generated which shows the AADT distributions with different colors for the divided traffic volume levels. In order to analyze the placement of the existing WIM stations in Indiana, ArcMap functions were utilized to visualize the relationship between AADT distributions and WIM stations locations. It was found that with log transformed AADT data the TIN map could clearly illustrate and distinguish different traffic volume levels on the 2D map. Adding the WIM stations as a layer on the 2D map, the WIM stations can be shown on the AADT distribution map. Therefore, the placement of the WIM stations in relation to the AADT distributions can be examined to determine the appropriate locations for the future new WIM stations. The coordinates of the proposed future WIM locations were determined. These coordinates were provided for INDOT to consider when new WIM devices are to be installed in the future.

In summary, this study has produced the traffic input for INDOT to implement the new pavement design method. The traffic input is an essential component for using the MEPDG to design pavement structures. In addition to the axle load spectra and truck traffic input, this study also analyzed the AADT distributions in Indiana through geostatistical analysis utilizing ArcGIS tools. The geostatistical analysis resulted in a series of results for spatial AADT predictions and future WIM station location determinations. It is believed that the results of this study will certainly facilitate INDOT's transition process from the current pavement design method to the MEPDG.

REFERENCES

- AASHTO. (1993). *Guide for Design of Pavement Structures*. American Association of State Highway and Transportation Officials.
- Al-Yagout, M. A., Mahoney, J. P., Pierce, L. M., & Hallenbeck, M. E. (2005). *Improving Traffic Characterization to Enhance Pavement Design and Performance: Load Spectra Development*. Washington State Transportation Center.
- Buchanan, M. S. (2004). *Traffic Load Spectra Development for the 2002 AASHTO Pavement Design Guide*. Mississippi Department of Transportation, FHWA/MS-DOT-RD-04-165. Mississippi State University.
- Box, G.E.P., and Cox, D.R. (1964). "An Analysis of Transformations," *Journal of the Royal Statistical Society, Series B*, 26, 455-575.
- Clark, I. (1979). *Practical Geostatistics*. Geostokos Limited.
- ESRI. (2007). *ArcGIS 9.2 Desktop Help*. <http://webhelp.esri.com/arcgisdesktop/9.2/>. ESRI Corporate.
- FHWA. (2001). *Traffic Monitoring Guide*. Office of Highway Policy Information, Federal Highway Administration, U.S. Department of Transportation, 2001.
- Haider, S. W., & Harichandran, R. S. (2007). "Characterizing Axle Load Spectra by Using Gross Vehicle Weights and Truck Traffic Volumes," *Transportation Research Board 86th Annual Meeting Compendium of Papers CD-ROM*.
- IRD. (1999). *Software Users' Manual, IRD Weigh-In-Motion (WIM) Data Collection System, Version 7.5.0*. International Road Dynamics (IRD) Inc.
- McBratney, A.B., & Webster, R. (1986). Choosing Functions for Semi-variograms of Soil Properties and Fitting Them to Sampling Estimates. *Journal of Soil Science* 37: 617-639.
- Myers, R.H., & Montgomery, D. C. (2002). *Response Surface Methodology*. John Wiley & Sons, Inc.
- NCHRP. (2004). *Guide for Mechanistic-Empirical Design of New and Rehabilitated Pavement Structures*. NCHRP 1-37A, Final Report, ERES Consultants Division, ARA Incorporation.
- Swan, D. J., Tardif, R., Hajek, J. J., Hein, D. K. (2008). "Development of Regional Traffic Data for the M-E Pavement Design Guide," *Transportation Research Board 87th Annual Meeting Compendium of Papers CD-ROM*.
- Timm, D. H., Bower, J. M., & Turochy, R. E. (2006). "Effect of Load Spectra on Mechanistic-Empirical Flexible Pavement Design," *Journal of the Transportation Research Board*, 1947.

APPENDIX: TRAFFIC INPUT AT A WIM STATION

**WIM Site 5300 (6170), I-74, RP 169.77, W Harrison
Two Lanes in Each Direction
Two Lane WIM Data in Each Direction**

AADTT: Two-way annual average daily truck traffic
MAF: Truck traffic monthly adjustment factors (note: twelve-month MAF total = 12.0)
DDF: Directional distribution factors, or percent trucks in the design direction
LDF: Truck lane distribution factors, or the percent trucks in the design lane
TCD: Truck class distribution (percent)
HDF: Hourly distribution factors (percent)
C4, C5, ... C13: Class 4, Class 5, ..., Class 13 of vehicle classifications

	AADTT Ln 1	AADTT Ln 2	AADTT Ln 3	AADTT Ln 4	Total	MAF
AADTT Jan	2410.40	280.10	1155.90	262.80	4109.20	0.56
AADTT Feb	2691.30	316.10	928.60	279.50	4215.50	0.57
AADTT Mar	2971.40	343.60	1687.80	316.50	5319.30	0.72
AADTT Apr	3203.20	358.90	3193.60	1224.20	7979.90	1.09
AADTT May	3491.60	336.60	3778.20	1127.00	8733.40	1.19
AADTT Jun	4077.60	367.60	4504.90	1213.50	10163.60	1.38
AADTT Jul	3653.40	371.20	4355.60	1242.20	9622.40	1.31
AADTT Aug	3480.20	370.60	3997.70	1241.60	9090.10	1.24
AADTT Sep	3314.80	354.30	3744.10	1182.90	8596.10	1.17
AADTT Oct	2852.50	322.80	3001.50	1149.00	7325.80	1.00
AADTT Nov	2618.80	331.10	2716.10	1100.40	6766.40	0.92
AADTT Dec	2395.90	326.80	2514.10	1082.40	6319.20	0.86
Avg	3096.76	339.98	2964.84	951.83	7353.41	
Sum	37161.10	4079.70	35578.10	11422.00	88240.90	12.00

	C4	C5	C6	C7	C8	C9	C10	C11	C12	C13	All Truck
DDF	0.51	0.64	0.59	0.92	0.53	0.55	0.55	0.52	0.52	0.80	0.53
LDF-dir1	0.91	0.83	0.87	0.85	0.95	0.94	0.94	0.94	0.94	0.80	0.90
LDF-dir2	0.84	0.56	0.93	0.92	0.86	0.93	0.98	0.94	0.97	1.00	0.76

All Lanes Combined AADTT											
	C4	C5	C6	C7	C8	C9	C10	C11	C12	C13	Total
Jan	31.90	1006.10	233.10	21.10	240.00	2419.60	10.10	124.20	18.50	4.60	4109.20
Feb	38.50	1158.80	208.30	17.70	226.50	2417.80	9.20	118.80	18.30	1.60	4215.50
Mar	50.70	1581.40	339.70	12.70	371.80	2781.70	9.90	149.20	22.10	0.10	5319.30
Apr	102.50	2886.20	127.50	21.20	389.00	4195.00	16.80	201.00	40.50	0.20	7979.90
May	112.70	3793.20	130.90	48.10	434.10	3971.30	12.40	190.60	40.10	0.00	8733.40
Jun	108.00	4819.70	142.30	52.90	490.10	4282.30	16.90	207.00	44.00	0.40	10163.60
Jul	97.30	4656.30	130.20	56.60	479.70	3957.40	13.30	192.80	38.70	0.10	9622.40
Aug	101.60	3841.40	141.30	49.80	469.40	4228.30	16.60	201.70	39.70	0.30	9090.10
Sep	107.40	3352.80	122.30	54.10	445.40	4260.70	15.50	197.10	40.70	0.10	8596.10
Oct	102.40	2296.80	118.80	42.60	361.30	4149.70	14.30	199.30	40.60	0.00	7325.80
Nov	93.90	1851.00	123.40	31.20	287.20	4140.90	14.60	184.90	39.20	0.10	6766.40
Dec	76.40	1772.10	123.10	26.50	266.60	3835.50	11.90	173.90	33.10	0.10	6319.20
Total	1023.30	33015.80	1940.90	434.50	4461.10	44640.20	161.50	2140.50	415.50	7.60	88240.90
Average AADTT Yearly Increase = 7.9%											

Monthly Adjustment Factor (MAF)											
	C4	C5	C6	C7	C8	C9	C10	C11	C12	C13	Total
Jan	0.37	0.37	1.44	0.58	0.65	0.65	0.75	0.70	0.53	7.26	0.56
Feb	0.45	0.42	1.29	0.49	0.61	0.65	0.68	0.67	0.53	2.53	0.57
Mar	0.59	0.57	2.10	0.35	1.00	0.75	0.74	0.84	0.64	0.16	0.72
Apr	1.20	1.05	0.79	0.59	1.05	1.13	1.25	1.13	1.17	0.32	1.09
May	1.32	1.38	0.81	1.33	1.17	1.07	0.92	1.07	1.16	0.00	1.19
Jun	1.27	1.75	0.88	1.46	1.32	1.15	1.26	1.16	1.27	0.63	1.38
Jul	1.14	1.69	0.80	1.56	1.29	1.06	0.99	1.08	1.12	0.16	1.31
Aug	1.19	1.40	0.87	1.38	1.26	1.14	1.23	1.13	1.15	0.47	1.24
Sep	1.26	1.22	0.76	1.49	1.20	1.15	1.15	1.10	1.18	0.16	1.17
Oct	1.20	0.83	0.73	1.18	0.97	1.12	1.06	1.12	1.17	0.00	1.00
Nov	1.10	0.67	0.76	0.86	0.77	1.11	1.08	1.04	1.13	0.16	0.92
Dec	0.90	0.64	0.76	0.73	0.72	1.03	0.88	0.97	0.96	0.16	0.86
Sum	12.00	12.00	12.00	12.00	12.00	12.00	12.00	12.00	12.00	12.00	12.00

Hourly Volume												
	StartTime	C4	C5	C6	C7	C8	C9	C10	C11	C12	C13	All Truck
Combined	0	2.38	15.27	3.67	0.55	6.54	99.43	0.18	5.77	1.19	0.03	135.00
	1	2.08	10.68	3.43	0.73	6.71	95.11	0.17	5.68	0.85	0.01	125.45
	2	1.66	10.46	3.64	0.93	6.13	95.84	0.15	6.72	1.04	0.00	126.57
	3	2.07	14.52	4.18	1.02	9.49	106.12	0.32	8.82	1.28	0.00	147.81
	4	3.04	33.75	5.68	1.63	11.73	123.33	0.41	10.18	1.71	0.05	191.52
	5	3.13	62.35	9.24	2.26	11.48	141.16	0.68	12.18	1.88	0.04	244.41
	6	2.93	76.76	9.04	2.06	11.30	151.99	0.77	8.99	1.64	0.11	265.59
	7	4.48	88.67	7.56	2.23	13.03	171.14	0.94	6.86	1.31	0.13	296.35
	8	5.05	109.06	8.08	2.23	16.82	191.46	0.93	7.63	1.34	0.03	342.62
	9	4.94	141.42	8.99	2.57	20.61	204.49	0.96	6.84	1.46	0.02	392.29
	10	4.71	164.66	9.53	2.33	23.06	213.11	1.13	7.03	1.68	0.05	427.28
	11	4.73	176.36	9.48	2.38	24.18	207.93	1.20	5.80	1.04	0.02	433.12
	12	4.62	191.24	9.58	1.76	25.53	203.07	0.84	4.69	0.96	0.03	442.32
	13	4.52	215.97	9.18	1.98	25.62	201.70	0.90	5.65	0.90	0.05	466.46
	14	4.67	265.48	9.39	1.60	25.82	191.26	0.91	6.33	1.03	0.03	506.50
	15	4.53	293.28	9.18	1.42	23.74	182.00	0.72	5.98	1.28	0.00	522.13
	16	4.08	264.75	7.82	1.38	20.89	169.33	0.59	5.83	1.58	0.01	476.24
	17	3.97	196.78	6.71	1.28	17.70	159.52	0.42	5.44	1.28	0.00	393.08
	18	3.32	134.32	5.65	1.15	15.13	152.31	0.33	4.77	1.23	0.00	318.19
	19	3.09	97.93	5.36	1.13	12.99	146.32	0.27	6.63	1.21	0.01	274.92
	20	3.08	75.63	4.58	1.05	11.73	144.81	0.21	9.78	2.15	0.00	252.99
	21	2.83	53.63	4.17	0.92	12.38	133.83	0.13	12.51	2.98	0.03	223.40
	22	2.96	36.04	4.15	0.83	11.75	123.98	0.19	10.69	2.16	0.00	192.75
	23	2.38	22.29	3.49	0.81	7.41	110.75	0.13	7.63	1.46	0.00	156.35
AADTT	Sum	85.23	2751.27	161.75	36.21	371.77	3719.96	13.46	178.43	34.62	0.63	7353.32
TCD	Percent	1.16	37.42	2.20	0.49	5.06	50.59	0.18	2.43	0.47	0.01	100.00

Hourly Distribution Factor (HDF) (%) Two Directions Combined											
StartTime	C4	C5	C6	C7	C8	C9	C10	C11	C12	C13	All Truck
0	2.80	0.55	2.27	1.52	1.76	2.67	1.36	3.23	3.44	3.95	1.84
1	2.43	0.39	2.12	2.03	1.80	2.56	1.24	3.19	2.46	1.32	1.71
2	1.95	0.38	2.25	2.55	1.65	2.58	1.11	3.76	3.01	0.00	1.72
3	2.42	0.53	2.59	2.81	2.55	2.85	2.35	4.94	3.71	0.00	2.01
4	3.57	1.23	3.51	4.51	3.16	3.32	3.03	5.71	4.94	7.89	2.60
5	3.68	2.27	5.71	6.24	3.09	3.79	5.08	6.82	5.44	6.58	3.32
6	3.44	2.79	5.59	5.68	3.04	4.09	5.70	5.04	4.74	17.11	3.61
7	5.26	3.22	4.67	6.14	3.51	4.60	7.00	3.84	3.78	21.05	4.03
8	5.92	3.96	4.99	6.14	4.52	5.15	6.87	4.28	3.88	5.26	4.66
9	5.80	5.14	5.56	7.09	5.54	5.50	7.12	3.83	4.21	2.63	5.33
10	5.52	5.98	5.89	6.44	6.20	5.73	8.36	3.94	4.84	7.89	5.81
11	5.55	6.41	5.86	6.58	6.50	5.59	8.92	3.25	3.01	2.63	5.89
12	5.42	6.95	5.92	4.86	6.87	5.46	6.25	2.63	2.77	5.26	6.02
13	5.30	7.85	5.67	5.48	6.89	5.42	6.69	3.17	2.60	7.89	6.34
14	5.48	9.65	5.81	4.42	6.94	5.14	6.75	3.55	2.96	3.95	6.89
15	5.32	10.66	5.67	3.91	6.39	4.89	5.33	3.35	3.68	0.00	7.10
16	4.78	9.62	4.83	3.80	5.62	4.55	4.40	3.27	4.55	1.32	6.48
17	4.65	7.15	4.15	3.54	4.76	4.29	3.10	3.05	3.68	0.00	5.35
18	3.89	4.88	3.49	3.18	4.07	4.09	2.41	2.67	3.54	0.00	4.33
19	3.63	3.56	3.31	3.11	3.49	3.93	1.98	3.71	3.49	1.32	3.74
20	3.61	2.75	2.83	2.90	3.15	3.89	1.55	5.48	6.21	0.00	3.44
21	3.31	1.95	2.58	2.53	3.33	3.60	0.99	7.01	8.62	3.95	3.04
22	3.47	1.31	2.57	2.30	3.16	3.33	1.42	5.99	6.23	0.00	2.62
23	2.80	0.81	2.16	2.23	1.99	2.98	0.99	4.27	4.21	0.00	2.13
Sum	100.00	100.00	100.00	100.00	100.00	100.00	100.00	100.00	100.00	100.00	100.00

Single-Axle Load Distribution (Percentages) for Each Truck Class

Class	4	5	6	7	8	9	10	11	12	13
3kips	0.59	51.34	14.72	2.07	5.61	3.52	2.31	0.14	0.23	0.20
4kips	0.38	20.56	3.28	4.30	12.30	3.34	2.17	4.30	4.08	7.08
5kips	0.47	10.23	4.11	3.48	10.63	3.79	3.15	6.14	6.09	9.96
6kips	0.89	5.09	4.65	3.44	9.59	4.60	4.61	7.67	8.62	9.76
7kips	8.06	3.22	5.25	3.42	9.13	5.92	7.22	8.84	9.55	9.18
8kips	14.35	2.27	6.81	4.00	9.24	8.29	10.22	10.38	11.30	9.07
9kips	14.31	1.69	9.18	4.83	8.52	11.77	14.19	11.28	12.01	9.43
10kips	12.70	1.25	11.13	5.96	7.00	15.83	17.16	10.33	11.71	9.59
11kips	10.64	0.90	10.00	6.34	5.27	15.00	15.03	8.87	9.89	9.43
12kips	8.58	0.64	7.18	7.19	3.88	10.13	10.29	6.93	7.74	6.24
13kips	6.45	0.46	4.95	7.59	2.93	5.77	5.41	5.45	5.50	4.64
14kips	4.74	0.34	3.42	7.78	2.32	3.00	2.42	4.60	4.00	3.24
15kips	3.54	0.27	2.56	7.16	1.93	2.04	1.55	3.69	2.72	2.05
16kips	2.64	0.22	2.03	6.75	1.63	1.68	1.09	2.95	1.90	1.81
17kips	2.07	0.18	1.75	5.92	1.33	1.40	0.79	2.27	1.31	2.13
18kips	1.59	0.15	1.52	5.48	1.12	1.09	0.58	1.64	0.99	2.18
19kips	1.25	0.13	1.29	4.35	0.92	0.79	0.43	1.18	0.65	1.35
20kips	0.97	0.11	1.04	3.00	0.75	0.54	0.30	0.84	0.49	0.54
21kips	0.87	0.10	0.90	1.74	0.64	0.37	0.23	0.59	0.27	0.43
22kips	0.65	0.09	0.73	1.11	0.52	0.25	0.17	0.38	0.25	0.32
23kips	0.50	0.08	0.61	0.72	0.45	0.18	0.12	0.26	0.13	0.29
24kips	0.43	0.07	0.51	0.61	0.39	0.13	0.11	0.17	0.10	0.21
25kips	0.38	0.07	0.41	0.42	0.35	0.10	0.08	0.13	0.08	0.17
26kips	0.31	0.06	0.34	0.35	0.31	0.08	0.07	0.11	0.05	0.14
27kips	0.25	0.06	0.29	0.27	0.28	0.07	0.05	0.08	0.04	0.07
28kips	0.25	0.05	0.24	0.21	0.26	0.05	0.05	0.09	0.04	0.08
29kips	0.20	0.05	0.21	0.28	0.24	0.04	0.04	0.08	0.04	0.09
30kips	0.22	0.05	0.17	0.17	0.22	0.04	0.03	0.07	0.03	0.05
31kips	0.14	0.04	0.14	0.14	0.21	0.03	0.03	0.04	0.03	0.05
32kips	0.16	0.04	0.11	0.16	0.19	0.02	0.02	0.05	0.02	0.05
33kips	0.18	0.03	0.08	0.13	0.18	0.02	0.02	0.04	0.02	0.03
34kips	0.11	0.03	0.06	0.13	0.17	0.02	0.01	0.05	0.02	0.03
35kips	0.12	0.03	0.05	0.08	0.16	0.02	0.01	0.03	0.02	0.02
36kips	0.11	0.02	0.04	0.07	0.15	0.01	0.01	0.04	0.02	0.01
37kips	0.10	0.01	0.04	0.06	0.13	0.01	0.01	0.03	0.02	0.02
38kips	0.10	0.01	0.03	0.09	0.12	0.01	0.01	0.03	0.01	0.01
39kips	0.12	0.01	0.03	0.05	0.12	0.01	0.00	0.03	0.01	0.01
40kips	0.10	0.01	0.03	0.04	0.11	0.01	0.01	0.02	0.01	0.01
41kips	0.54	0.06	0.15	0.15	0.72	0.05	0.03	0.17	0.03	0.03

Tandem-Axle Load Distribution (Percentages) for Each Truck Class

Class	4	5	6	7	8	9	10	11	12	13
6kips	5.69	0.00	30.22	17.66	34.71	7.92	5.11	0.00	0.00	0.00
8kips	6.06	0.00	10.38	6.75	13.23	7.12	5.45	0.00	5.25	3.78
10kips	5.96	0.00	8.57	5.44	11.71	8.15	7.42	0.00	9.13	7.72
12kips	6.77	0.00	7.49	5.51	9.77	8.04	7.82	0.00	11.89	9.57
14kips	7.38	0.00	6.00	5.95	7.45	7.49	7.57	0.00	14.32	8.81
16kips	7.28	0.00	4.76	5.59	5.53	7.26	7.35	0.00	14.42	8.58
18kips	7.88	0.00	3.89	4.87	4.27	7.02	6.98	0.00	13.23	7.46
20kips	8.83	0.00	3.43	4.16	3.37	6.59	6.48	0.00	10.49	7.89
22kips	8.72	0.00	3.08	4.04	2.59	6.20	6.26	0.00	6.96	6.32
24kips	7.05	0.00	2.93	4.24	1.84	5.71	6.45	0.00	4.98	6.05
26kips	6.46	0.00	2.77	4.57	1.32	5.29	6.03	0.00	3.10	6.63
28kips	5.66	0.00	2.60	4.69	0.98	4.98	5.94	0.00	1.73	5.56
30kips	4.29	0.00	2.43	5.07	0.72	4.75	5.41	0.00	1.12	3.91
32kips	3.10	0.00	2.11	5.16	0.54	4.21	4.37	0.00	0.83	3.91
34kips	2.22	0.00	1.70	4.12	0.43	3.04	3.65	0.00	0.68	2.39
36kips	1.61	0.00	1.42	3.19	0.35	2.21	2.67	0.00	0.47	2.33
38kips	1.14	0.00	1.21	1.68	0.27	1.61	1.81	0.00	0.28	2.63
40kips	0.85	0.00	0.89	1.05	0.19	0.95	0.92	0.00	0.24	1.74
42kips	0.55	0.00	0.63	0.91	0.14	0.46	0.62	0.00	0.20	1.48
44kips	0.41	0.00	0.49	0.66	0.11	0.23	0.41	0.00	0.13	0.74
46kips	0.33	0.00	0.41	0.58	0.10	0.14	0.32	0.00	0.12	0.98
48kips	0.31	0.00	0.35	0.69	0.07	0.10	0.21	0.00	0.08	0.38
50kips	0.22	0.00	0.32	0.67	0.07	0.08	0.16	0.00	0.08	0.27
52kips	0.17	0.00	0.27	0.40	0.05	0.06	0.11	0.00	0.07	0.20
54kips	0.15	0.00	0.25	0.39	0.04	0.05	0.12	0.00	0.05	0.15
56kips	0.12	0.00	0.22	0.38	0.03	0.04	0.08	0.00	0.04	0.10
58kips	0.11	0.00	0.19	0.28	0.03	0.03	0.05	0.00	0.04	0.08
60kips	0.10	0.00	0.16	0.22	0.02	0.03	0.04	0.00	0.02	0.10
62kips	0.09	0.00	0.15	0.16	0.02	0.02	0.03	0.00	0.02	0.07
64kips	0.08	0.00	0.13	0.16	0.01	0.02	0.03	0.00	0.01	0.04
66kips	0.07	0.00	0.11	0.18	0.01	0.02	0.02	0.00	0.01	0.03
68kips	0.06	0.00	0.09	0.12	0.01	0.02	0.02	0.00	0.01	0.02
70kips	0.05	0.00	0.07	0.15	0.00	0.02	0.02	0.00	0.01	0.01
72kips	0.05	0.00	0.06	0.08	0.00	0.02	0.01	0.00	0.01	0.02
74kips	0.03	0.00	0.05	0.06	0.00	0.01	0.01	0.00	0.00	0.01
76kips	0.03	0.00	0.04	0.05	0.00	0.01	0.01	0.00	0.00	0.01
78kips	0.03	0.00	0.03	0.04	0.00	0.01	0.01	0.00	0.00	0.01
80kips	0.02	0.00	0.02	0.01	0.00	0.01	0.01	0.00	0.00	0.01
82kips	0.06	0.00	0.09	0.09	0.01	0.05	0.03	0.00	0.00	0.02

Tridem-Axle Load Distribution (Percentages) for Each Truck Class

Class	4	5	6	7	8	9	10	11	12	13
12kips	0.00	0.00	0.00	3.11	0.00	0.00	26.31	0.00	0.00	0.00
15kips	0.00	0.00	0.00	2.08	0.00	0.00	8.61	0.00	0.00	0.00
18kips	0.00	0.00	0.00	2.30	0.00	0.00	7.49	0.00	0.00	0.00
21kips	0.00	0.00	0.00	3.10	0.00	0.00	6.75	0.00	0.00	0.00
24kips	0.00	0.00	0.00	3.60	0.00	0.00	6.40	0.00	0.00	0.00
27kips	0.00	0.00	0.00	3.88	0.00	0.00	6.43	0.00	0.00	0.00
30kips	0.00	0.00	0.00	4.36	0.00	0.00	7.08	0.00	0.00	0.00
33kips	0.00	0.00	0.00	5.37	0.00	0.00	7.13	0.00	0.00	0.00
36kips	0.00	0.00	0.00	6.61	0.00	0.00	6.70	0.00	0.00	0.00
39kips	0.00	0.00	0.00	7.92	0.00	0.00	5.27	0.00	0.00	0.00
42kips	0.00	0.00	0.00	9.15	0.00	0.00	3.69	0.00	0.00	0.00
45kips	0.00	0.00	0.00	9.59	0.00	0.00	2.81	0.00	0.00	0.00
48kips	0.00	0.00	0.00	9.18	0.00	0.00	1.93	0.00	0.00	0.00
51kips	0.00	0.00	0.00	8.18	0.00	0.00	1.23	0.00	0.00	0.00
54kips	0.00	0.00	0.00	6.58	0.00	0.00	0.62	0.00	0.00	0.00
57kips	0.00	0.00	0.00	4.73	0.00	0.00	0.36	0.00	0.00	0.00
60kips	0.00	0.00	0.00	3.30	0.00	0.00	0.30	0.00	0.00	0.00
63kips	0.00	0.00	0.00	2.33	0.00	0.00	0.24	0.00	0.00	0.00
66kips	0.00	0.00	0.00	1.46	0.00	0.00	0.21	0.00	0.00	0.00
69kips	0.00	0.00	0.00	0.76	0.00	0.00	0.11	0.00	0.00	0.00
72kips	0.00	0.00	0.00	0.71	0.00	0.00	0.06	0.00	0.00	0.00
75kips	0.00	0.00	0.00	0.36	0.00	0.00	0.06	0.00	0.00	0.00
78kips	0.00	0.00	0.00	0.25	0.00	0.00	0.05	0.00	0.00	0.00
81kips	0.00	0.00	0.00	0.22	0.00	0.00	0.04	0.00	0.00	0.00
84kips	0.00	0.00	0.00	0.13	0.00	0.00	0.04	0.00	0.00	0.00
87kips	0.00	0.00	0.00	0.18	0.00	0.00	0.03	0.00	0.00	0.00
90kips	0.00	0.00	0.00	0.10	0.00	0.00	0.02	0.00	0.00	0.00
93kips	0.00	0.00	0.00	0.08	0.00	0.00	0.02	0.00	0.00	0.00
96kips	0.00	0.00	0.00	0.07	0.00	0.00	0.02	0.00	0.00	0.00
99kips	0.00	0.00	0.00	0.05	0.00	0.00	0.02	0.00	0.00	0.00
102kips	0.00	0.00	0.00	0.06	0.00	0.00	0.01	0.00	0.00	0.00

Quad-Axle Load Distribution (Percentages) for Each Truck Class

Class	4	5	6	7	8	9	10	11	12	13
12kips	0.00	0.00	0.00	3.04	0.00	0.00	9.31	0.00	0.00	0.00
15kips	0.00	0.00	0.00	1.23	0.00	0.00	0.37	0.00	0.00	0.00
18kips	0.00	0.00	0.00	1.42	0.00	0.00	0.73	0.00	0.00	0.00
21kips	0.00	0.00	0.00	2.28	0.00	0.00	0.84	0.00	0.00	0.00
24kips	0.00	0.00	0.00	2.38	0.00	0.00	3.96	0.00	0.00	0.00
27kips	0.00	0.00	0.00	2.13	0.00	0.00	3.89	0.00	0.00	0.00
30kips	0.00	0.00	0.00	2.65	0.00	0.00	13.24	0.00	0.00	0.00
33kips	0.00	0.00	0.00	3.33	0.00	0.00	17.85	0.00	0.00	0.00
36kips	0.00	0.00	0.00	4.27	0.00	0.00	12.34	0.00	0.00	0.00
39kips	0.00	0.00	0.00	6.39	0.00	0.00	14.77	0.00	0.00	0.00
42kips	0.00	0.00	0.00	7.97	0.00	0.00	7.00	0.00	0.00	0.00
45kips	0.00	0.00	0.00	9.11	0.00	0.00	5.66	0.00	0.00	0.00
48kips	0.00	0.00	0.00	10.07	0.00	0.00	6.20	0.00	0.00	0.00
51kips	0.00	0.00	0.00	10.54	0.00	0.00	0.64	0.00	0.00	0.00
54kips	0.00	0.00	0.00	8.74	0.00	0.00	0.61	0.00	0.00	0.00
57kips	0.00	0.00	0.00	6.66	0.00	0.00	0.74	0.00	0.00	0.00
60kips	0.00	0.00	0.00	5.38	0.00	0.00	0.09	0.00	0.00	0.00
63kips	0.00	0.00	0.00	4.25	0.00	0.00	1.21	0.00	0.00	0.00
66kips	0.00	0.00	0.00	2.52	0.00	0.00	0.17	0.00	0.00	0.00
69kips	0.00	0.00	0.00	1.73	0.00	0.00	0.38	0.00	0.00	0.00
72kips	0.00	0.00	0.00	0.94	0.00	0.00	0.00	0.00	0.00	0.00
75kips	0.00	0.00	0.00	0.63	0.00	0.00	0.00	0.00	0.00	0.00
78kips	0.00	0.00	0.00	0.43	0.00	0.00	0.00	0.00	0.00	0.00
81kips	0.00	0.00	0.00	0.31	0.00	0.00	0.00	0.00	0.00	0.00
84kips	0.00	0.00	0.00	0.23	0.00	0.00	0.00	0.00	0.00	0.00
87kips	0.00	0.00	0.00	0.21	0.00	0.00	0.00	0.00	0.00	0.00
90kips	0.00	0.00	0.00	0.16	0.00	0.00	0.00	0.00	0.00	0.00
93kips	0.00	0.00	0.00	0.16	0.00	0.00	0.00	0.00	0.00	0.00
96kips	0.00	0.00	0.00	0.13	0.00	0.00	0.00	0.00	0.00	0.00
99kips	0.00	0.00	0.00	0.10	0.00	0.00	0.00	0.00	0.00	0.00
102kips	0.00	0.00	0.00	0.09	0.00	0.00	0.00	0.00	0.00	0.00

All-Axle Load Distribution (Percentages) for Each Truck Class

Class	4	5	6	7	8	9	10	11	12	13
3kips	3.82	26.47	42.37	20.17	18.02	28.43	25.52	9.90	5.83	7.05
4kips	5.37	12.00	15.60	17.67	9.92	21.70	13.50	13.65	14.10	18.47
5kips	7.62	7.12	12.37	14.33	8.98	14.45	11.82	14.30	16.78	14.75
6kips	9.40	5.87	9.37	10.83	7.40	10.30	10.58	13.42	13.37	14.67
7kips	14.87	5.45	6.33	7.20	6.67	6.92	7.68	10.45	9.83	8.52
8kips	14.33	7.15	3.93	6.27	6.27	4.50	5.83	7.87	6.60	5.97
9kips	11.18	2.88	2.77	5.07	5.22	2.90	4.83	6.28	5.32	7.83
10kips	7.53	2.43	2.07	4.10	4.37	2.02	3.85	4.90	4.12	4.55
11kips	6.12	1.18	1.53	2.67	3.42	1.52	3.28	3.55	3.03	3.30
12kips	4.12	4.63	1.00	1.80	3.10	1.15	2.72	3.05	2.43	3.48
13kips	2.18	2.17	0.57	1.37	2.40	0.88	1.85	2.47	1.98	2.12
14kips	2.13	2.17	0.33	1.37	1.98	0.65	1.42	1.68	1.50	1.67
15kips	1.22	4.88	0.27	1.37	1.80	0.50	1.22	0.90	1.22	1.47
16kips	1.58	1.53	0.13	0.97	1.63	0.38	0.95	1.17	1.13	1.00
17kips	1.32	0.65	0.20	0.90	1.43	0.30	0.65	0.63	0.90	1.18
18kips	1.32	1.28	0.07	1.10	1.05	0.22	0.50	0.98	0.80	0.82
19kips	0.50	3.12	0.03	0.33	1.12	0.20	0.45	0.77	0.68	0.42
20kips	0.05	1.85	0.03	0.43	0.97	0.17	0.35	0.72	0.67	0.25
21kips	0.92	0.00	0.00	0.40	0.88	0.13	0.33	0.17	0.60	0.27
22kips	0.80	0.00	0.00	0.17	0.90	0.10	0.27	0.30	0.55	0.37
23kips	0.03	0.00	0.00	0.27	0.80	0.10	0.18	0.27	0.48	0.28
24kips	0.85	0.63	0.00	0.03	0.72	0.10	0.17	0.27	0.48	0.13
25kips	0.25	0.00	0.00	0.07	0.72	0.08	0.12	0.27	0.47	0.22
26kips	0.05	0.00	0.00	0.03	0.55	0.08	0.12	0.17	0.42	0.03
27kips	0.25	0.00	0.00	0.13	0.53	0.08	0.08	0.05	0.37	0.03
28kips	0.00	0.00	0.00	0.00	0.48	0.08	0.03	0.03	0.38	0.02
29kips	0.00	0.00	0.00	0.03	0.43	0.05	0.03	0.05	0.35	0.02
30kips	0.00	1.27	0.00	0.00	0.50	0.05	0.03	0.03	0.35	0.07
31kips	0.00	0.00	0.00	0.07	0.45	0.05	0.03	0.08	0.33	0.00
32kips	0.00	0.00	0.00	0.00	0.45	0.05	0.00	0.10	0.32	0.00
33kips	0.00	0.00	0.00	0.00	0.38	0.05	0.02	0.00	0.30	0.00
34kips	0.00	0.00	0.00	0.00	0.38	0.03	0.02	0.00	0.27	0.00
35kips	0.00	1.85	0.00	0.00	0.40	0.03	0.00	0.00	0.25	0.00
36kips	0.00	0.00	0.00	0.00	0.30	0.03	0.03	0.00	0.25	0.00
37kips	0.00	0.00	0.00	0.00	0.35	0.03	0.02	0.03	0.22	0.00
38kips	0.00	1.27	0.00	0.00	0.35	0.03	0.00	0.02	0.22	0.00
39kips	0.00	0.00	0.00	0.00	0.35	0.02	0.00	0.00	0.22	0.00
40kips	0.00	0.00	0.00	0.00	0.33	0.03	0.00	0.02	0.18	0.00
41kips	1.23	1.27	0.00	0.10	2.52	0.28	0.12	0.22	1.48	0.02

Average Axle Weight (kip) and Average Axle Spacing (inches)

Class	4	5	6	7	8	9	10	11	12	13
W1	14.70	5.33	7.78	9.44	8.51	8.44	8.08	8.60	9.62	6.66
W2	13.88	5.12	6.20	7.55	10.98	6.14	5.81	12.21	7.23	5.59
W3	9.26	0.00	6.20	7.51	10.03	6.00	5.71	12.88	7.66	5.77
W4	0.00	0.00	0.00	7.73	6.64	5.76	4.97	11.25	9.71	5.19
W5	0.00	0.00	0.00	4.39	0.00	5.73	4.90	11.31	11.35	5.57
W6	0.00	0.00	0.00	0.00	0.00	0.00	5.24	0.00	8.74	7.08
W7	0.00	0.00	0.00	0.00	0.00	0.00	2.47	0.00	0.00	6.31
W8	0.00	0.00	0.00	0.00	0.00	0.00	0.00	0.00	0.00	7.79
W9	0.00	0.00	0.00	0.00	0.00	0.00	0.00	0.00	0.00	4.20
S12	23.18	13.06	18.97	5.68	12.35	13.88	13.85	10.42	12.58	9.45
S23	3.70	0.00	3.24	20.55	18.41	3.93	3.64	17.62	4.05	5.28
S34	0.00	0.00	0.00	3.35	14.91	27.22	19.77	7.94	17.31	7.50
S45	0.00	0.00	0.00	1.85	0.00	4.21	5.67	17.98	8.78	10.96
S56	0.00	0.00	0.00	0.00	0.00	0.00	3.50	0.00	18.88	6.27
S67	0.00	0.00	0.00	0.00	0.00	0.00	1.88	0.00	0.00	5.62
S78	0.00	0.00	0.00	0.00	0.00	0.00	0.00	0.00	0.00	5.09
S89	0.00	0.00	0.00	0.00	0.00	0.00	0.00	0.00	0.00	3.58

Average Axle Spacing (inches) and Average Number of Axle Types

Class	4	5	6	7	8	9	10	11	12	13
S12	23.18	13.05	18.98	5.68	12.36	13.88	13.85	10.43	12.62	9.45
S23	3.70	0.00	3.24	20.59	18.41	3.93	3.64	17.61	4.05	5.28
S34	0.00	0.00	0.00	3.35	14.92	27.22	19.82	7.93	17.33	7.50
S45	0.00	0.00	0.00	1.85	0.00	4.21	5.66	8.97	8.78	10.96
S56	0.00	0.00	0.00	0.00	0.00	0.00	3.50	0.00	18.90	6.27
S67	0.00	0.00	0.00	0.00	0.00	0.00	1.88	0.00	0.00	5.62
S78	0.00	0.00	0.00	0.00	0.00	0.00	0.00	0.00	0.00	5.09
S89	0.00	0.00	0.00	0.00	0.00	0.00	0.00	0.00	0.00	3.58
Single	1.78	2.00	1.00	1.75	2.36	1.27	1.05	4.74	3.72	2.10
Tandem	0.22	0.00	1.00	0.75	0.63	1.86	1.03	0.08	1.09	1.08
Tridem	0.00	0.00	0.00	0.12	0.00	0.00	0.92	0.03	0.02	0.45
Quad	0.00	0.00	0.00	0.12	0.00	0.00	0.02	0.00	0.01	0.15
Quinate	0.00	0.00	0.00	0.00	0.00	0.00	0.00	0.00	0.00	0.05
Hexad	0.00	0.00	0.00	0.00	0.00	0.00	0.01	0.00	0.00	0.14